

Process Characteristics of Liquid Core Hydrogel Beads for Radish Leaves Utilization

January 2018

Fu-Hsuan TSAI

Process Characteristics of Liquid Core Hydrogel Beads for Radish Leaves Utilization

A Dissertation Submitted to
the Graduate School of Life and Environmental Science
the University of Tsukuba
in Partial Fulfillment of the Requirements
for the Degree of Philosophy in Agriculture Science
(Doctoral Program in Appropriate Technology and Sciences for Sustainable Development)

Fu-Hsuan TSAI

Abstract

Hydrogel bead is a type of capsulation, which has been widely used to reduce the reactivity between the specific compound and environmental factors. In the study, reverse spherification is used to prepare liquid-core hydrogel beads with ionic biopolymers, alginate, in order to encapsulate the radish by-product juice which was prepared with a micro wet milling system. The thesis was separated into 6 chapters.

The chapter 1 and chapter 6 were overall introduction and conclusion, respectively.

In chapter 2, the radish by-product juice was prepared by the micro wet milling system and the particle size (D50) and particle size distribution were investigated. The particle size of radish by-product juice was approximately 6.63 μm to 9.84 μm after being milled with micro wet milling system, and the lowest D50 was obtained with a rotation of 30 rpm.

In chapter 3, I identified the effect of gelation time and calcium lactate concentration in primary and secondary gelation on the physical properties and *in vitro* release behavior of the liquid-core hydrogel beads. A central composite design with response surface methodology was used for the optimization of liquid-core hydrogel bead properties. The effect of four independent variables: primary gelation time (X_1), calcium lactate concentration in primary gelation (X_2), secondary gelation time (X_3), and calcium lactate concentration in secondary gelation (X_4), on seven physical properties of liquid-core hydrogel bead: average diameter, hardness (Y_1), encapsulation efficiency (Y_2), release profile of total phenolic compounds in simulated gastric (Y_3) and small intestinal (Y_4) digestion, swelling capacity (Y_5), and sphericity (Y_6), were evaluated. The optimal conditions of liquid-core hydrogel bead formulation were primary gelation time of 23.99 min, 0.13 M of calcium lactate in the primary gelation, secondary gelation time of 6.04 min, and 0.058 M of calcium lactate in secondary gelation. The optimized formulation of liquid-core hydrogel bead demonstrated 25.5 N of hardness, 85.67 % of encapsulation efficiency and 27.38 % of total phenolic compounds release in a simulated gastric

digestion with the small error-values (-2.47 to 2.21 %).

In chapter 4, I prepared liquid-core hydrogel bead from alginate combined with gum arabic or glycerol and evaluated average diameter, sphericity, hardness, encapsulation efficiency, swelling capacity, and morphology. The hardness of alginate/gum arabic bead (6.53 N to 26.68 N) changed significantly than the alginate/glycerol bead (19.91 N to 24.08 N). The alginate/gum arabic bead showed the higher encapsulation efficiency and the lower swelling capacity than the alginate/ glycerol bead. The SEM results showed that there are some cracks on the surface of the alginate/ glycerol bead, resulting in the relatively lower hardness and encapsulation efficiency.

In chapter 5, the characterizes of alginate/gum arabic bead were analyzed in depth. The change of hardness, swelling behavior, total phenolic compounds release behavior, and release kinetics of alginate/gum arabic bead in an *in vitro* digestion system the stability of stored total phenolic compounds during storage were investigated. The liquid-core hydrogel bead formulated with 25 % gum arabic (GA0.25) was effective in preventing total phenolic compounds from loss during storage with a decay rate (k) of $6.10 \times 10^{-3} \text{ day}^{-1}$ and a half-life ($t_{1/2}$) of 113.63 days, it showed the slowest release of total phenolic compounds in simulated gastric digestion and the release mechanism followed Fickian diffusion.

As I know, the study provided the first report on the preparation of radish by-product juice with micro wet milling system (chapter 2), the effect of four independent variables: primary gelation time, calcium lactate concentration in primary gelation, secondary gelation time, and calcium lactate concentration in secondary gelation on the physical properties of liquid-core hydrogel beads (chapter 3), the preparation of liquid-core hydrogel bead from alginate combined with gum arabic or glycerol by reverse spherification (chapter 4), and their physical properties, release behavior in an *in vitro* digestion system, and storage stability (chapter 5). I believe that this study may be useful for the development and quality improvement of a delivery system.

要旨

ハイドロゲルビーズ (hydrogel beads) は、特定の化合物と環境因子との間の反応を減少させるためによく使用されているカプセルの一種である。この研究では、マイクロウェットミリング (micro wet milling) により粉砕された大根副産物ジュースをカプセル化するために、スフェリフィケーション (spherification) を用い、イオンバイオポリマー (アルギン酸塩) により液体コアハイドロゲルビーズを作成した。本論文は 6 つの章に分かれていた。

第 1 章と第 6 章はそれぞれ全体的な紹介と結論である。

第 2 章では、マイクロウェットミリングにより大根副産物ジュースを調製し、粒径 (D50) 及び粒径分布を調べた。マイクロウェットミリングにより粉砕後、大根副産物ジュースの粒度は約 $6.63\mu\text{m}$ ~ $9.84\mu\text{m}$ であり、30rpm の回転速度で最小 D50 を得た。

第 3 章では、一回及び二回ゲル化における時間及び乳酸カルシウム濃度が液体コアハイドロゲルビーズの物理的特性及びインビトロ放出挙動 (*in vitro* release profile) に与える影響を解明した。応答表面法中央複合体設計を使用し、液体コアハイドロゲルビーズ特性を最適化した。一回ゲル化時間 (X_1)、一回ゲル化における乳酸カルシウム濃度 (X_2)、二回ゲル化時間 (X_3)、二回ゲル化における乳酸カルシウム濃度 (X_4) が液体コアハイドロゲルビーズの 7 つの物理的特性【直径、硬度 (Y_1)、カプセル化効率 (Y_2)、模擬胃液 (Y_3) 及び小腸 (Y_4) におけるポリフェノール放出挙動、膨潤能力 (Y_5)、真球度 (Y_6)】に及ぼす影響を調べた。液体コアハイドロゲルビーズの最適条件は、一回ゲル化時間 23.99 分であり、乳酸カルシウム濃度 0.13M、二回ゲル化時間 6.04 分であり、乳酸カルシウム濃度 0.058M であった。上記の状況を用い、わずかな誤差値 (-2.47~2.21%) で硬度 25.5 N、カプセル化効率 85.67 %、模擬胃液における 27.38 %ポリフェノール放出の液体コアハイドロゲルビーズを得ることができた。

第 4 章では、アルギン酸塩とアラビアゴム又はグリセリンとを組み合わせた液体コアハイドロゲルビーズを作成し、直径、真球度、硬度、カプセル化効率、膨潤能力、形態

を評価した。アルギン酸塩/アラビアゴムビーズ (6.53 N~26.68 N) の硬度は、アルギン酸塩/グリセロールビーズ (19.91 N~24.08 N) よりも著しく変化した。アルギン酸塩/アラビアゴムビーズはアルギン酸塩/グリセロールビーズより、高いカプセル化効率及び低い膨潤能力を示した。SEM 結果は、アルギン酸塩/グリセロールビーズの表面にいくらの亀裂が存在し、比較的低い硬度及びカプセル化効率に致した。

第 5 章では、アルギン酸塩/アラビアゴムビーズの特徴を深く分析した。インビトロ放出システムにおける硬度、膨潤能力、ポリフェノール放出挙動、放出動力学及び貯蔵安定性を調べた。25%アラビアゴム (GA0.25) で配合した液体コアハイドロゲルビーズは、ポリフェノールが保存中に損失速度 (k) が $6.10 \times 10^{-3} \text{ day}^{-1}$ 、半減期 ($t^{1/2}$) が 113.63 日であり、模擬胃液におけるポリフェノールの放出が最も遅く、放出仕組がフィックの拡散に従うと分かった。

私が知っている限り、この論文は初めてのマイクロウェットミリング (第 2 章) を用い、大根副産物ジュースを作成することであり (第 2 章)、一回ゲル化時間、一回ゲル化における乳酸カルシウム濃度、二回ゲル化時間、二回ゲル化における乳酸カルシウム濃度という 4 つの自変数が液体コアハイドロゲルビーズの物理的特性に与える影響であり (第 3 章)、スフェリフィケーションを用い、アルギン酸塩とアラビアゴム又はグリセロールとを組み合わせ、液体コアハイドロゲルビーズの作成 (第 4 章)、更に、それらの物理的な特性、インビトロ放出挙動及び貯蔵安定性 (第 5 章) である。この研究がデリバリーシステムの開発と品質向上に役立つと考えておる。

Keywords

Liquid-core hydrogel bead

Reverse sphericity

Radish by-product

Micro wet milling system

In vitro release profile

Storage stability

Alginate

Gum arabic

Glycerol

Abbreviations

ANOVA: analysis of variance

CCD: central composite design

CL: calcium lactate

G-blocks: α -L-guluronic acid unit of alginate

LCM: liquid-core material

M-block: β -D-mannuronic acid unit of alginate

RSM: response surface methodology

RSREG: response surface regression

Contents

Abstract	i
要旨	iii
Keywords	v
Abbreviations	v
Contents.....	vi
List of Tables	x
List of Figures	xii
1. General introduction	1
1.1. Encapsulation	1
1.1.1. Hydrogel beads.....	1
1.1.2. Crosslinking in hydrogels.....	4
1.2. Alginate	5
1.3. Spherification	5
1.3.1. Basic spherification	8
1.3.2. Reverse spherification	8
1.4. Radish by-product	10
1.5. Structure of the thesis	15
2. Preparation of radish by-product juice by micro wet milling system.....	17
2.1. Introduction	17
2.2. Objectives	19
2.3. Materials and methods.....	19
2.3.1. Materials.....	19
2.3.2. Micro wet milling processing.....	21
2.3.3. Particle size.....	21

2.3.4. Statistical analysis	21
2.4. Results and Discussion	21
2.4.1. Particle size and particle distribution	21
2.5. Conclusions	23
3. Optimization of liquid-core hydrogel bead prepared by reverse spherification	24
3.1. Introduction	25
3.2. Objectives	27
3.3. Materials and methods	27
3.3.1. Materials	27
3.3.2. Formulation of liquid-core hydrogel beads	28
3.3.3. Average diameter and sphericity	29
3.3.4. Hardness	29
3.3.5. Encapsulation efficiency	29
3.3.6. <i>In vitro</i> release profile	31
3.3.7. Swelling capacity	32
3.3.8. Experimental design and data analysis	32
3.4. Results and Discussion	34
3.4.1. Average diameter	34
3.4.2. Hardness	37
3.4.3. Encapsulation efficiency	40
3.4.4. <i>In vitro</i> release experiment	43
3.4.5. Swelling capacity	48
3.4.6. Sphericity	51
3.4.7. Optimization of the liquid-core hydrogel bead	54
3.5. Conclusions	58
4. Physical properties of liquid-core hydrogel beads with gum arabic and glycerol	60

4.1. Introduction	61
4.2. Objectives	62
4.3. Materials and methods.....	63
4.3.1. Materials	63
4.3.2. Formulation of liquid-core hydrogel bead.....	63
4.3.3. Average diameter and sphericity	64
4.3.4. Hardness	64
4.3.5. Encapsulation efficiency	64
4.3.6. Swelling capacity	64
4.3.7. Differential scanning calorimetry.....	64
4.3.8. Morphology	65
4.3.9. Statistical analysis	65
4.4. Results and Discussion	65
4.4.1. Average diameter	65
4.4.2. Sphericity.....	67
4.4.3. Hardness	67
4.4.4. Encapsulation efficiency	68
4.4.5. Swelling capacity	70
4.4.6. Microstructure	70
4.5. Conclusions	72
5. Release behavior improvement of liquid-core hydrogel beads with gum arabic	74
5.1. Introduction	75
5.2. Objectives	76
5.3. Materials and methods.....	76
5.3.1. Materials	76
5.3.2. Formulation of alginate/gum arabic bead and storage test.....	76

5.3.3. Total phenolic content	77
5.3.4. Antioxidant ability	77
5.3.5. <i>In vitro</i> release profile and release kinetic.....	78
5.3.6. Hardness	78
5.3.7. Swelling capacity	78
5.4. Results and Discussion	80
5.4.1. Loss of total phenolic compounds.....	80
5.4.2. Antioxidant activity	80
5.4.3. <i>In vitro</i> release profile and kinetics	85
5.4.4. Hardness	88
5.4.5. Swelling capacity	89
5.5. Conclusions	91
6. Conclusions and future prospective.....	92
References	94

List of Tables

Table 1-1 Methods for preparation of microcapsules.....	2
Table 1-2 Summary of the characteristics of common microencapsulation technologies.	3
Table 1-3 Nutrition information of Japanese radish (amounts per 100 g).....	11
Table 1-4 Typical Japanese radish cultivars and their characteristic.....	12
Table 3-1 Independent variables in the central composite design for the preparation of liquid-core hydrogel bead.....	30
Table 3-2 Central composite design for liquid-core hydrogel bead.	33
Table 3-3 Experimental results of average diameter.	35
Table 3-4 Regression coefficients of the fitted quadratic equations for average diameter.....	35
Table 3-5 Summary of ANOVA for average diameter.	36
Table 3-6 Experimental results of hardness (Y_1) for different formulations of the liquid-core hydrogel bead.....	38
Table 3-7 Regression coefficients of the fitted quadratic equations for hardness (Y_1).....	38
Table 3-8 Summary of ANOVA for hardness (Y_1).....	39
Table 3-9 Experimental results of encapsulation efficiency (Y_2) for different formulations of the liquid-core hydrogel bead.	41
Table 3-10 Regression coefficients of the fitted quadratic equations for encapsulation efficiency (Y_2).	41
Table 3-11 Summary of ANOVA for encapsulation efficiency (Y_2).....	42
Table 3-12 Experimental results of the release profile of total phenolic compounds in simulated gastric digestion (Y_3) and simulated intestinal digestion (Y_4).....	44
Table 3-13 Regression coefficients of the fitted quadratic equations for the release profile of total phenolic compounds in simulated gastric digestion (Y_3) and simulated intestinal digestion (Y_4).....	45

Table 3-14 Summary of ANOVA for the release profile of total phenolic compounds in simulated gastric digestion (Y ₃) and simulated intestinal digestion (Y ₄).....	46
Table 3-15 Experimental results of swelling capacity (Y ₅) for different formulations of the liquid-core hydrogel bead.....	49
Table 3-16 Regression coefficients of the fitted quadratic equations for swelling capacity (Y ₅).	49
Table 3-17 Summary of ANOVA for swelling capacity (Y ₅).....	50
Table 3-18 Experimental results of sphericity (Y ₆) for different formulations of liquid-core hydrogel bead.....	52
Table 3-19 Regression coefficients of the fitted quadratic equations for sphericity (Y ₆)	52
Table 3-20 Summary of ANOVA for sphericity (Y ₆).....	53
Table 3-21 Optimum conditions for the preparation of the liquid-core hydrogel bead.	55
Table 4-1 Formulation of alginate/gum arabic and alginate/glycerol bead.....	66
Table 4-2 Average diameter of alginate/gum arabic and alginate/glycerol beads.....	66
Table 4-3 Sphericity of alginate/gum arabic and alginate/glycerol beads.	66
Table 4-4 Hardness of alginate/gum arabic and alginate/glycerol beads.	69
Table 4-5 Encapsulation efficiency of alginate/gum arabic and alginate/glycerol beads.	69
Table 4-6 Swelling capacity of alginate/gum arabic and alginate/glycerol beads.	69
Table 5-1 Release mechanism from polymeric delivery system.....	79
Table 5-2 Kinetic parameters for total phenolic compounds change during storage.	81
Table 5-3 Kinetic parameters for DPPH scavenging ability change during storage.....	84
Table 5-4 Kinetic parameters for total phenolic compounds release from alginate/gum arabic beads in an <i>in vitro</i> digestion system.	87

List of Figures

Figure 1-1 The structure of sodium alginate.	6
Figure 1-2 The structure of guluronic chains and mannuronate chains.....	6
Figure 1-3 The multiple-step binding of calcium ion to alginate.....	7
Figure 1-4 Gelation mechanism of basic and reverse spherification.	9
Figure 1-5 Typical Japanese radish.	14
Figure 2-1 Micro wet milling system.	18
Figure 2-2 Pretreatment of radish by-product.	20
Figure 2-3 Effect of rotation on the particle size of radish by-product juice.	22
Figure 3-1 Liquid-core hydrogel bead preparation via reverse spherification.....	26
Figure 3-2 Two-dimensional corresponding contour plot for average diameter.	36
Figure 3-3 Two-dimensional corresponding contour plot for hardness	39
Figure 3-4 Two-dimensional corresponding contour plot for encapsulation efficiency (Y_2). .	42
Figure 3-5 Two-dimensional corresponding contour plot for the release profile of total phenolic compounds in simulated gastric digestion (Y_3) and simulated intestinal digestion (Y_4).	47
Figure 3-6 Two-dimensional corresponding contour plot for swelling capacity (Y_5).	50
Figure 3-7 Two-dimensional corresponding contour plot for sphericity (Y_6).....	53
Figure 3-8 Overlay plot indicating the region of optimal process variable settings.	57
Figure 4-1 Microstructure of alginate/gum arabic and alginate/glycerol beads ($\times 500$).....	71
Figure 5-1 The amount of total phenolic compounds of alginate/gum arabic beads during storage.....	79
Figure 5-2 Total phenolic compounds loss kinetic during storage.....	81
Figure 5-3 DPPH scavenging activity of alginate/gum arabic beads during storage.....	83
Figure 5-4 DPPH scavenging activity reducing kinetic during storage.	83

Figure 5-5 The correlation between DPPH scavenging activity and total phenolic compounds amount. 84

Figure 5-6 Total phenolic compounds release from alginate/gum arabic beads in an *in vitro* digestion system..... 87

Figure 5-7 Hardness of alginate/gum arabic beads in an *in vitro* digestion system. 90

Figure 5-8 Swelling capacity of alginate/gum arabic beads in an *in vitro* digestion system. .. 90

1. General introduction

1.1. Encapsulation

In recent years, novel methods for delivering bioactive substances with natural, biocompatible, and biodegradable polysaccharides have been developed. Encapsulation is a technique where the coating or embedding materials surround a specific compound into a matrix, producing small capsules with many properties. This technique has been used for many years in the pharmaceutical industry to design delivery systems, and in the food industry to protect functional components (Li, Hu, Du, Xiao, & McClements, 2011). Table 1-1 and Table 1-2 shows the common encapsulation technologies and their characteristics, respectively.

1.1.1. Hydrogel beads

Hydrogel beads are often termed as hydrocolloid gel particles or hydrogel particles, and have been used widely in fields such as food technology, biotechnology, medical and pharmaceutical sciences, and waste treatment, with objectives such as treatment of waste water, enzyme immobilization, drug delivery and controlled release, and covering bad flavors of ingredients (Belščak-Cvitanović et al., 2015; Burey, Bhandari, Howes, & Gidley, 2008; Luo, Chen, & Wang, 2005). The utilization of hydrogel particles, capsules or microcapsules which could be produced entirely by edible biopolymers such as proteins and polysaccharides, to deliver functional compounds and drugs has attracted attention for decades (Li et al., 2011).

The wall material of hydrogel bead plays an important role in protecting the core and controlling its release (Trugo & Finglas, 2003). Much attention has been focused on hydrogel bead formed by food-grade biopolymers as a delivery system to protect and encapsulate some food ingredients, drugs, and bioactive compounds and/or control their release behavior (Gouin, 2004; Matalanis, Jones, & McClements, 2011). Hydrogel beads composed of alginate have been reported for the delivery of bioactive substance, drugs, and food ingredients in the

Table 1-1 Methods for preparation of microcapsules

Mechanism	Method
Physical methods	Spray drying
	Spray chilling
	Spray cooling
	Fluid bed coating (spray coating in fluidized bed)
	Extrusion
	Multiorifice centrifugal extrusion
	Cocrystallization
Freeze drying	
Chemical methods	Molecular inclusion (inclusion complexation)
	Interfacial polymerization
Physicochemical methods	Coacervation (aqueous phase separation)
	Organic phase separation
	Liposome

(Shahidi & Han, 1993)

Table 1-2 Summary of the characteristics of common microencapsulation technologies.

		Fluidized bed	Coacervation	Spray drying	Spray cooling	Spinning disk	Liposome entrapment
Nature of the ingredient	Hydrophilic	Light Gray	Dark Gray	Black	Light Gray	Light Gray	Light Gray
	Lipophilic	Light Gray	Light Gray	Light Gray	Black	Black	Light Gray
	Amphiphilic	Light Gray	Dark Gray	Dark Gray	Dark Gray	Dark Gray	Light Gray
	Solid	Light Gray	Light Gray	Dark Gray	Light Gray	Light Gray	Black
	Liquid	Black	Light Gray	Light Gray	Dark Gray	Dark Gray	Light Gray
	>100 μm	Light Gray	Light Gray	n/a	Light Gray	Light Gray	n/a
	<100μm	Black	Light Gray	White	Light Gray	Light Gray	White
Cost-in-use*		Med	High	Low	Lowest	Med	High
Production capacity	Batchwise	1T	0.5T				
	Continuous			2T/h	5T/h	1T/h	0.5T/h
Controlled release mechanism	Thermal	Light Gray	Light Gray	Light Gray	Light Gray	Light Gray	Light Gray
	Time	Light Gray	Light Gray	Dark Gray	Light Gray	Light Gray	Light Gray
	Mechanical	Dark Gray	Light Gray	Dark Gray	Dark Gray	Dark Gray	Black
	Digestion	Light Gray	Light Gray	Black	Black	Black	Black



(Gouin, 2004)

* Cost-in-use: the cost of owning, running, or using something (“CollinsDictionary.com,” 2017)

pharmaceutical, biotechnology, and food technology fields due to their ability to control release, cover bad flavors, and protect active molecules from environmental conditions such as heat, light, enzymes, and oxygen. (Belščak-Cvitanović et al., 2015; Jantrawut, Assifaoui, & Chambin, 2013; Lupo, Maestro, Gutiérrez, & González, 2015).

1.1.2. Crosslinking in hydrogels

Crosslinking is the main step which gives hydrophilic polymers (wall materials) the ability to deliver and protect core material because it results in the following physical changes of polymer (Maitra & Shukla, 2014):

- A. Elasticity decrease or increase
- B. Viscosity decrease
- C. Hydrophobicity of the polymer
- D. Lower melting point and higher glass transition temperature
- E. Increase in polymer strength and toughness
- F. Thermoplastic change to thermoset plastics

Crosslinkings can be classified into chemical and physical crosslinking based on their gelation mechanism. Chemical crosslinking is an efficient method for improving the mechanical property by connecting polymers with covalent binding (Connell, 1975); however, some toxic crosslinker could resulting in detrimental consequences to the environment. Physical crosslinking involves ionic interaction, stereocomplex formation, protein interaction, hydrogen bond, and crystallization (Liang et al., 2011; Nguyen & West, 2002). The use of physical crosslinking techniques such as an ionotropic gelation are attracting attention because the techniques are simple, gentle, and undesirable effects and possible toxicity arising from crosslink reagents during chemical crosslinking can be avoided (A. K. Nayak, Das, & Maji, 2012; A. K. Nayak, Pal, & Santra, 2016).

1.2. Alginate

Alginate is a natural anionic linear polysaccharide derived from algae, and is composed randomly of (1-4)-linked β -D-mannuronate (M residues) and α -L-guluronate units (G residues) and divided into homopolymeric blocks (G- and M-blocks) and heteropolymeric blocks (MG-blocks) (Mohy Eldin, Kamoun, Sofan, & Elbayomi, 2014; Pawar & Edgar, 2012) (Figure 1-1). G residues result in the strengthening and stiffness of the polysaccharide, while M residues provide flexibility and elasticity (Jost, Kobsik, Schmid, & Noller, 2014; Zhao, Hu, Evans, & Harris, 2011) (Figure 1-2). Therefore, the M/G ratio has a major impact on alginate gelation characteristics. It is a biodegradable, low-cost, biocompatible, and non-immunogenic biopolymer that is generally regarded as safe (GRAS) by the FDA.

Some multivalent cations such as Ca^{2+} , Ba^{2+} , Zn^{2+} , Cd^{2+} , and Al^{3+} (crosslink agents), can combine with G residues by a ionotropic gelation (Figure 1-3). These cations replace sodium ions in alginate polymer and form an egg-box dimers. Egg-box dimers further aggregate and compose egg-box multimers (Fang et al., 2007; George & Abraham, 2006; A. K. Nayak et al., 2012; Sinha, Ubaidulla, Hasnain, Nayak, & Rama, 2015) (Figure 1-3). Ionotropically gelled alginate is a pH-sensitive polymer that shrinks in acidic conditions and swells in a high-pH environment (Wang, Zhang, & Wang, 2009). This characteristic makes alginate widely used for the delivery of proteins, drugs, and probiotics, protecting these compounds from destruction by stomach fluid (Cai et al., 2014; Mohy Eldin et al., 2014).

1.3. Spherification

Spherification is a technique used in avant-garde and modernist cuisine, which was invented by Peschardt in 1946 and carried forward by elBulli, one of the most distinguished restaurants in the world. It is a technique where a liquid material is coated by a polymer film, forming a sphere with a liquid core (Fu et al., 2014; Hoffman, 2009; Lee & Rogers, 2012). For many years, the use of the term spherification has been limited to the field of cooking, I consider it an adequate

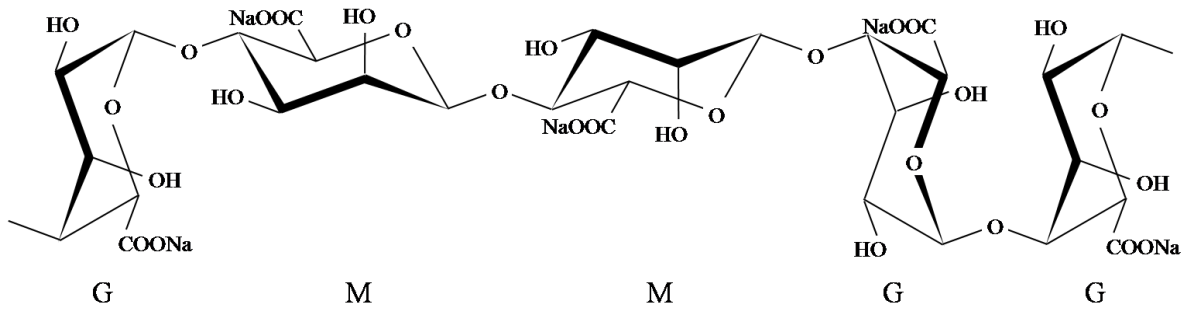
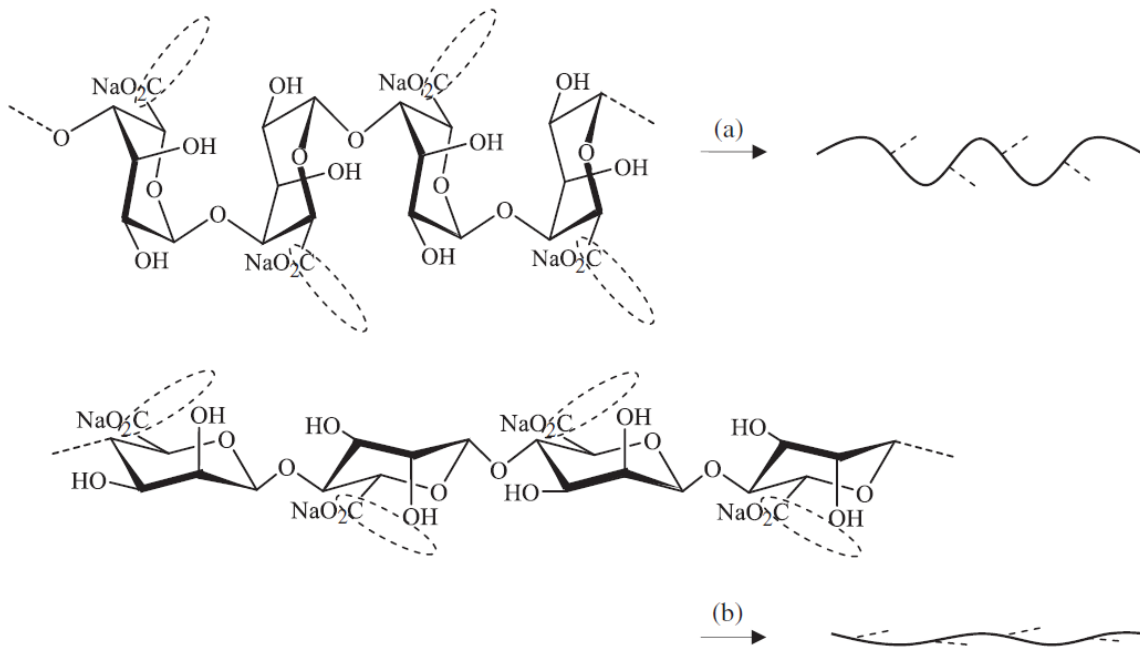


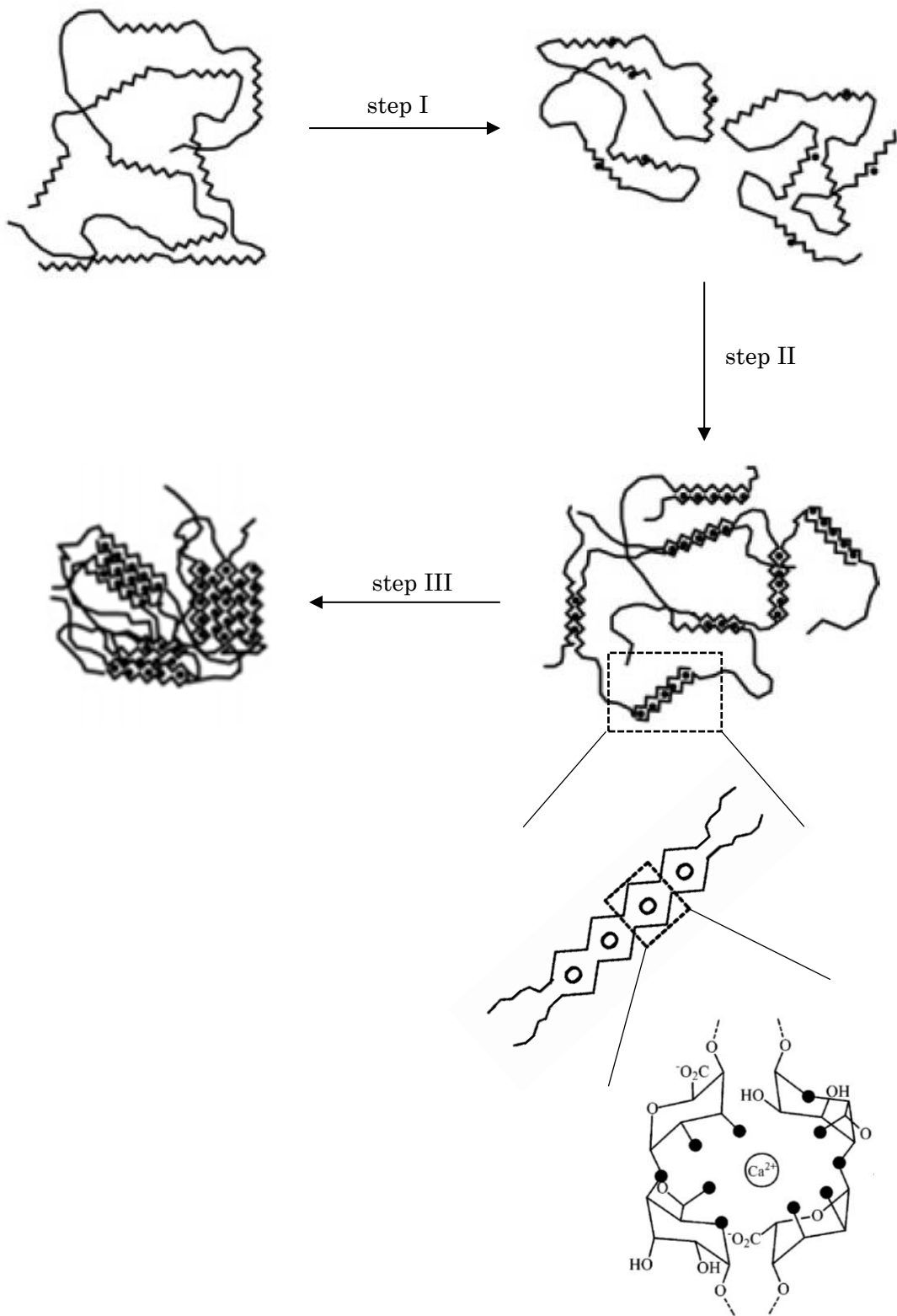
Figure 1-1 The structure of sodium alginate.



(Zhao et al., 2011)

Figure 1-2 The structure of guluronicate chains and mannuronate chains.

(a) Guluronicate chains; (b) Mannuronate chains



(Fang et al., 2007).

Figure 1-3 The multiple-step binding of calcium ion to alginate.

term to be used in other fields such as food technology since it accurately captures the formation of the hydrogel bead. The hydrogel bead which prepared by spherification has a liquid center, it is named liquid-core hydrogel bead. Liquid-core hydrogel beads are formed by a droplet surrounded by a thin layer of membrane. In a cell delivery system, liquid-core allows cells to grow to a greater and uniform density (K. Koyama & Seki, 2004).

Depending on the preparing method, spherification techniques can be divided into two types: basic spherification and reverse spherification.

1.3.1. Basic spherification

Basic spherification is a well-known and tradition method for forming hydrogel particles by mixing drugs, food ingredients, or bioactive substances with an ionic biopolymer (ex: alginate) and dropping the mixture into a multivalent cation (ex: Ca^{2+}) solution. The osmotic gradient between the mixture droplet and calcium solution causes the cation to permeate into the droplet. Ionotropic gelation occurs from the surface to inside the droplet, creating the outer layer of the beads (Figure 1-4a).

However, the process cannot be used to encapsulate compounds or materials which have low pH or low polarity, for example, acid or alcoholic solutions, because they would cause alginate gelation to occur before the alginate combines with calcium ions. Thus, the modification of basic spherification is necessary.

1.3.2. Reverse spherification

In reverse spherification, specific compounds mix with the calcium solution and then inject into alginate, causing calcium ions to diffuse from the calcium solution to the surrounding alginate, and a calcium alginate outer layer is formed (Figure 1-4) (Lee & Rogers, 2012). Because most of functional compounds or medicine components can be mixed with calcium solution, easily, the reverse spherification can be used to encapsulate a wider range of ingredients than basic

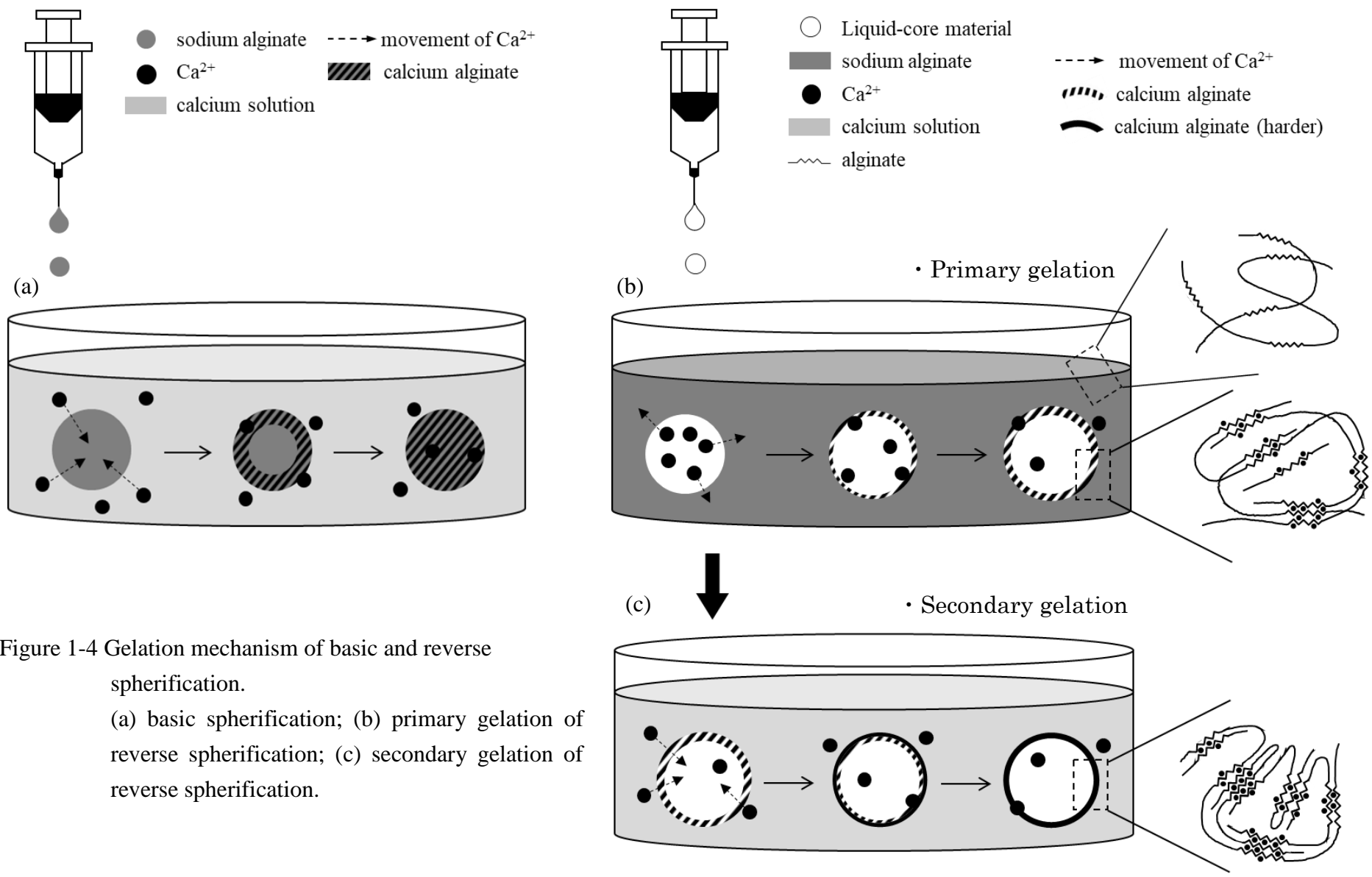


Figure 1-4 Gelation mechanism of basic and reverse spherification.
 (a) basic spherification; (b) primary gelation of reverse spherification; (c) secondary gelation of reverse spherification.

spherification.

The procedure of reverse spherification is separated into two steps:

Primary gelation is a step of outer layer formation (Figure 1-4b). The step occurs when the core material, a mixture of cation and a specific compound, is extruded into the alginate solution. The osmotic gradient between the droplet and alginate solution causes the calcium ions to diffuse from the droplet to the surrounding alginate. When G-blocks are coordinated with calcium ions, a water insoluble calcium alginate outer layer is formed. The thickness of the coating layer increases with time until the osmotic pressures are balanced. Afterward, the semifinished beads are moved to an ion solution again for an additional hardening, and this step is called secondary gelation.

Secondary gelation (Figure 1-4c), where cation permeates into the network of outer layer. Cation fills into the G blocks that were not combined with cation in primary gelation. The stability of outer layer is increased and hardness of liquid-core hydrogel bead is strengthened.

1.4. Radish by-product

Radish (*Raphanus sativus* L.) is consumed with pickled, dried, cooked, and raw forms in Asia, European, and America (Mowlick et al., 2014). Japanese radish, or daikon, is one of the most popular varieties of radish in East Asia and is rich in vitamin C, folate, potassium, dietary fiber, and has low calorie (Table 1-3) (SELFNutritionData, 2014). Over 100 varieties of Japanese radish have been cultivated year-round in Japan (Table 1-4 and Figure 1-5).

According to the statistics data of the Ministry of Agriculture, Forestry and Fisheries (MAFF) of Japan, about 1,362,000 tons of Japanese radish were harvested in 2016 (MAFF, 2017). The average top-root ratio (T/R ratio) of Japanese daikon is approximately 4 (Ohi & Isomura, 2000). T/R ratio is the ratio of the weight of the aerial part of the crop to the weight of the underground part. In other words, approximately 4 kg of leaf and stem are got when per kilogram Japanese daikon is produced, more than 5 million tons of leaf and stem, so-called by-products, were

Table 1-3 Nutrition information of Japanese radish (amounts per 100 g).

Calories	58.6 kJ	Protein	0.5 g
Water	95.4 g	Tryptophan	3.0 mg
Ash	0.8 g	Serine	16.5 mg
Total carbohydrate	2.6 g	Proline	14.0 mg
Dietary fiber	1.4 g	Glycine	17.0 mg
Total fat	0.1 g	Glutamic acid	104.0 mg
Saturated Fat		Aspartic acid	37.5 mg
16:00	26.0 mg	Alanine	17.0 mg
18:00	4.0 mg	Histidine	10.5 mg
Monounsaturated Fat		Arginine	32.0 mg
18:1 undifferentiated	16.0 mg	Valine	25.5 mg
Polyunsaturated Fat		Tyrosine	10.5 mg
18:2 undifferentiated	16.0 mg	Phenylalanine	18.0 mg
18:03	29 mg	Cystine	4.5 mg
Total Omega-3 fatty acids	29 mg	Methionine	5.0 mg
Total Omega-6 fatty acids	16.0 mg	Lysine	27.5 mg
Minerals		Leucine	29.0 mg
Calcium	27.0 mg	Isoleucine	24.0 mg
Iron	0.8 mg	Threonine	22.5 mg
Magnesium	9.0 mg	Vitamins	
Phosphorus	28.0 mg	Vitamin C	29 mg
Potassium	280 mg	Niacin	0.3 mg
Sodium	16.0 mg	Vitamin B6	0.1 mg
Zinc	0.1 mg	Folate	14.0 mcg
Copper	0.1 mg	Pantothenic Acid	0.2 mg
Selenium	0.7 mcg		

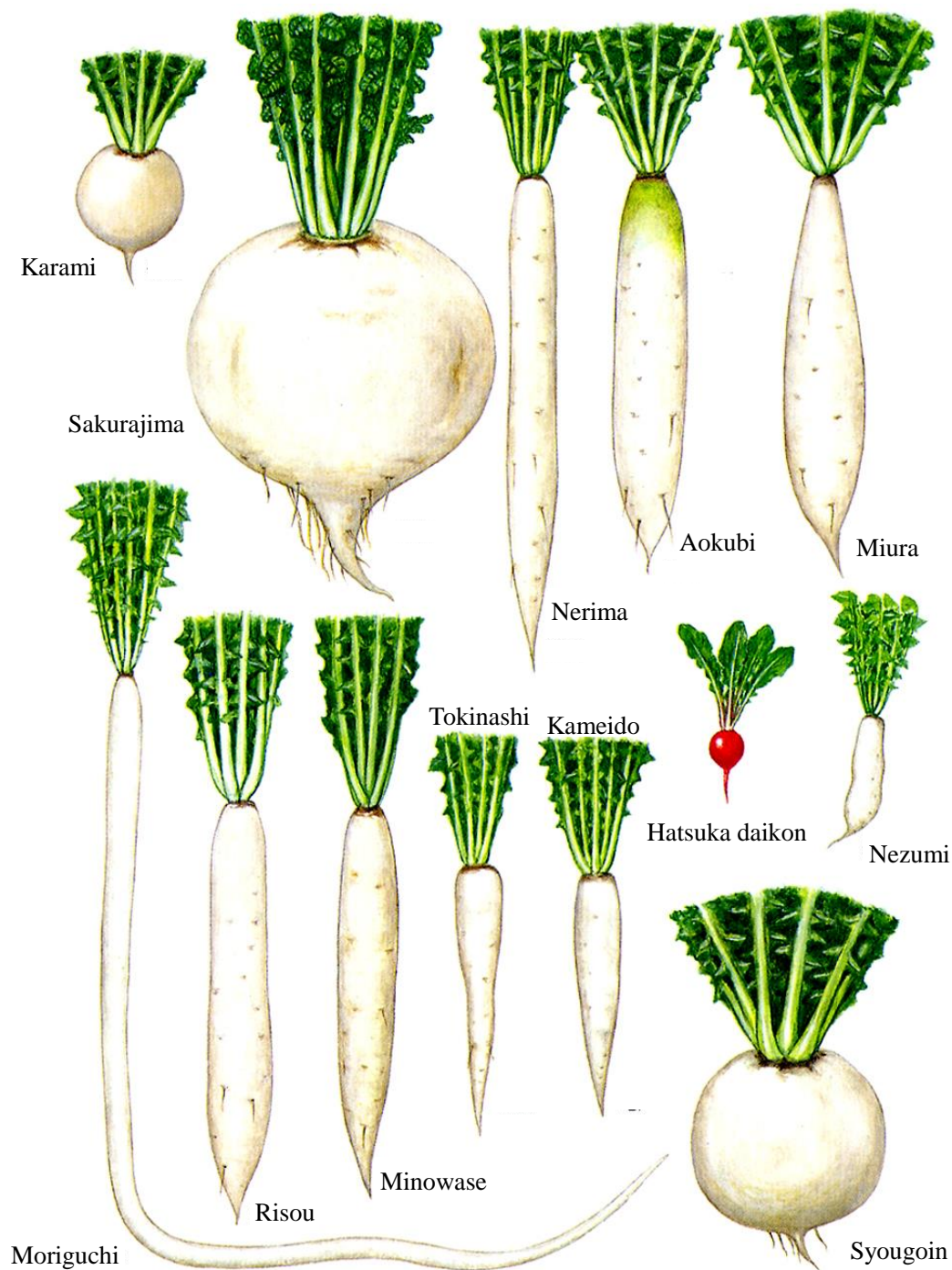
(SELFNutritionData, 2014)

Table 1-4 Typical Japanese radish cultivars and their characteristic.

Cultivar	Characteristic
Aokubi daikon	Aokubi means “green head” in Japanese. The mainstream variety of radish in Japan from the 1970's. It contains a lot of moisture, soft, sweet, and hard to collapse during cooking. The thickness is almost the same from the top to the bottom.
Miura daikon	It was a popular cultivar for preparing Oden in the past, which is rich in flavor; however, comparing to other cultivars, it is too bulky to arrange at the shop, only a small number of daikon can be planted in the same area, and the volume is so large that it is not easy to use by the consumers. It had been replaced by Aokubi daikon since the 1970's and hardly been seen now.
Syougoin daikon	Syougoin daikon is sweet and soft. It contains a lot of moisture and less fiber, is a perfect material for simmered or pickled food, for example, the traditional Kyoto pickles, Senmaidzuke.
Minowase daikon	The representative cultivar of daikon in summer. The growing season is long, from March to October, and can be harvested in 50 to 60 days after seeding. It is a popular cultivar because of the good appearance. It has a bitter taste with little sweetness and is suitable for simmering.
Nerima daikon	A preservation species with only small production, currently. It is characterized by the length of the root, as long as 70 cm, and the large spreading leaves. Because the low moisture content, it is mainly prepared as the pickled vegetables, Takuantsuke.

Cultivar	Characteristic
Kameido daikon	A small and elongated spindle radish which is cultivated in Tokyo with a low production. It has a sweet taste with a slight scent, and soft leaves. A delicious pickled vegetable can be made by pickling the Kameido daikon with its leaves.
Sakurajima daikon	The biggest radish in the world, the big one exceeds 20 kg. It has soft sweetness and its texture can be kept after a long boiling. Therefore, it is suitable for salad, simmered dishes, dried vegetables, and pickles.
Moriguchi daikon	The longest radish in the world, the length of the root is approximately 200 cm and the thickness is 2 cm. It is famous for the material of the pickle, Moriguchiduke.
Karami daikon	It is small radish, about 20 cm in length. The material of grated daikon and being used as condiments for the soba, tempura, and sashimi in a raw form.
Gensuke daikon	It is used for simmered dishes and pickles because it has little bitterness.
Hatsuka daikon	Hatsuka means 20 days in Japanese because it can be harvested in about 20 days. A spherical daikon with a diameter of 2 to 3 cm. Because of the crisp texture and beautiful color, it is widely used for the decoration of dishes and salad.

(Anonymous, 2015)



(Anonymous, 2017)

Figure 1-5 Typical Japanese radish.

created in 2016. Young leaves are cooked as the vegetable (Mowlick et al., 2014); however, the radish by-product is not accepted by most of the consumers due to the fuzz on the skin of the stem, and the pungent and bitter taste. Thus, a lot of residues is disposed of as waste after marketable parts are collected, which creates significant food waste for producers. Mowlick et al. (2014) suggest that radish by-product could be used as the material of biological soil disinfestation for controlling soilborne diseases. On the other hand, Okine et al. (2007) indicate that the by-product of radish contains a high amount of mineral salts, resulting in detrimental consequences when it returns to the soil; conversely, it is a good animal feed resource because it contains high crude protein and easily digestible nutrients.

According to the study of (Ohi & Isomura, 2000). However, they have an abundance of minerals and the content of phenolic compounds and flavonoids in leaves are approximately 2.0-fold and 3.9-fold that of their content in roots, which are the parts which are normally consumed (Goyeneche et al., 2015). The total flavonoid and phenol content of radish by-product is 100.8 mg/100 g and 52.48 mg/100 g, respectively (Kim, Park, Kim, Cho, & Chang, 2010). Studies have shown that radish leaves are natural antioxidants, and have anticancer properties and antihypertensive effects. Ingesting the radish leaf may increase antioxidant activities and the concentration of NO in the serum and concentration of Na⁺ in the fecal (Chung, Kim, Myung, Cho, & Chang, 2012).

1.5. Structure of the thesis

The aim of this study is encapsulating the radish by-product juice with a liquid-core hydrogel bead via reverse spherification.

In chapter 1, the background of this research is introduced.

In chapter 2, micro wet milling system was used to prepare a radish by-product juice, for reducing the particle size of radish by-product. In order to prepare the radish by-product with the smallest particle size, the optimal rotation rate of milling stone was analyzed

In chapter 3, I provided the first report on liquid-core hydrogel beads preparation with calcium lactate by reverse spherification, and is the first study which synthetically identified the effect of gelation time and calcium lactate concentration in first and secondary gelation on the physical properties and *in vitro* release behavior of the liquid-core hydrogel beads.

In chapter 4, I prepared liquid-core hydrogel bead from alginate combined with gum arabic or glycerol by reverse phase spherification, and evaluated physical properties of the alginate/gum arabic bead and alginate/glycerol bead and their out-layer.

In chapter 5, the characterizes of alginate/gum arabic bead were analyzed in depth. The change of hardness, swelling behavior, total phenolic compounds release behavior, and release kinetics of alginate/gum arabic bead in an *in vitro* digestion system were investigated. And then, the stability of stored total phenolic compounds, including their antioxidant ability and kinetics of total phenolic compounds loss, were examined.

In chapter 6, the conclusion of my research and some future plans of reverse spherification are given.

2. Preparation of radish by-product juice by micro wet milling system

2.1. Introduction

In the past few decades, the demand for functional food has increased considerably, and some novel ingredients with high functionality have been searched for. Recently, much attention has been devoted to the recycling of harvest by-products and wastes during harvesting and processing. This work used radish by-product juice as the ingredient.

Japanese radish, or daikon (*Raphanus sativus* L.), is one of the most popular varieties of radish in East Asia and is rich in vitamin C, folate, potassium, dietary fiber, and has low calorie (SELFNutritionData, 2014). About 1,362,000 tons of radish were harvested in 2016 (MAFF, 2017) and approximately 5 million tonnes of by-product, the leaf and stem, was created. After commercial parts are collected, most of by-product of radish are disposed of as waste.

However, they have an abundance of minerals, crude protein and the content of phenolic compounds and flavonoids in leaves are approximately 2.0-fold and 3.9-fold that of their content in roots, which are the parts which are normally consumed (Goyeneche et al., 2015). The total flavonoid and phenol content of radish by-product are 100.8 mg/100 g and 52.48 mg/100 g, respectively (Kim et al., 2010). Studies have shown that radish leaves are natural antioxidants, and have anticancer properties and antihypertensive effects. Ingesting the radish leaf may increase antioxidant activities and the concentration of NO in the serum and concentration of Na⁺ in the fecal (Chung et al., 2012). Young leaves are cooked as vegetable; however, the radish by-product is not accepted by most of consumers due to the fuzz on the skin of the stem, and the bitter and strong taste. Thus, a lot of residue including the leaf and stem are disposed as waste during harvesting and processing every year, which creates significant food waste for producers.

Micro wet milling system is a micronization processing which reduces particle size to a micrometer scale by the shear and frictional stress between two milling stones (Figure 2-1). The

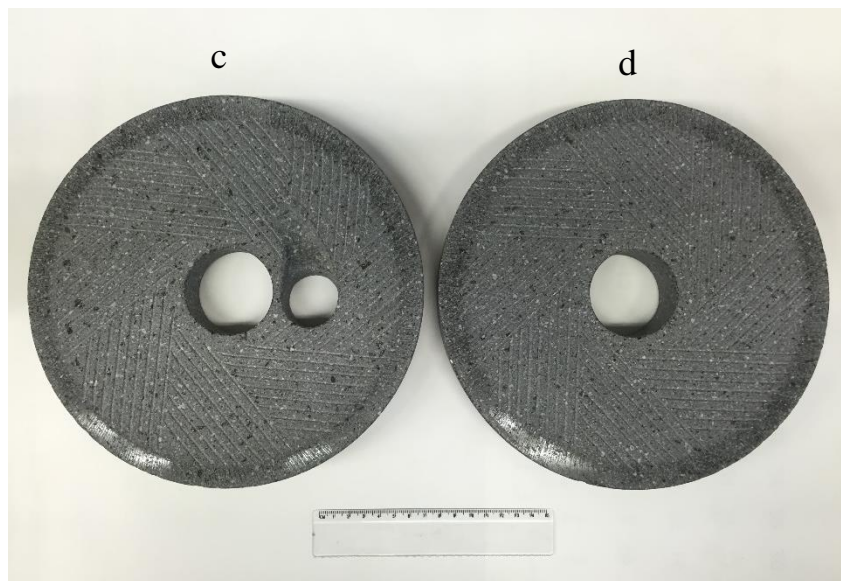
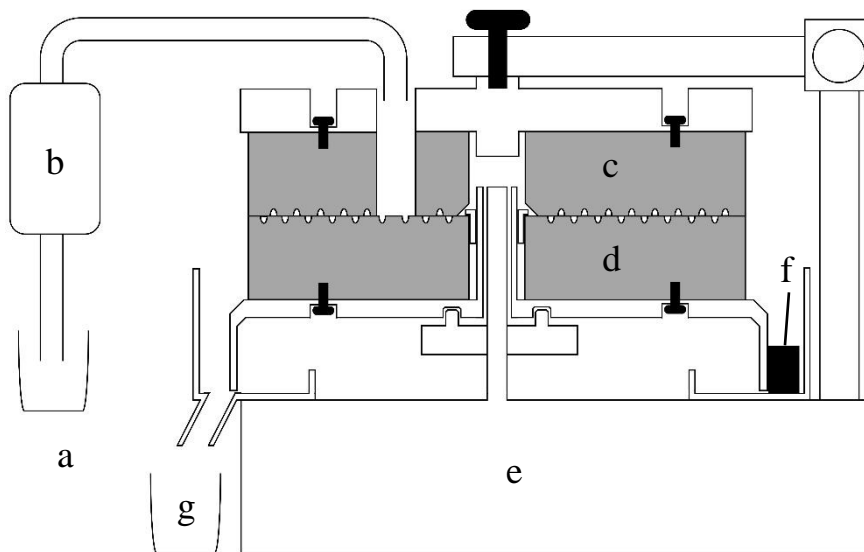


Figure 2-1 Micro wet milling system.

- (a) Sample; (b) Tubing Pump; (c) Upper milling stone; (d) Lower milling stone;
 (e) Motor; (f) Rubber spatula; (g) Sample receiver.

upper milling stone was fixed on the system and the lower milling stone connected with a rubber spatula was rotated by an electric motor. There are no grooves on the edge of milling stones and the gap between milling stones approaches zero; therefore, the mixture will not drain out of the milling stones until the particle size reaches micrometer scale (M. Koyama & Kitamura, 2014). Comparing to a traditional blender, the sample is milled with a relatively lower rotation speed by the micro wet milling system (the maximum rotation is 50 rpm), the temperature of sample doesn't increase during milling processing, thus, less nutritional compounds degrade (中村, 2016). Some studies indicated that the functional compound could be released efficiently with the reduction of particle size of the fruit tissue and the orange juice, which was prepared micro wet milling system, had a higher content of ascorbic acid, total polyphenol, and total flavonoid as well as a higher antioxidant ability than the commercial orange juice (Islam, Kitamura, Kokawa, Monalisa, et al., 2017; Stinco et al., 2012).

2.2. Objectives

The leaves and stems of radish is a potential ingredient of functional food. However, the fuzzy texture is not accepted by most of the consumer. Micro wet milling system was used to prepare a radish by-product juice, for reducing the particle size of radish by-product. The optimal rotation rate, which could prepare the radish by-product with the smallest particle size, of milling stone was analyzed in this part.

2.3. Materials and methods

2.3.1. Materials

Radish leaves were obtained from a local farmer. Following washing and cutting, the leaves were stored at -20°C (Figure 2-2).



(a)



(b)



(c)



(d)



(e)



(f)

Figure 2-2 Pretreatment of radish by-product.

- (a) Radish leaf and stem; (b) Washing; (c) Removing the water on the surface;
(d) Cutting; (e) Mixing; (f) Packaging.

2.3.2. Micro wet milling processing

Radish by-product juice was produced by micro wet milling system (Figure 2-1). The lower milling stone connected with a rubber spatula was rotated by an electric motor at 10 to 50 rpm. Radish leaves and distilled water were initially mixed at a ratio of 1:2 by a blender (SBC-1000J, Cuisinart, Ualginate) for 1 min at approximately 15,000 rpm. The sample was fed into micro wet milling system by a tubing pump at 10 mL/min.

2.3.3. Particle size

The particle size of radish by-product juice was analyzed with a laser particle size analyzer at room temperature (alginatELD-2200, Shimadzu, Japan). A wet measurement model was performed with a humidity of 60 %.

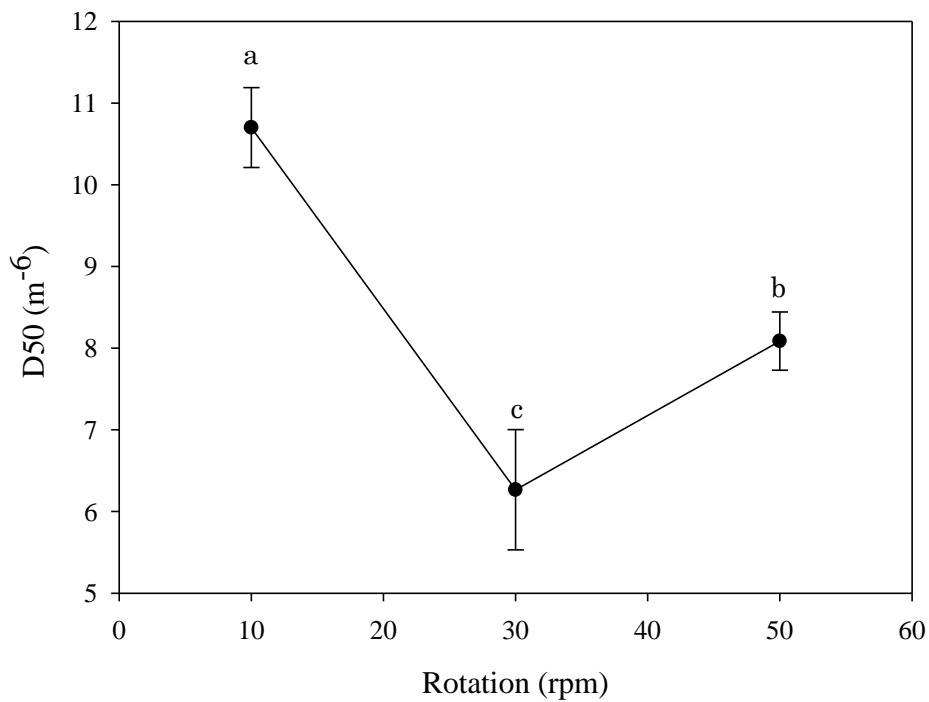
2.3.4. Statistical analysis

All experiments were run at least in triplicate. The results were presented as the mean \pm standard deviation and analyzed using Statistical Analysis System software (Version 8.01, alginatES Institute Inc., Ualginate). One-way analysis of variance (ANOVA), followed by Duncan's multiple comparison test, was performed. Responses with p values <0.05 were considered significant.

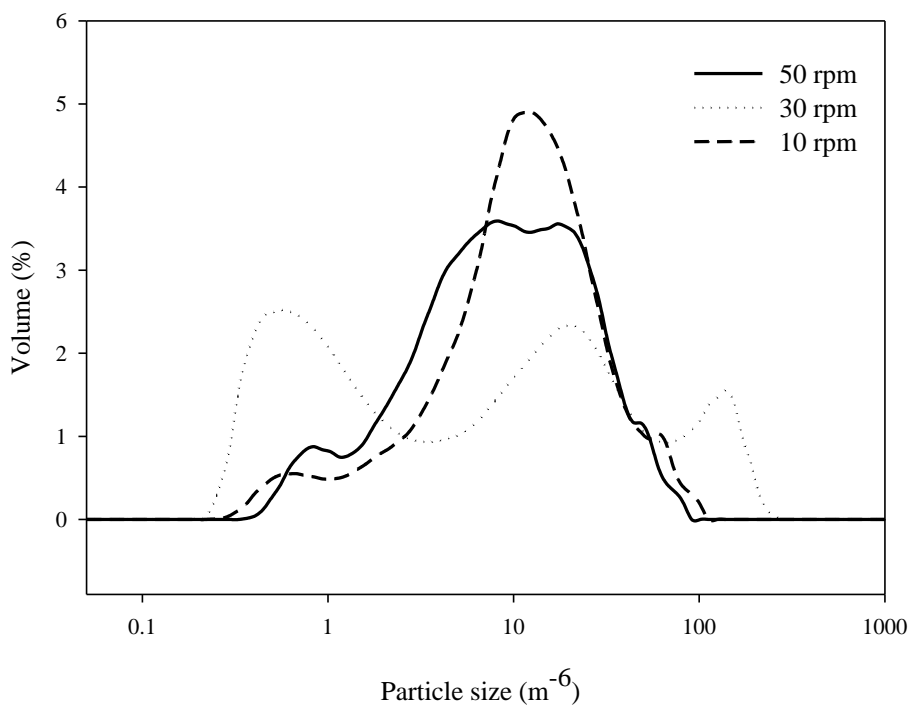
2.4. Results and Discussion

2.4.1. Particle size and particle distribution

The particle size is expressed using D50. D50 means the median value of the particle size and the median value shows the point where half of particles above and half of them below this value. Figure 2-3 shows that the D50 of radish by-product juice decreased and then increased with the increase of rotation from 10 to 50 rpm. The lowest D50 was obtained (6.63 μ m) with a rotation of 30 rpm. The rotation speed effects on the feeding rate and delivery rate of the



(a)



(b)

Figure 2-3 Effect of rotation on the particle size of radish by-product juice.

(a) D50; (b) Particle size distribution.

sample, the milling processing speeds up, where indicates a shorter time was taken from the sample is fed to it is delivered, with a higher rotation of milling stone. Meanwhile, the shear and frictional stress between two milling stones is larger. I inferred that a lower rotation speed (10 rpm) required a longer milling processing, where the tissue of radish by-product was smashed, properly; however, the relatively weaker milling force was provided. On the other hand, a stronger milling force was provided when rotation speed increased (50 rpm), but the sample stayed in the micro wet system in the relatively shorter time, the tissue of radish by-product couldn't be smashed properly.

2.5. Conclusions

According to the result of this part, the particle size of radish by-product juice was approximately 6.63 μm to 9.84 μm after being milled with micro wet milling system, and the lowest D50 was obtained with a rotation of 30 rpm. Because the functional compound could be released efficiently with the reduction of particle size of the fruit tissue, I will use the condition to prepare the radish by-product juice in the following part.

3. Optimization of liquid-core hydrogel bead prepared by reverse spherification

Liquid-core hydrogel beads were formulated through reverse spherification, by sodium alginate and using calcium lactate to replace the common calcium source, calcium chloride. The effect of four independent variables: primary gelation time (X_1), calcium lactate concentration in primary gelation (X_2), secondary gelation time (X_3), and calcium lactate concentration in secondary gelation (X_4), on seven physical properties of liquid-core hydrogel bead: average diameter, hardness (Y_1), encapsulation efficiency (Y_2), release profile of total phenolic compounds in simulated gastric (Y_3) and small intestinal (Y_4) digestion, swelling capacity (Y_5), and sphericity (Y_6), were evaluated. Furthermore, a central composite design with response surface methodology was used for the optimization of liquid-core hydrogel bead properties. Y_1 to Y_6 , and the importance of the four independent variables to physical properties was analyzed. The average diameter of liquid-core hydrogel bead was in the range of 4.17 to 5.84 mm. The optimal conditions of liquid-core hydrogel bead formulation were primary gelation time of 23.99 min, 0.13 M of calcium lactate in the primary gelation, secondary gelation time of 6.04 min, and 0.058 M of calcium lactate in secondary gelation. The optimized formulation of liquid-core hydrogel bead demonstrated 25.5 N of hardness, 85.67 % of encapsulation efficiency and 27.38 % of total phenolic compounds release in simulated gastric digestion with the small error-values (-2.47 to 2.21 %).

3.1. Introduction

Hydrogel bead is a type of encapsulation, which has been widely used for various purposes, such as: reduce the reactivity between the specific compound and environmental factors; to adjust the controlled-release ability of the core material; to make the material easier to handle; to change the appearance of materials; to cover bad flavors (Shahidi & Han, 1993). In this study, hydrogel bead was used to wrap the radish by-product juice, which contains rich nutrition, but is not accepted by most of consumers, due to the bitter and strong taste.

Reverse spherification is an encapsulation technique used to prepare liquid-core hydrogel beads with ionic biopolymers. Unlike basic spherification, during reverse spherification, food ingredients, or bioactive substances mix with cation solution and then inject into an ionic biopolymer solution (Schmidt, Bohn, Rasmussen, & Sutherland, 2012). On the other hand, basic spherification is processed by mixing food ingredients, or bioactive substances with an ionic biopolymer solution. Ionic biopolymer gelation may occur before the biopolymer reacts with cations, especially when the ingredients have low polarity and pH values. Thus, reverse spherification can be used to encapsulate a wider range of ingredients than basic spherification. The procedure of reverse spherification is separated into two steps (Figure 3-1). These steps were defined as primary gelation, the step of outer layer forming, and secondary gelation, the step of strengthening (Fu Hsuan Tsai, Chuang, Kitamura, Kokawa, & Islam, 2017). In the primary gelation, the core material, a mixture of ion and a specific compound, was suspended in an ionic biopolymer. Ions diffuse from the droplet into the surrounding ionic biopolymer, and an outer layer is formed. Afterward, the semifinished beads are moved to an ion solution again for an additional hardening, and this step was called secondary gelation.

Calcium lactate was used as a source of calcium ion, replacing calcium chloride, which is a common curing agent used in alginate gelation processing but tastes bitter, in this study (Neyraud & Dransfield, 2004). Previous studies indicated that calcium chloride combine rapidly with alginate; however, there was no significant difference between the hardness of

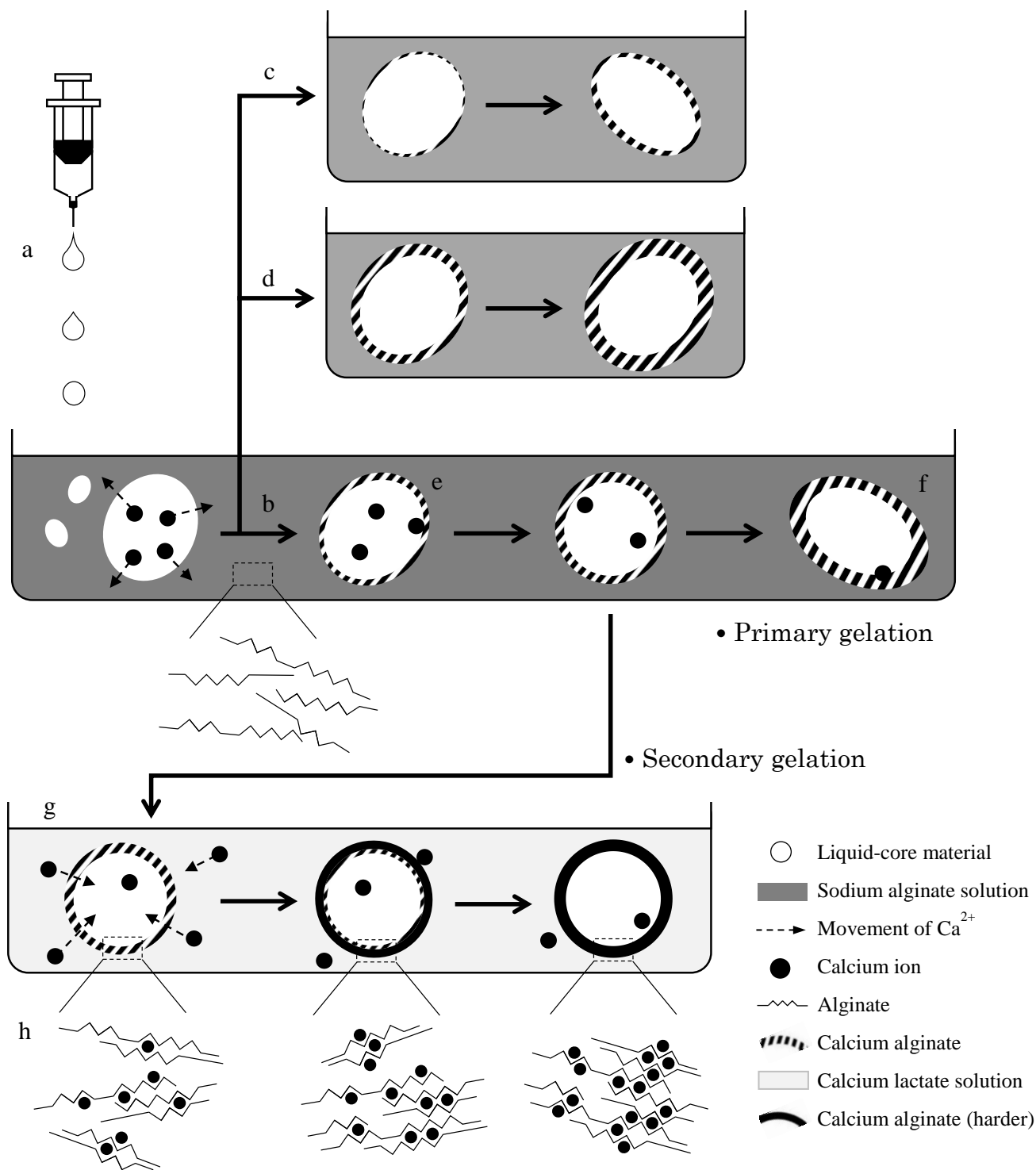


Figure 3-1 Liquid-core hydrogel bead preparation via reverse spherification.

(a) Droplets were extruded into sodium alginate solution with a hypodermic needle; liquid-core hydrogel bead was prepared with the (b) optimal calcium lactate concentration in primary gelation, (c) lower calcium lactate concentration in primary gelation, (d) higher calcium lactate concentration in primary gelation, (e) shorter primary gelation time, (f) longer primary gelation; (g) mechanism of secondary gelation; (h) the change of outer layer structure during secondary gelation.

beads which were produced by calcium chloride and calcium lactate (Lee & Rogers, 2012).

The optimal conditions for producing liquid-core hydrogel beads were investigated by the response surface methodology (RSM). RSM, a branch of experiment design, is a collection of statistical and mathematical techniques (Carley, Kamneva, & Reminga, 2004). It is used to describe the interrelation between independent and dependent variables, analyzing the influence and importance of independent variables to one or several dependent variables to improve a process and obtain an optimal response (Ji, Cho, Gu, & Kim, 2007; Šumić et al., 2016).

3.2. Objectives

The objectives of this part were to increase the palatability of radish by-products while retaining all of the functional compounds, and to prevent these functional compounds from releasing and being destroyed by stomach tract. To cover the bitter flavor of radish by-product juice, it was encapsulated by reverse spherification. This part provided the first report on liquid-core hydrogel beads preparation with calcium lactate by reverse spherification, and is the first study which synthetically identified the effect of four independent variables: primary gelation time, calcium lactate concentration in primary gelation, secondary gelation time, and calcium lactate concentration in secondary gelation, on the average diameter, hardness, encapsulation efficiency, release profile of total phenolic compounds in an *in vitro* release system, swelling capacity, and sphericity of the liquid-core hydrogel beads.

3.3. Materials and methods

3.3.1. Materials

Radish leaves were obtained from a local farmer and prepared as described in the section 2.3.1. All chemicals in the investigation were commercially available and of analytical grade. Sodium alginate, chitosan 100, acetic acid, calcium lactate, ethanol, sodium chloride (NaCl), hydrochloric acid (HCl), sodium carbonate (Na₂CO₃) were purchased from Wako Pure

Chemical Industries, Ltd. (Japan). The viscosity of a 1 % solution of sodium alginate was 80-120 m Pa · s at 20°C, the molecular weight was 1325 kDa, the percentage of guluronate content was 34.4 %, and guluronate–gulursodionate diad frequency was 18.9 % (Nakata, Kyoui, Takahashi, Kimura, & Kuda, 2016). The molecular weight of chitosan 100 was approximately 1.3×10^5 Da and the degree of deacetylation was 78 % (Bhattarai, Bahadur K.C., Aryal, Khil, & Kim, 2007). Pepsin (1:10,000, from porcine stomach mucosa) and pancreatin U.S.P. were purchased from MP Biomedicals, Inc. (Ualginate). Folin-Ciocalteu reagent was purchased from Merck Millipore Corporation (Ualginate).

3.3.2. Formulation of liquid-core hydrogel beads

Radish by-product juice was produced with a blender and the micro wet milling system as described in the section 2.3.2. The rotation of the lower milling stone was 30 rpm. The feeding rate of radish by-product juice was 10 mL/min.

Liquid-core hydrogel bead consists of the liquid-core and the outer layer. The liquid-core material was made by mixing 2 g chitosan, 1 mL acetic acid, and 1.23-6.17 g calcium lactate, and then adding radish by-product juice to achieve a final concentration of 0.04-0.2 M of calcium lactate solution. Chitosan was used as a thickener to modulate the viscosity and density of radish by-product juice for preventing the liquid-core being deformed by shear stress during primary gelation.

The preparation of liquid-core hydrogel bead was separated into the two steps of gelation. In the primary gelation, liquid-core material was extruded into 1% alginate solution through a 20G flat-tipped hypodermic needle with gentle stirring for 5 to 45 min. The semifinished beads were collected and washed with distilled water and 95 % ethanol, and then secondary gelation was carried out. In the secondary gelation, semifinished beads were suspended in 0 to 0.1 mole/L calcium lactate solution for 2 to 10 min, and then liquid-core hydrogel bead was prepared by collecting and rinsing these beads with distilled water and 95 % ethanol again. The process

variables and levels are shown in Table 3-1.

3.3.3. Average diameter and sphericity

Liquid-core hydrogel beads were recorded with a digital camera. The diameter of each variation was measured by ImageJ software (version 1.50i, National Institutes of Health, Ualginat) and the sphericity was calculated with the following equation:

$$\text{Sphericity} = (d_{max} - d_{min}) / (d_{max} + d_{min})$$

where d_{max} and d_{min} are the largest and the smallest diameters of the same bead, respectively (López Córdoba, Deladino, & Martino, 2013). A perfect sphere has a sphericity of 0, while a sphericity of 1 indicates a line (López Córdoba, Deladino, & Martino, 2013).

3.3.4. Hardness

A compression test was carried out with a texture analyzer (EZ-SX 100N C05 KIT, Shimadzu Ltd. Japan) at room temperature. A 25 mm cylinder probe was used to compress the liquid-core hydrogel bead with a test speed of 20.0 mm/min to 4 mm from the start position, when the probe stopped and returned to start position. The maximum force (N) of compression was represented as the hardness of the liquid-core hydrogel bead (Belščak-Cvitanović et al., 2015). The data were calculated and analyzed with TrapeziumX software (version 1.4.2, Shimadzu Ltd. Japan).

3.3.5. Encapsulation efficiency

Encapsulation efficiency was determined by the method of Gong et al. (2011) with some modifications. Liquid-core hydrogel beads were broken by a homogenizer (NS-52K, Microtec, Japan) at 10,000 rpm for 30 s with 10 mL 1% acetic acid. The samples were centrifuged at 4000 rpm for 5 min and the amount of total phenolic compounds in the supernatant was determined with Folin–Ciocalteu method (Goyeneche et al., 2015) as follows: 0.5 mL of Folin-Ciocalteu reagent and 2 mL of 20% Na₂CO₃ were added to 0.5 mL of supernatant, the mixture was

Table 3-1 Independent variables in the central composite design for the preparation of liquid-core hydrogel bead.

Codes levels	Independent variables			
	Primary gelation time	CL ¹ concentration in primary gelation	Secondary gelation time	CL concentration in secondary gelation
	Z ₁ (min)	Z ₂ (mole/L)	Z ₃ (min)	Z ₄ (mole/L)
2	45	0.2	10	0.1
1	35	0.16	8	0.075
0	25	0.12	6	0.05
-1	15	0.08	4	0.025
-2	5	0.04	2	0
X _i	$X_1=(Z_1-25)/10$	$X_2=(Z_2-0.12)/0.04$	$X_3=(Z_3-6)/2$	$X_4=(Z_4-0.05)/0.025$

¹CL, calcium lactate

incubated for 15 min at room temperature and centrifuged at 4000 rpm for 5 min. The absorbance of the supernatant of the mixture was measured by a spectrophotometer (U-2800-A, Hitachi, Japan) at 735 nm. The same method was applied to measure the amount of total phenolic compounds in the liquid-core material. The encapsulation efficiency was calculated with the following equation:

$$\text{Encapsulation efficiency (\%)} = M_1/M_2 \times 100$$

where M_1 and M_2 are the total phenolic compounds in liquid-core hydrogel bead and liquid-core material, respectively.

3.3.6. *In vitro* release profile

In vitro release experiments were performed by the method of Tsai, Chuang, Kitamura, Kokawa, & Islam (2017), using United States Pharmacopeia apparatus 2 (PJP-32N, Miyamoto Riken, Japan). Simulated gastric fluid was prepared by mixing 2 g of NaCl, 3.2 g of pepsin, and 7 mL of HCl in 500 mL of distilled water, and adding distilled water to 1 L, simulated intestinal fluid was prepared by mixing 6.8 g of NaOH, 77 mL 0.2 N of KH_2PO_4 , and 10 g of pancreatin, and adding distilled water to reach 1 L (Robertson, 2013).

Liquid-core hydrogel beads were left in 300 mL of simulated gastric fluid for 30 min and simulated intestinal fluid for 60 min at 37 °C, respectively, with a paddle rotation speed of 50 rpm. Liquid-core hydrogel beads were collected and excess bathing fluid on the surface was removed with a paper towel. Liquid-core hydrogel beads were broken and the amount of total phenolic compounds was determined with the section 3.3.5. Release profiles of total phenolic compounds in simulated gastric digestion and simulated intestinal digestion were calculated with the following equation:

$$\text{Release profile of total phenolic compounds (\%)} = 100 - [M_1/M_2 \times 100]$$

where M_1 and M_2 are the total phenolic compounds in liquid-core hydrogel bead and liquid-core material, respectively.

3.3.7. Swelling capacity

Swelling capacity was determined by the method of Gong et al. (Gong et al., 2011) with some modifications. Liquid-core hydrogel beads (W_1) were placed in 10 mL of distilled water at room temperature for 10 min. After gently removing excess water on the surface of liquid-core hydrogel bead with a paper towel, the weight of swollen liquid-core hydrogel beads were weighed (W_2), and the swelling capacity was calculated as follows:

$$\text{Swelling capacity (\%)} = [(W_2 - W_1)/W_1] \times 100$$

3.3.8. Experimental design and data analysis

The processing parameters were optimized by RSM with central composite design (CCD). The effects of four processing variables: primary gelation time (X_1), calcium lactate concentration in the primary gelation (X_2), secondary gelation time (X_3), and calcium lactate concentration in secondary gelation (X_4) on seven physical properties: average diameter (d), hardness (Y_1 , N), encapsulation efficiency (Y_2 , %), release profile of total phenolic compounds in simulated gastric digestion (Y_3 , %) and simulated intestinal digestion (Y_4 , %), swelling capacity (Y_5 , %), and sphericity (Y_6) were evaluated. The range and the levels of the variables in this study are given in Table 3-1 and the design matrix for the experiment is shown in Table 3-2. Data were expressed as mean \pm SD of three individual measurements and analyzed by the Analysis of Variance (ANOVA) of Statistical Analysis System software (Version 8.01, alginateS Institute Inc., Ualginate). The parameter was regarded as significant when the p-value was less than 0.05.

The data of dependent variables were fitted to a second-order polynomial equation:

$$Y = \beta_0 + \sum_{i=1}^4 \beta_i X_i + \sum_{i=1}^4 \beta_{ii} X_i^2 + \sum_{i=4}^3 \sum_{j=i+1}^4 \beta_{ij} X_i X_j$$

where Y is the dependent variable, β_0 , β_i , β_{ii} and β_{ij} are regression coefficients obtained by the response surface regression (RSREG) of the experimental data, and X_i and X_j are independent

Table 3-2 Central composite design for liquid-core hydrogel bead.

Run	Independent variables ¹							
	Coded				Uncoded			
	X ₁	X ₂	X ₃	X ₄	Z ₁ (min)	Z ₂ (mole/L)	Z ₃ (min)	Z ₄ (mole/L)
1	1	1	1	1	35	0.16	8	0.075
2	1	1	1	-1	35	0.16	8	0.025
3	1	1	-1	1	35	0.16	4	0.075
4	1	1	-1	-1	35	0.16	4	0.025
5	1	-1	1	1	35	0.08	8	0.075
6	1	-1	1	-1	35	0.08	8	0.025
7	1	-1	-1	1	35	0.08	4	0.075
8	1	-1	-1	-1	35	0.08	4	0.025
9	-1	1	1	1	15	0.16	8	0.075
10	-1	1	1	-1	15	0.16	8	0.025
11	-1	1	-1	1	15	0.16	4	0.075
12	-1	1	-1	-1	15	0.16	4	0.025
13	-1	-1	1	1	15	0.08	8	0.075
14	-1	-1	1	-1	15	0.08	8	0.025
15	-1	-1	-1	1	15	0.08	4	0.075
16	-1	-1	-1	-1	15	0.08	4	0.025
17	2	0	0	0	45	0.12	6	0.05
18	-2	0	0	0	5	0.12	6	0.05
19	0	2	0	0	25	0.2	6	0.05
20	0	-2	0	0	25	0.04	6	0.05
21	0	0	2	0	25	0.12	10	0.05
22	0	0	-2	0	25	0.12	2	0.05
23	0	0	0	2	25	0.12	6	0.1
24	0	0	0	-2	25	0.12	6	0
25	0	0	0	0	25	0.12	6	0.05
26	0	0	0	0	25	0.12	6	0.05
27	0	0	0	0	25	0.12	6	0.05
28	0	0	0	0	25	0.12	6	0.05
29	0	0	0	0	25	0.12	6	0.05
30	0	0	0	0	25	0.12	6	0.05

¹X₁, primary gelation time; X₂, concentration of calcium lactate in primary gelation; X₃, secondary gelation time; X₄, concentration of calcium lactate in secondary gelation.

variables. Multiple response optimization was analyzed by MINITAB statistical software (Version 17, Minitab Inc., Ualginate).

3.4. Results and Discussion

3.4.1. Average diameter

The average diameter of the liquid-core hydrogel bead was between 4.17 to 5.84 mm (Table 3-3) and related to the following second-order polynomial equation after simplifying the model by eliminating non-significant terms ($p > 0.05$) (A. Nayak, Laha, & Sen, 2011) (Table 3-4):

$$d = 2.37 \times 10^{-2} - 1.04 \times 10^{-2}X_1 - 7.52 \times 10^{-3}X_2 + 2.73 \times 10^{-3}X_3^2 + 2.39 \times 10^{-3}X_4^2$$

The results of the lack-of-fit test indicates the fitness of the model (Ji et al., 2007). The model of average diameter showed no lack-of-fit ($p > 0.05$), indicating that it was adequate to represent the relationship between the responses and the independent variables. The average diameter increased with the increase of primary gelation time (X_1) and calcium lactate concentration in the primary gelation (X_2) (Figure 3-2). Primary gelation is the step of outer layer formation in the reverse spherification process. When the liquid-core material containing calcium ions is extruded into alginate solution, a calcium alginate film immediately forms around the droplet. With the increase of primary gelation time, more and more calcium ions are released from the liquid-core material and combine with alginate (Figure 3-1b), increasing the droplet diameter and membrane thickness.

The importance of each independent variable on the dependent variables can be estimated by the sum of square of independent variables. The larger sum of square of independent variables indicates a relatively larger effect on dependent variables. The sum of square of independent variables was as follows: $X_1 > X_2 > X_4$ (calcium lactate concentration in the secondary gelation) $> X_3$ (secondary gelation time), demonstrating X_1 had the largest influence on average diameter. Moreover, X_3 had no significant influence on the average diameter of the liquid-core hydrogel bead (Table 3-5).

Table 3-3 Experimental results of average diameter.

Run	Average diameter (mm)	Run	Average diameter (mm)	Run	Average diameter (mm)
1	5.23±0.06 ^{bcd}	11	4.75±0.11 ^{fghi}	21	4.58±0.15 ^{ghijk}
2	5.59±0.13 ^{ab}	12	4.70±0.22 ^{ghij}	22	4.89±0.01 ^{efgh}
3	5.26±0.09 ^{bcd}	13	4.17±0.15 ^k	23	4.50±0.18 ^{hijk}
4	5.51±0.16 ^{abc}	14	4.39±0.12 ^{ijk}	24	5.84±0.16 ^a
5	4.66±0.07 ^{ghij}	15	4.35±0.14 ^{ijk}	25	4.58±0.15 ^{ghijk}
6	4.90±0.05 ^{efgh}	16	4.72±0.21 ^{ghi}	26	4.71±0.11 ^{ghij}
7	4.92±0.12 ^{defg}	17	5.16±0.12 ^{cdef}	27	4.73±0.21 ^{fghi}
8	4.92±0.12 ^{defg}	18	4.29±0.08 ^{jk}	28	4.49±0.11 ^{hijk}
9	4.67±0.12 ^{ghij}	19	5.34±0.07 ^{bcd}	29	4.63±0.04 ^{ghij}
10	4.84±0.21 ^{efgh}	20	4.39±0.07 ^{ijk}	30	4.53±0.12 ^{ghijk}

^{a-k} Means each treatment with different superscript letters are significantly different at $p < 0.05$.

Table 3-4 Regression coefficients of the fitted quadratic equations for average diameter.

Parameter ¹	DF ²	Estimate	Standard error	t value	p value
Intercept	1	4.61	0.07	64.47	<0.001
X ₁	1	0.26	0.03	7.28	<0.001
X ₂	1	0.23	0.04	6.42	<0.001
X ₃	1	-0.05	0.04	-1.55	0.143
X ₄	1	-0.18	0.04	-5.02	<0.001
X ₁ ×X ₂	1	0.05	0.04	1.25	0.231
X ₁ ×X ₃	1	0.01	0.04	0.29	0.778
X ₁ ×X ₄	1	-0.01	0.04	-0.20	0.841
X ₂ ×X ₃	1	0.06	0.04	1.31	0.209
X ₂ ×X ₄	1	0.004	0.04	0.11	0.913
X ₃ ×X ₄	1	-0.03	0.04	-0.61	0.553
X ₁ ²	1	0.02	0.03	0.71	0.491
X ₂ ²	1	0.06	0.03	1.81	0.091
X ₃ ²	1	0.03	0.03	0.81	0.429
X ₄ ²	1	0.14	0.03	4.10	<0.001

¹X₁, primary gelation time; X₂, concentration of calcium lactate in primary gelation; X₃, secondary gelation time; X₄, concentration of calcium lactate in secondary gelation.

²DF, degrees of freedom

Table 3-5 Summary of ANOVA for average diameter.

Sources	DF ¹	SS ¹	R square	MS ¹	F value	p value
Model	14	4.29	0.91		10.28	<0.001
Linear	4	3.63	0.77		30.46	<0.001
Quadratic	4	0.55	0.12		4.59	0.013
Crossproduct	6	0.11	0.02		0.63	0.703
Residual	15	0.45		0.03		
Lack of fit	10	0.40		0.04	4.36	0.059
Pure error	5	0.05		0.01		
Factor						
X ₁ ²	5	1.64		0.33	11.03	<0.001
X ₂	5	1.42		0.28	9.56	<0.001
X ₃	5	0.16		0.03	1.05	0.427
X ₄	5	1.26		0.25	8.49	<0.001

¹SS, sum of squares; DF, degrees of freedom; MS, mean squares.

²X₁, primary gelation time; X₂, concentration of calcium lactate in primary gelation; X₃, secondary gelation time; X₄, concentration of calcium lactate in secondary gelation.

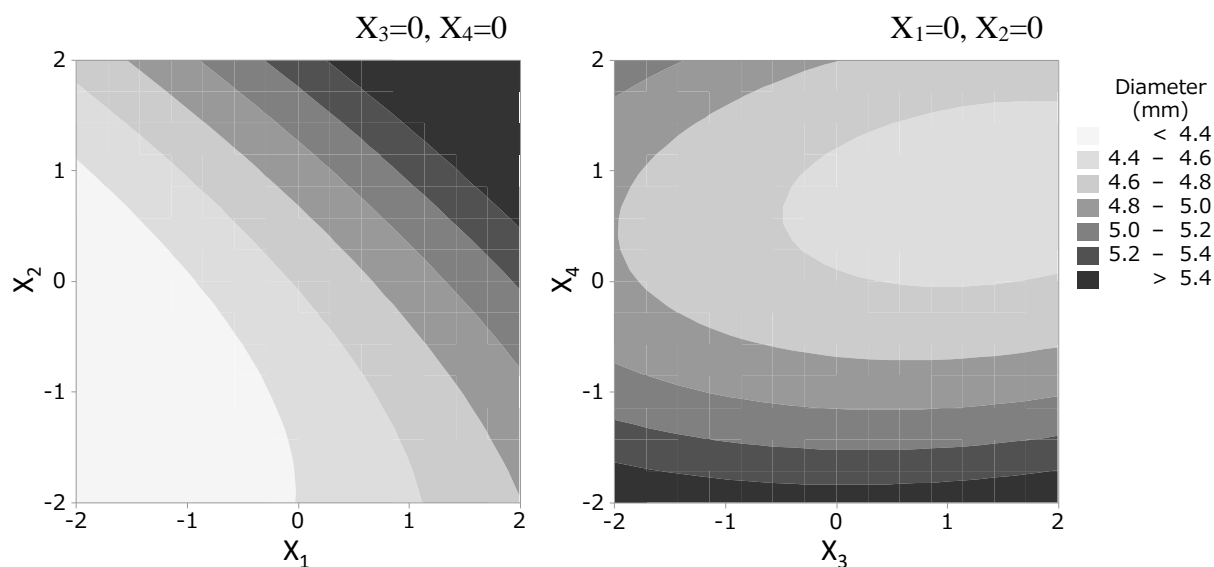


Figure 3-2 Two-dimensional corresponding contour plot for average diameter.

Although the lack-of-fit test of the model of the average diameter was not significant, the average diameter was not considered as one of the dependent variables in the following multiple response optimization because it was a minor parameter in evaluating the quality of the liquid-core hydrogel bead.

3.4.2. Hardness

Hardness is regarded as one of the most important physical properties of hydrogel capsules because it indicates the bead stability under processing and gelation efficiency between ionic biopolymer and ions (Lozano-Vazquez et al., 2015; Lupo et al., 2015). An earlier study indicated that hardness affected the survivability of probiotics in the capsule (Cai et al., 2014). High hardness could prevent the liquid-core hydrogel bead from bursting during transportation and storage. The hardness of all liquid-core hydrogel beads was found within the range of 2.00 to 26.15N (Table 3-6). The model equations was:

$$Y_1 = 24.65 + 1.53X_1 + 1.68X_2 + 5.10X_4 - 1.36X_1^2 - 3.36X_2^2 - 1.60X_3^2 - 2.73X_4^2$$

and there was no significance in the lack-of-fit test (Table 3-7 and Table 308). When considering the result of ANOVA (Table 3-8), all of the independent variables had significant effect on hardness; however, X_4 had a relatively larger effect among four independent variables as shown by the large sum of squares (823.77). In a previous study (Fu Hsuan Tsai et al., 2017), I demonstrated that secondary gelation is an important step in strengthening the liquid-core hydrogel bead. The calcium alginate outer layer is formed during primary gelation, when calcium ions are combined with the carboxyl group (-COOH) in the G-block of alginate; however, semifinished beads are fragile because some carboxyl groups do not coordinate with calcium ions. Therefore, I operated secondary gelation, where semifinished beads are suspended into the calcium lactate solution so that calcium ions could combine with remnants of carboxyl groups, and showed that the hardness of the liquid-core hydrogel bead increased through this process (Figure 3-1h). The results obtained in this study also show the importance

Table 3-6 Experimental results of hardness (Y_1) for different formulations of the liquid-core hydrogel bead.

Run	Y_1 (N)	Run	Y_1 (N)	Run	Y_1 (N)
1	23.70±1.47 ^{abcd}	11	20.40±1.65 ^{cdef}	21	18.73±1.21 ^{fg}
2	12.69±0.93 ^{ijk}	12	10.94±1.73 ^{jkl}	22	18.42±0.42 ^{fgh}
3	23.24±1.44 ^{abcde}	13	17.12±1.30 ^{fgh}	23	26.15±1.31 ^a
4	12.41±1.19 ^{ijk}	14	9.14±0.79 ^{kl}	24	2.00±0.17 ^m
5	19.41±1.32 ^{defg}	15	16.63±1.27 ^{fghi}	25	23.86±1.18 ^{abc}
6	10.42±1.02 ^{jkl}	16	9.00±0.38 ^{kl}	26	25.24±2.14 ^a
7	19.07±1.53 ^{efg}	17	24.65±1.44 ^{abc}	27	24.99±1.73 ^{ab}
8	10.68±0.82 ^{jkl}	18	14.41±0.97 ^{hij}	28	25.57±1.80 ^a
9	20.89±1.35 ^{bdcef}	19	15.65±0.86 ^{ghi}	29	23.29±1.92 ^{abcde}
10	11.17±1.07 ^{jkl}	20	7.48±0.72 ^l	30	24.94±2.28 ^{ab}

^{a-1} Means each treatment with different superscript letters are significantly different at $p < 0.05$.

Table 3-7 Regression coefficients of the fitted quadratic equations for hardness (Y_1).

Parameter ¹	DF ²	Estimate	Standard error	t value	p value
Intercept	1	24.65	0.58	42.59	<0.001
X_1	1	1.53	0.29	5.30	<0.001
X_2	1	1.68	0.29	5.81	<0.001
X_3	1	0.11	0.29	0.40	0.696
X_4	1	5.10	0.29	17.61	<0.001
$X_1 \times X_2$	1	0.06	0.35	0.17	0.870
$X_1 \times X_3$	1	-0.03	0.35	-0.09	0.926
$X_1 \times X_4$	1	0.27	0.35	0.78	0.446
$X_2 \times X_3$	1	0.05	0.35	0.13	0.896
$X_2 \times X_4$	1	0.50	0.35	1.42	0.177
$X_3 \times X_4$	1	0.09	0.35	0.24	0.810
X_1^2	1	-1.36	0.27	-5.04	<0.001
X_2^2	1	-3.36	0.27	12.40	<0.001
X_3^2	1	-1.60	0.27	-5.92	<0.001
X_4^2	1	-2.73	0.27	-10.07	<0.001

¹ X_1 , primary gelation time; X_2 , concentration of calcium lactate in primary gelation; X_3 , secondary gelation time; X_4 , concentration of calcium lactate in secondary gelation.

²DF, degrees of freedom

Table 3-8 Summary of ANOVA for hardness (Y₁).

Sources	DF ¹	SS ¹	R square	MS ¹	F value	p value
Model	14	1231.38	0.97		43.77	<0.001
Linear	4	748.02	0.59		93.06	<0.001
Quadratic	4	477.88	0.38		59.45	<0.001
Crossproduct	6	5.49	0.004		0.45	0.831
Residual	15	30.14		2.01		
Lack of fit	10	26.28		2.63	3.40	0.095
Pure error	5	3.87		0.77		
Factor						
X ₁ ²	5	108.82		21.76	10.83	<0.001
X ₂	5	380.70		76.14	37.89	<0.001
X ₃	5	70.86		14.17	7.05	0.001
X ₄	5	832.77		166.55	82.88	<0.001

¹SS, sum of squares; DF, degrees of freedom; MS, mean squares. SS

²X₁, primary gelation time; X₂, concentration of calcium lactate in primary gelation; X₃, secondary gelation time; X₄, concentration of calcium lactate in secondary gelation.

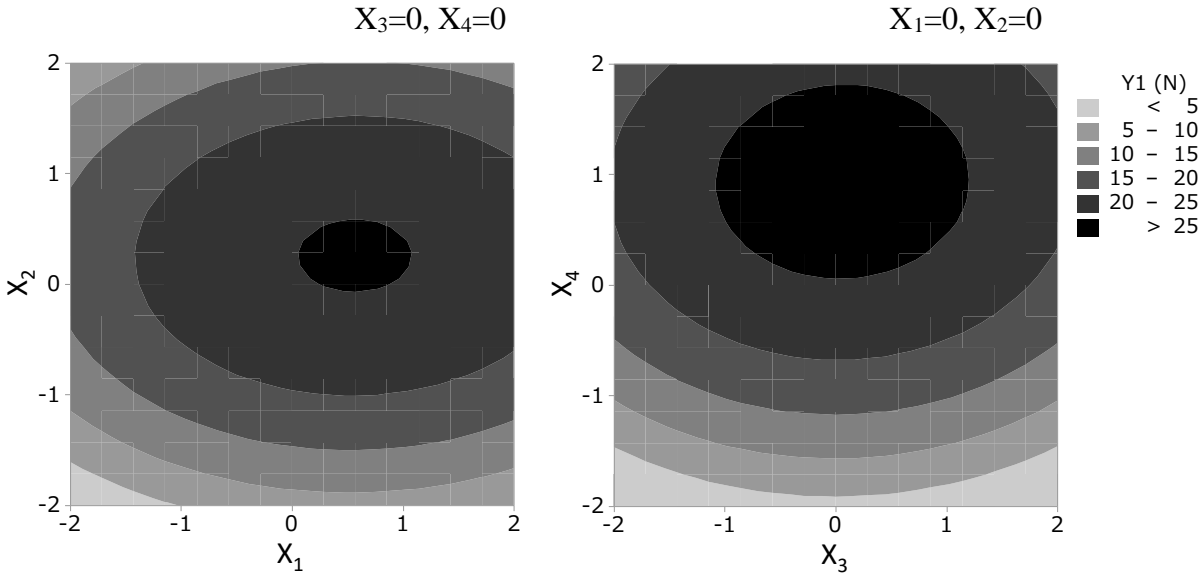


Figure 3-3 Two-dimensional corresponding contour plot for hardness

of secondary gelation. The reason of why secondary gelation plays an important role in the liquid-core hydrogel bead formulation is demonstrated in section 3.4.5., by the swelling capacity of the liquid-core hydrogel bead.

The maximum of hardness (27.99 N) was found under the following experimental conditions: primary gelation time of 31.70 min, calcium lactate concentration of 0.13 mole/L in the primary gelation, secondary gelation time of 6.12 min, and calcium lactate concentration of 0.075 mole/L in secondary gelation (Figure 3-3).

3.4.3. Encapsulation efficiency

The encapsulation efficiency associates with the cost of processing. A low encapsulation efficiency usually reflects on a non-valuable product (Zucker, Marcus, Barenholz, & Goldblum, 2009). The encapsulation efficiency of the liquid-core hydrogel bead varied from 60.85 to 87.91 % (Table 3-9). The model of the encapsulation efficiency was as follows (Table 3-10):

$$Y_2 = 85.04 - 5.18X_1 + 1.74X_2 + 0.92X_4 - 1.27X_2X_3 - 3.76X_1^2 - 3.07X_2^2 - 4.18X_3^2 - 1.03X_4^2.$$

The highest encapsulation efficiency was observed on X_1 , 25 min; X_2 , 0.12 mole/L; X_3 , 6 min; X_4 , 0.05 mole/L. According to *p*-statistics, the lack-of-fit showed a significant difference ($p > 0.05$), only X_4 exhibited no significant influence on the encapsulation efficiency ($p > 0.05$). X_1 had a relatively larger effect on the encapsulation efficiency, the sum of square of X_1 was 1045.06 (Table 3-11). Figure 3-4 showed that the encapsulation efficiency increased and then decreased with the increase of primary gelation time. I inferred that calcium ion tended to diffuse from the liquid-core material to the surrounding alginate during primary gelation; meanwhile, total phenolic compounds also leaked out to alginate, the phenomenon resulted in the decrease of the encapsulation efficiency when primary gelation was long. On the other hand, primary gelation is the main step of outer layer formation of the liquid-core hydrogel bead, the outer layer was thin when preparing the liquid-core hydrogel bead in a short primary gelation

Table 3-9 Experimental results of encapsulation efficiency (Y_2) for different formulations of the liquid-core hydrogel bead.

Run	Y_2 (%)	Run	Y_2 (%)	Run	Y_2 (%)
1	66.99±1.34 ^{klm}	11	82.44±1.46 ^{bcdef}	21	72.31±1.56 ^{ij}
2	64.47±1.85 ^{mn}	12	79.51±1.12 ^{defgh}	22	66.43±3.06 ^{lm}
3	72.11±1.34 ^{ijk}	13	78.43±0.72 ^{efgh}	23	83.88±1.09 ^{abcd}
4	69.76±0.73 ^{jkl}	14	76.34±0.77 ^{ghi}	24	80.06±1.40 ^{cdefgh}
5	65.92±0.83 ^{lmn}	15	72.65±1.82 ^{ij}	25	84.92±4.10 ^{abc}
6	65.52±1.45 ^{lmn}	16	75.54±0.64 ^{hi}	26	83.68±2.54 ^{abcde}
7	68.64±0.97 ^{jklm}	17	60.85±1.09 ⁿ	27	83.88±0.78 ^{abcd}
8	64.80±0.91 ^{lmn}	18	81.30±1.87 ^{bcdefg}	28	85.64±1.99 ^{ab}
9	79.84±1.47 ^{cdefgh}	19	78.27±1.28 ^{fgh}	29	87.91±1.87 ^a
10	76.75±0.78 ^{ghi}	20	69.39±1.84 ^{jklm}	30	84.19±1.00 ^{abcd}

^{a-n} Means each treatment with different superscript letters are significantly different at $p < 0.05$.

Table 3-10 Regression coefficients of the fitted quadratic equations for encapsulation efficiency (Y_2).

Parameter ¹	DF ²	Estimate	Standard error	t value	p value
Intercept	1	85.04	0.86	99.34	<0.001
X ₁	1	-5.18	0.43	-12.09	<0.001
X ₂	1	1.74	0.43	4.07	0.001
X ₃	1	0.02	0.43	0.06	0.956
X ₄	1	0.92	0.43	2.14	0.049
X ₁ ×X ₂	1	-0.44	0.52	-0.85	0.410
X ₁ ×X ₃	1	-0.85	0.52	-1.62	0.125
X ₁ ×X ₄	1	-0.24	0.52	0.47	0.648
X ₂ ×X ₃	1	-1.27	0.52	-2.43	0.028
X ₂ ×X ₄	1	0.47	0.52	0.89	0.389
X ₃ ×X ₄	1	0.12	0.52	0.22	0.829
X ₁ ²	1	-3.76	0.40	-9.38	<0.001
X ₂ ²	1	-3.07	0.40	-7.66	<0.001
X ₃ ²	1	-4.18	0.40	10.44	<0.001
X ₄ ²	1	-1.03	0.40	-2.57	0.021

¹X₁, primary gelation time; X₂, concentration of calcium lactate in primary gelation; X₃, secondary gelation time; X₄, concentration of calcium lactate in secondary gelation.

²DF, degrees of freedom

Table 3-11 Summary of ANOVA for encapsulation efficiency (Y_2).

Sources	DF ¹	SS ¹	R square	MS ¹	F value	p value
Model	14	1662.66	0.96		27.01	<0.001
Linear	4	735.66	0.43		41.83	<0.001
Quadratic	4	881.74	0.51		50.13	<0.001
Crossproduct	6	45.26	0.02		1.72	0.185
Residual	15	65.95		4.40		
Lack of fit	10	53.41		5.34	2.13	0.209
Pure error	5	12.54		2.51		
Factor						
X_1^2	5	1045.06		209.01	47.54	<0.001
X_2	5	362.93		72.59	16.51	<0.001
X_3	5	517.00		103.40	23.52	<0.001
X_4	5	53.85		10.77	2.45	0.082

¹SS, sum of squares; DF, degrees of freedom; MS, mean squares. SS

² X_1 , primary gelation time; X_2 , concentration of calcium lactate in primary gelation; X_3 , secondary gelation time; X_4 , concentration of calcium lactate in secondary gelation.

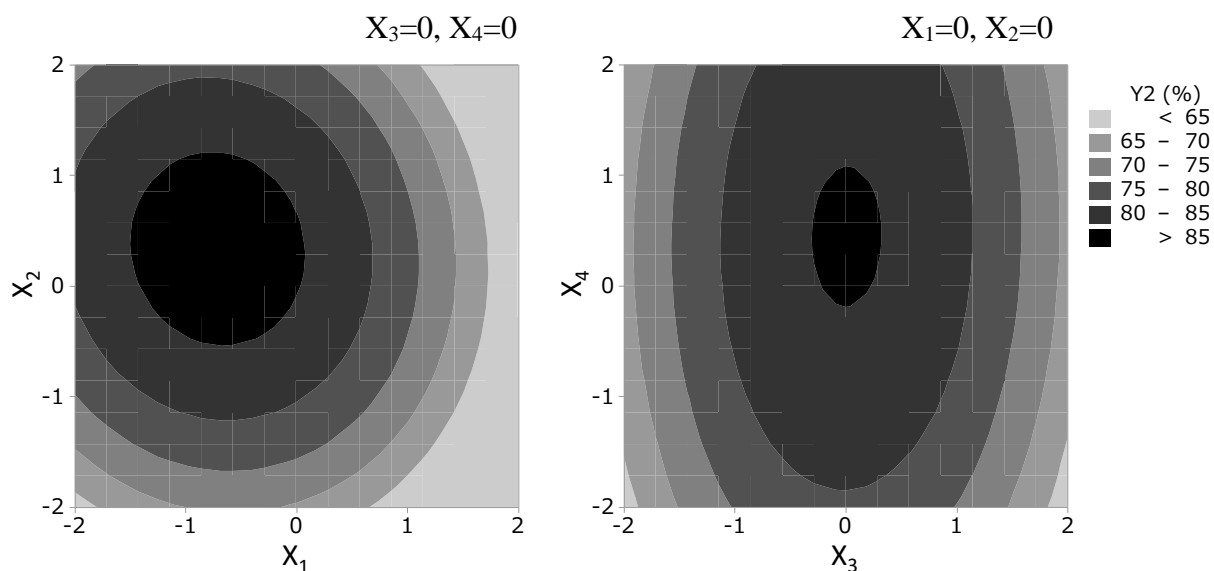


Figure 3-4 Two-dimensional corresponding contour plot for encapsulation efficiency (Y_2).

(Figure 3-1c). Therefore, total phenolic compound was easy to run off during secondary gelation. Furthermore, X_2 and X_3 were also two significant parameters in the liquid-core hydrogel bead formulation. According to the sum of square of independent variables, gelation time had a larger effect on the encapsulation efficiency than calcium lactate concentration, no matter in first or secondary gelation.

3.4.4. *In vitro* release experiment

As shown in Table 3-12, the release profile of total phenolic compounds in simulated gastric digestion and simulated intestinal digestion ranged from 19.63 to 34.60 % and 34.28 to 65.27 %, respectively. To efficiently deliver total phenolic compounds to the intestine and to ensure efficient absorption, the release profile and rate of total phenolic compounds should be kept low in the stomach and high in the intestine. The model of total phenolic compounds release in simulated gastric digestion was (Table 3-13):

$$Y_3 = 21.68 - 1.06X_1 - 1.53X_2 + 1.95X_1^2 + 2.67X_2^2 + 1.07X_3^2 + 1.46X_4^2$$

A minimum was found under the following experimental conditions: X_1 of 25 min, X_2 of 0.12 mole/L, X_3 of 6 min, and X_4 of 0.05 mole/L.

Figure 3-5 present the effects of the four independent variables on release profile of total phenolic compounds in simulated gastric digestion. The model of total phenolic compounds release in simulated intestinal digestion was (Table 3-13):

$$Y_4 = 39.65 - 2.48X_1 - 5.87X_2 - 4.11X_4 + 3.98X_1^2 + 1.91X_2^2 + 1.39X_3^2 + 3.00X_4^2.$$

Release profile of total phenolic compounds decreased and then increased with an increase in independent variables from -2 to 2 and the release profile of total phenolic compounds exhibit a more considerable variation when X_1 and X_2 change than X_3 and X_4 . The result of ANOVA also showed that the effect of X_1 and X_2 were larger than X_3 and X_4 and X_3 showed no significant difference on the effect of total phenolic compounds release in simulated gastric digestion and simulated intestinal digestion. The porous structure of alginate causes the release

Table 3-12 Experimental results of the release profile of total phenolic compounds in simulated gastric digestion (Y₃) and simulated intestinal digestion (Y₄).

Run	Y ₃ (%)	Y ₄ (%)	Run	Y ₃ (%)	Y ₄ (%)
1	27.65±1.41 ^{cdefgh}	38.39±2.25 ^{ijkl}	16	30.65±1.41 ^{abcd}	61.19±1.16 ^{ab}
2	25.02±0.13 ^{efghijk}	43.67±0.59 ^{ghij}	17	27.24±0.13 ^{cdefghi}	50.52±3.28 ^{defg}
3	27.57±1.36 ^{cdefgh}	40.36±2.01 ^{hijkl}	18	30.16±1.36 ^{abcde}	58.99±1.70 ^{ab}
4	25.54±1.97 ^{defghij}	44.37±2.24 ^{fghi}	19	28.81±1.97 ^{bcdef}	34.28±1.68 ^l
5	30.72±2.26 ^{abcd}	50.29±3.41 ^{defg}	20	34.35±2.26 ^a	58.68±2.14 ^{abc}
6	27.37±1.27 ^{cdefghi}	55.41±3.00 ^{bcd}	21	24.63±1.27 ^{fghijk}	43.19±2.04 ^{hijk}
7	32.07±0.68 ^{abc}	51.89±1.71 ^{cde}	22	25.69±0.68 ^{defghij}	45.64±3.16 ^{efgh}
8	28.11±0.85 ^{bcdefg}	56.92±1.77 ^{bcd}	23	24.55±0.85 ^{fghijk}	36.39±1.20 ^{kl}
9	29.75±1.50 ^{abcdef}	43.98±2.82 ^{ghi}	24	28.94±1.50 ^{bcdef}	65.27±1.44 ^a
10	27.20±2.60 ^{cdefghi}	50.98±0.95 ^{def}	25	22.81±2.60 ^{jk}	37.70±2.40 ^{ijkl}
11	30.13±1.48 ^{abcde}	44.37±1.61 ^{fghi}	26	19.63±1.48 ^{hijk}	37.00±2.69 ^{ijkl}
12	28.17±2.35 ^{bcdefg}	50.51±2.13 ^{defg}	27	20.33±2.35 ^k	38.13±2.92 ^{ijkl}
13	33.26±1.79 ^{ab}	56.08±1.47 ^{bcd}	28	22.11±1.79 ^{ijk}	40.84±1.14 ^{hijkl}
14	29.83±1.79 ^{abcdef}	60.02±1.76 ^{ab}	29	20.24±1.79 ^{ghijk}	41.71±1.78 ^{hijk}
15	34.60±1.90 ^a	56.83±1.89 ^{bcd}	30	21.46±1.90 ^{jk}	42.50±2.36 ^{hijk}

^{a-l} Means each treatment of Y₃ or Y₄ with different superscript letters are significantly different at p < 0.05.

Table 3-13 Regression coefficients of the fitted quadratic equations for the release profile of total phenolic compounds in simulated gastric digestion (Y_3) and simulated intestinal digestion (Y_4).

Parameter ¹	DF ²	Estimate	Standard error	t value	p value
Simulated gastric digestion					
Intercept	1	21.68	0.75	28.86	<0.001
X ₁	1	-1.06	0.38	-2.82	0.013
X ₂	1	-1.53	0.38	-4.07	0.001
X ₃	1	-0.34	0.38	-0.91	0.379
X ₄	1	0.63	0.38	1.67	0.115
X ₁ ×X ₂	1	0.04	0.46	0.08	0.936
X ₁ ×X ₃	1	0.06	0.46	0.13	0.896
X ₁ ×X ₄	1	0.005	0.46	0.01	0.992
X ₂ ×X ₃	1	0.16	0.46	0.33	0.744
X ₂ ×X ₄	1	-0.35	0.46	-0.75	0.465
X ₃ ×X ₄	1	0.01	0.46	0.01	0.991
X ₁ ²	1	1.95	0.35	5.55	<0.001
X ₂ ²	1	2.67	0.35	0.08	0.936
X ₃ ²	1	1.07	0.35	3.04	0.008
X ₄ ²	1	1.46	0.35	4.17	<0.001
Simulated intestinal digestion					
Intercept	1	39.65	1.32	30.13	<0.001
X ₁	1	-2.48	0.66	-3.77	0.002
X ₂	1	-5.87	0.66	-8.91	<0.001
X ₃	1	-0.52	0.66	-0.79	0.441
X ₄	1	-4.11	0.66	-6.25	<0.001
X ₁ ×X ₂	1	-0.21	0.81	-0.27	0.793
X ₁ ×X ₃	1	-0.25	0.81	-0.30	0.765
X ₁ ×X ₄	1	0.13	0.81	0.16	0.878
X ₂ ×X ₃	1	0.15	0.81	0.19	0.853
X ₂ ×X ₄	1	-0.25	0.81	-0.31	0.762
X ₃ ×X ₄	1	-0.11	0.81	-0.14	0.892
X ₁ ²	1	3.98	0.62	6.47	<0.001
X ₂ ²	1	1.91	0.62	3.10	0.007
X ₃ ²	1	1.39	0.62	2.27	0.039
X ₄ ²	1	3.00	0.62	4.87	<0.001

¹X₁, primary gelation time; X₂, concentration of calcium lactate in primary gelation; X₃, secondary gelation time; X₄, concentration of calcium lactate in secondary gelation.

²DF, degrees of freedom

Table 3-14 Summary of ANOVA for the release profile of total phenolic compounds in simulated gastric digestion (Y₃) and simulated intestinal digestion (Y₄).

Sources	DF ¹	SS ¹	R square	MS ¹	F value	p value
Simulated gastric digestion						
Model	14	389.00	0.88		8.20	<0.001
Linear	4	95.10	0.22		7.02	0.002
Quadratic	4	291.53	0.66		21.52	<0.001
Crossproduct	6	2.36	0.01		0.12	0.993
Residual	15	50.80		3.39		
Lack of fit	10	45.13		4.51	3.98	0.070
Pure error	5	5.57		1.13		
Factor						
X ₁ ²	5	131.38		26.28	7.76	0.001
X ₂	5	254.13		50.83	15.01	<0.001
X ₃	5	34.46		6.89	2.03	0.132
X ₄	5	70.13		14.03	4.14	0.015
Simulated intestinal digestion						
Model	14	2023.96	0.93		15.28	<0.001
Linear	4	1385.53	0.64		0.06	<0.001
Quadratic	4	634.92	0.29		13.91	<0.001
Crossproduct	6	3.52	0.001		33.34	0.999
Residual	15	155.85		10.39		
Lack of fit	10	128.95		12.89	2.40	0.173
Pure error	5	26.90		5.38		
Factor						
X ₁ ²	5	584.26		116.85	11.25	<0.001
X ₂	5	927.81		185.56	17.86	<0.001
X ₃	5	61.37		12.17	1.18	0.364
X ₄	5	653.24		130.65	12.57	<0.001

¹SS, sum of squares; DF, degrees of freedom; MS, mean squares.

²X₁, primary gelation time; X₂, concentration of calcium lactate in primary gelation; X₃, secondary gelation time; X₄, concentration of calcium lactate in secondary gelation.

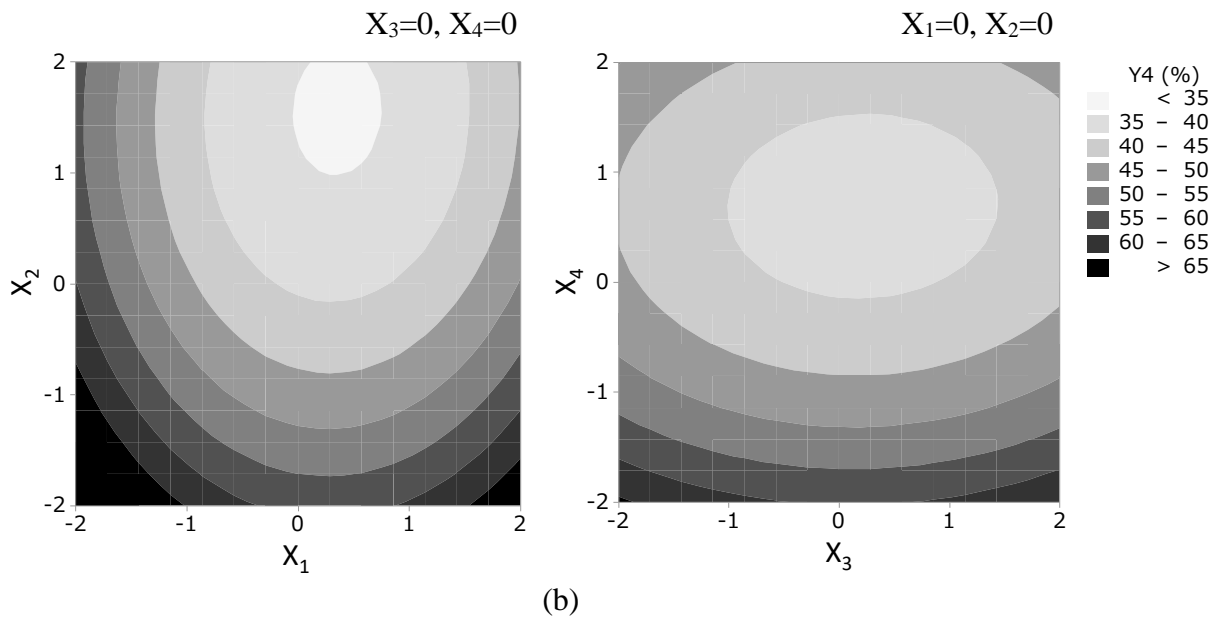
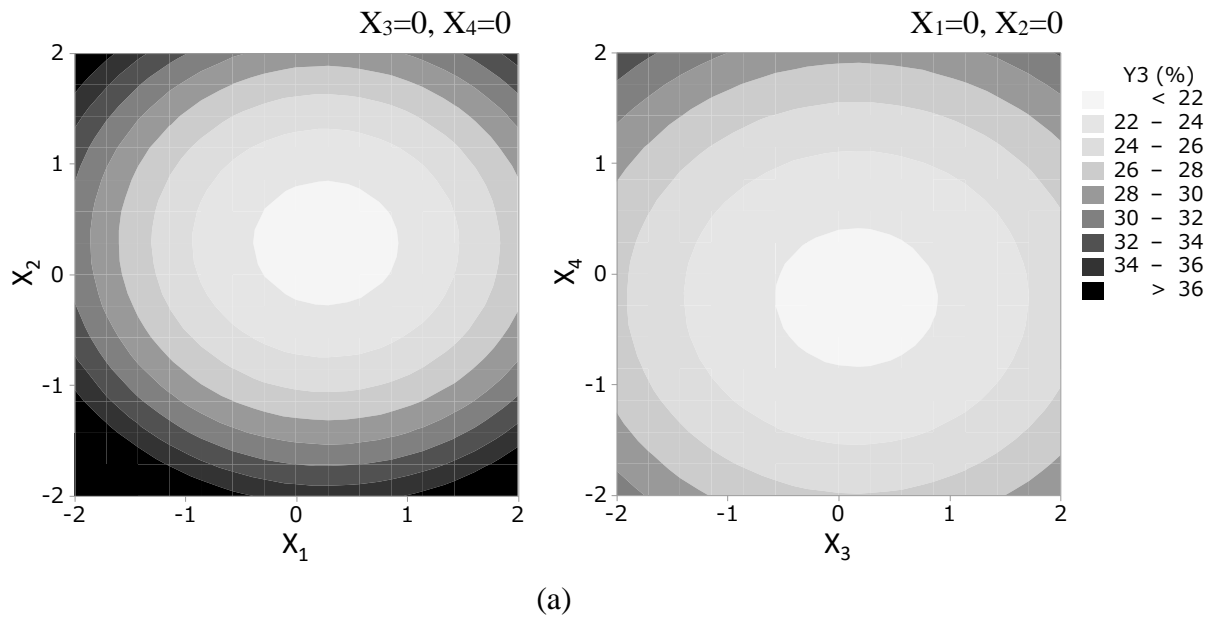


Figure 3-5 Two-dimensional corresponding contour plot for the release profile of total phenolic compounds in simulated gastric digestion (Y_3) and simulated intestinal digestion (Y_4).

(a) simulated gastric digestion; (b) simulated intestinal digestion

of entrapped material (Lozano-Vazquez et al., 2015). Our previous work (Fu Hsuan Tsai et al., 2017) observed the microstructure of the liquid-core hydrogel bead after *in vitro* treatment with SEM and showed that calcium alginate outlayers shrunk in simulated gastric fluid and were eroded in simulated intestinal fluid. The work also demonstrated that secondary gelation plays an important role in preventing the entrapped material release from the liquid-core hydrogel bead during thermal and *in vitro* treatment because some apertures, where G-block does not combine with calcium ion during the primary gelation, were filled by calcium ion during secondary gelation. Considering with the result of the work, I can infer that calcium ion could fill these pores in a short time in the step; therefore, secondary gelation time did have a significant effect on total phenolic compounds release in the *in vitro* environment. The lack-of-fit test of both dependent variables showed no significant difference (Table 3-14).

3.4.5. Swelling capacity

Swelling of hydrogel capsule indicates the decrease of ionic strength and usually leads to the release of compounds from the capsule (McKenna, Nicholson, Wehr, & Menzies, 2010; Siepmann & Peppas, 2001). A lower swelling capacity indicates higher stability of the liquid-core hydrogel bead. In all of the liquid-core hydrogel bead, the swelling capacity was between 2.79 and 23.33%. The lowest swelling capacity, i.e. the highest stability, was obtained when a higher level of X_4 was applied (Table 3-15). The model of the swelling capacity was:

$$Y_5 = 5.54 - 3.21X_1 - 1.53X_2 - 0.95X_3 - 3.36X_4 + 1.13X_1^2 + 0.94X_2^2 + 2.22X_4^2$$

The lack-of-fit test showed a significant difference. The sum of square of X_4 was largest among the four independent variables, indicating that X_4 contributed to the swelling capacity of the beads to a larger extent than other factors, and suggesting that a small change in X_4 could have large effects on the swelling capacity (Table 3-17). As mentioned before, G-blocks of alginate do not completely combine with calcium ion in primary gelation, leaving some pores in calcium alginate structure (Figure 3-1f); therefore, secondary gelation plays an important role in filling

Table 3-15 Experimental results of swelling capacity (Y_5) for different formulations of the liquid-core hydrogel bead.

Run	Y_5 (%)	Run	Y_5 (%)	Run	Y_5 (%)
1	8.45±0.50 ^{ijk}	11	5.32±0.70 ^{mno}	21	6.02±0.57 ^{lmno}
2	14.35±0.96 ^{ef}	12	9.17±0.73 ^{hij}	22	8.79±0.78 ^{ij}
3	10.20±0.85 ^{hi}	13	6.46±0.64 ^{klmn}	23	2.79±0.16 ^{pq}
4	17.53±0.88 ^c	14	10.91±0.70 ^{gh}	24	23.33±0.78 ^a
5	12.57±1.05 ^{fg}	15	7.96±0.63 ^{jkl}	25	5.70±0.56 ^{mno}
6	17.43±0.95 ^{cd}	16	13.48±0.63 ^{ef}	26	5.97±0.37 ^{lmno}
7	15.45±0.28 ^{de}	17	15.26±0.27 ^e	27	5.13±0.45 ^{no}
8	20.06±0.85 ^b	18	2.20±0.21 ^q	28	5.34±0.27 ^{mno}
9	4.39±0.39 ^{op}	19	5.70±0.12 ^{mno}	29	5.42±0.52 ^{mno}
10	7.35±0.62 ^{jklm}	20	10.24±0.56 ^{hi}	30	5.71±0.49 ^{mno}

^{a-q} Means each treatment with different superscript letters are significantly different at $p < 0.05$.

Table 3-16 Regression coefficients of the fitted quadratic equations for swelling capacity (Y_5).

Parameter ¹	DF ²	Estimate	Standard error	t value	p value
Intercept	1	5.54	0.86	6.46	<0.001
X_1	1	3.21	0.43	7.48	<0.001
X_2	1	-1.53	0.43	-3.56	0.003
X_3	1	-0.95	0.43	-2.21	0.043
X_4	1	-3.36	0.43	-7.81	<0.001
$X_1 \times X_2$	1	-0.15	0.53	-0.29	0.779
$X_1 \times X_3$	1	-0.23	0.53	-0.43	0.674
$X_1 \times X_4$	1	-0.37	0.53	-0.70	0.493
$X_2 \times X_3$	1	0.12	0.53	0.22	0.826
$X_2 \times X_4$	1	-0.04	0.53	-0.07	0.945
$X_3 \times X_4$	1	0.20	0.53	0.37	0.715
X_1^2	1	1.13	0.40	2.82	0.013
X_2^2	1	0.94	0.40	2.35	0.033
X_3^2	1	0.80	0.40	2.00	0.064
X_4^2	1	2.22	0.40	5.52	<0.001

¹ X_1 , primary gelation time; X_2 , concentration of calcium lactate in primary gelation; X_3 , secondary gelation time; X_4 , concentration of calcium lactate in secondary gelation.

²DF, degrees of freedom

Table 3-17 Summary of ANOVA for swelling capacity (Y_5).

Sources	DF ¹	SS ¹	R square	MS ¹	F value	p value
Model	14	764.48***	0.92		12.34	<0.001
Linear	4	595.85***	0.71		33.66	<0.001
Quadratic	4	164.41***	0.20		9.29	<0.001
Crossproduct	6	4.22 ^{ns}	0.01		0.16	0.984
Residual	15	66.39		4.43		
Lack of fit	10	65.93***		6.59	71.32	<0.001
Pure error	5	0.46		0.09		
Factor						
X_1^2	5	286.54***		57.31	12.95	<0.001
X_2	5	81.05*		16.21	3.66	0.023
X_3	5	41.00 ^{ns}		8.20	1.85	0.163
X_4	5	407.90***		81.58	18.43	<0.001

¹SS, sum of squares; DF, degrees of freedom; MS, mean squares.

² X_1 , primary gelation time; X_2 , concentration of calcium lactate in primary gelation; X_3 , secondary gelation time; X_4 , concentration of calcium lactate in secondary gelation.

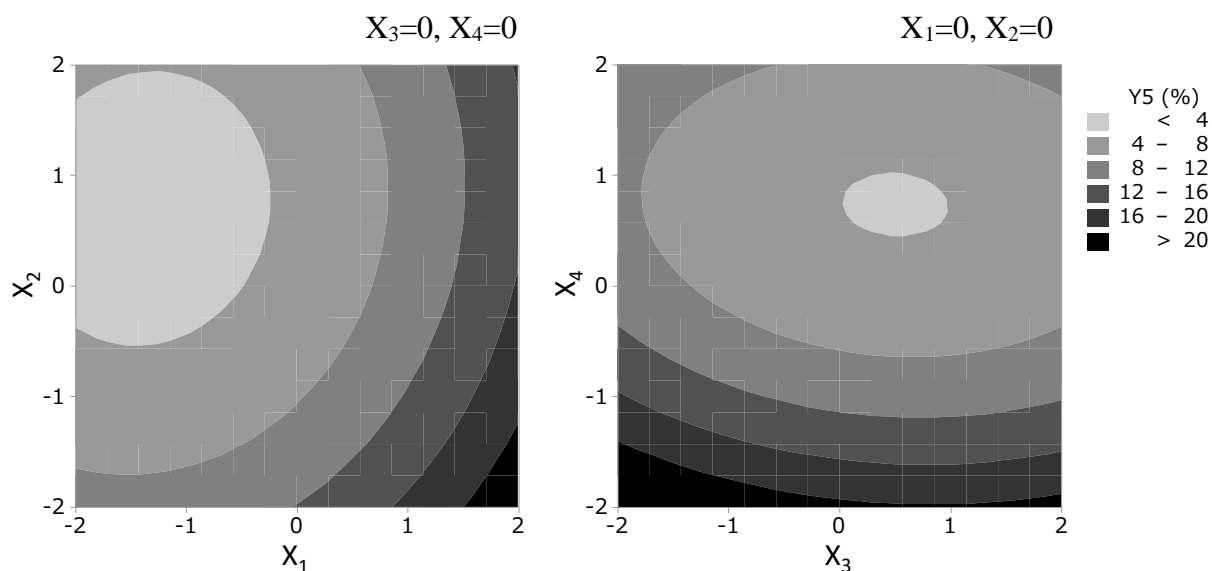


Figure 3-6 Two-dimensional corresponding contour plot for swelling capacity (Y_5).

these rooms by additional calcium ions. Not only the swelling phenomenon was inhibited when proper conditions were applied in the secondary gelation, but the hardness of the liquid-core hydrogel bead also increased when these pores were filled. Therefore, it can be demonstrated that secondary gelation plays an important role in improving the quality of the liquid-core hydrogel bead by increasing its hardness and decreasing the swelling capacity. The highest swelling capacity was observed in primary gelation time of 25 min, calcium lactate concentration of 0.12 mole/L in the primary gelation, secondary gelation time of 6 min, and calcium lactate concentration of 0 mole/L in secondary gelation. The result also indicated that the lower the calcium lactate concentration in secondary gelation, the lower the stability of the liquid-core hydrogel bead.

3.4.6. Sphericity

Sphericity is a factor that evaluates the roundness of the microcapsule. A larger sphericity indicates a more significant distortion and conversely, the microcapsule is a perfect sphere when sphericity is zero (Chew & Nyam, 2016). The hydrogel particle can be considered spherical when sphericity is smaller than 0.05 (Chan, Lee, Ravindra, & Poncelet, 2009). As shown in Table 3-18, the sphericity of the liquid-core hydrogel bead was in the range of 2.22×10^{-2} to 11.41×10^{-2} . The model of sphericity was:

$$Y_6 = 4.61 + 0.26X_1 + 0.23X_2 - 0.18X_4 + 0.14X_4^2$$

The lowest sphericity was obtained in primary gelation time of 25 min, calcium lactate concentration of 0.12 mole/L in the primary gelation, secondary gelation time of 6 min, and calcium lactate concentration of 0.05 mole/L in secondary gelation; however, lack-of-fit test showed a significant difference. The p-value of X_1 and X_2 was smaller than 0.05, indicating the effect of X_1 and X_2 on sphericity was significant, and X_1 was the most important independent variable of sphericity.

The liquid-core hydrogel bead were formulated by extruding liquid-core material into the

Table 3-18 Experimental results of sphericity (Y_6) for different formulations of liquid-core hydrogel bead.

Run	$Y_6 (\times 10^{-2})$	Run	$Y_6 (\times 10^{-2})$	Run	$Y_6 (\times 10^{-2})$
1	4.37±0.21 ^{gh}	11	6.52±0.12 ^{cdef}	21	2.46±0.17 ⁱ
2	4.62±0.25 ^g	12	6.80±0.51 ^{bcd}	22	2.57±0.23 ⁱ
3	4.40±0.07 ^{gh}	13	7.41±0.36 ^{bcd}	23	2.40±0.18 ⁱ
4	4.27±0.31 ^{gh}	14	7.91±0.56 ^b	24	2.36±0.14 ⁱ
5	6.24±0.47 ^{def}	15	7.52±0.48 ^{bc}	25	2.58±0.25 ⁱ
6	6.04±0.37 ^{ef}	16	7.50±0.61 ^{bc}	26	2.32±0.23 ⁱ
7	6.15±0.25 ^{ef}	17	6.40±0.49 ^{cdef}	27	2.29±0.12 ⁱ
8	5.89±0.78 ^f	18	11.41±0.90 ^a	28	2.22±0.20 ⁱ
9	6.51±0.56 ^{cdef}	19	3.33±0.26 ^{hi}	29	2.33±0.21 ⁱ
10	6.81±0.19 ^{bcd}	20	7.18±0.46 ^{bcd}	30	2.49±0.06 ⁱ

^{a-i} Means each treatment with different superscript letters are significantly different at $p < 0.05$.

Table 3-19 Regression coefficients of the fitted quadratic equations for sphericity (Y_6)

Parameter ¹	DF ²	Estimate	Standard error	t value	p value
Intercept	1	2.37×10^{-2}	3.66×10^{-3}	6.47	<0.001
X ₁	1	-1.04×10^{-2}	1.83	-5.69	<0.001
X ₂	1	-7.52×10^{-3}	1.83	-4.11	<0.001
X ₃	1	2.64×10^{-4}	1.83	0.14	0.887
X ₄	1	-2.60×10^{-4}	1.83	-0.14	0.889
X ₁ ×X ₂	1	-1.85×10^{-3}	2.24	-0.82	0.423
X ₁ ×X ₃	1	1.62×10^{-4}	2.24	0.07	0.943
X ₁ ×X ₄	1	8.83×10^{-4}	2.24	0.39	0.700
X ₂ ×X ₃	1	-1.42×10^{-4}	2.24	-0.06	0.951
X ₂ ×X ₄	1	-4.29×10^{-4}	2.24	-0.19	0.851
X ₃ ×X ₄	1	-6.21×10^{-4}	2.24	-0.28	0.786
X ₁ ²	1	1.87×10^{-2}	1.71	10.92	<0.001
X ₂ ²	1	9.58×10^{-3}	1.71	5.59	<0.001
X ₃ ²	1	2.73×10^{-3}	1.71	1.59	0.133
X ₄ ²	1	2.39×10^{-3}	1.71	1.40	0.183

¹X₁, primary gelation time; X₂, concentration of calcium lactate in primary gelation; X₃, secondary gelation time; X₄, concentration of calcium lactate in secondary gelation.

²DF, degrees of freedom

Table 3-20 Summary of ANOVA for sphericity (Y_6).

Sources	DF ¹	SS ¹	R square	MS ¹	F value	p value
Model	14	1.50×10^{-2}	0.93		13.34	<0.001
Linear	4	3.97×10^{-3}	0.24		12.33	<0.001
Quadratic	4	1.10×10^{-2}	0.68		34.12	<0.001
Crossproduct	6	7.68×10^{-5}	0.004		0.16	0.984
Residual	15	1.21×10^{-3}		8.05×10^{-5}		
Lack of fit	10	1.20×10^{-3}		1.20×10^{-4}	65.08	<0.001
Pure error	5	9.21×10^{-6}		1.84×10^{-6}		
Factor						
X_1^2	5	1.22×10^{-2}		2.46×10^{-3}	30.50	<0.001
X_2	5	3.9×10^{-3}		7.86×10^{-4}	9.77	<0.001
X_3	5	2.0×10^{-4}		4.25×10^{-5}	0.53	0.752
X_4	5	2.0×10^{-4}		3.60×10^{-5}	0.45	0.809

¹SS, sum of squares; DF, degrees of freedom; MS, mean squares.

² X_1 , primary gelation time; X_2 , concentration of calcium lactate in primary gelation; X_3 , secondary gelation time; X_4 , concentration of calcium lactate in secondary gelation.

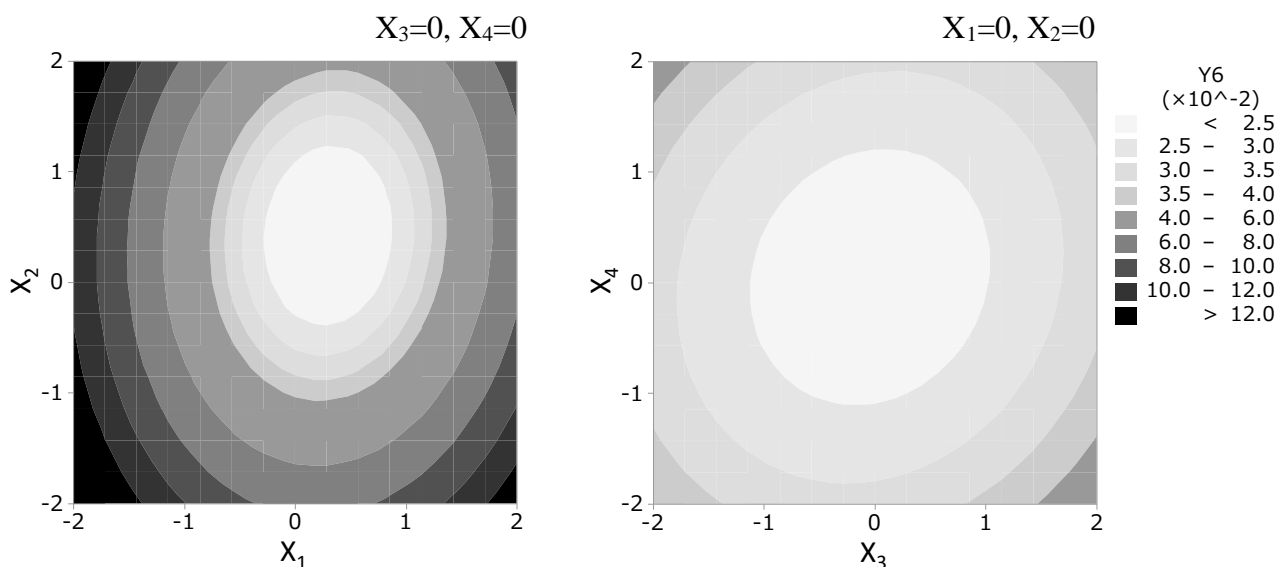


Figure 3-7 Two-dimensional corresponding contour plot for sphericity (Y_6).

alginate solution with a hypodermic needle (Figure 3-1a). The droplet of the liquid-core material changed from a drop-like shape to a sphere as it was extruded into the alginate solution; however, the droplet could not become a perfect sphere even when the distance between the front end of the needle and the surface of alginate solution was enlarged to 30 cm. On the other hand, the sphericity of the liquid-core hydrogel bead decreased and then increased with the increase of X_1 and X_2 . This can be explained as follows: the droplet of the liquid-core material was fragile and it was deformed as it passed through the surface of alginate solution. The droplet gradually returned to sphere during primary gelation (Figure 3-1e), but it deformed into an elongated blob when primary gelation time was too long (Figure 3-1f). Moreover, the rate of gelation is positively correlated with the concentration of calcium ions (Lee & Rogers, 2012), and in low calcium lactate concentration, gelation was so slow that liquid-core hydrogel beads were disrupted before their structure was stable enough to resist the deformation (Figure 3-1c). Conversely, in high calcium lactate concentration, gelation was so fast that a thick calcium alginate outer layer was formed before the shape of droplet returned to sphere (Figure 3-1d).

3.4.7. Optimization of the liquid-core hydrogel bead

All the p-values of linear and quadratic term of models were lower than 0.05, and all the p-values of the cross-product were higher than 0.05. The results indicated the linear and quadratic terms were significantly important, and interactions between independent variables were not significant. Because the swelling capacity and the sphericity were rather unsatisfactory statistical parameters for the lack-of-fit testing, these two dependent variables could not be applied for optimization of the liquid-core hydrogel bead formulation.

The response of optimizing the four independent variables in the CCD are shown in Table 3-21. The hardness (Y_1), encapsulation efficiency (Y_2), and release profile of total phenolic compounds in simulated gastric digestion (Y_3) were the main factors that determine the quality of liquid-core hydrogel bead, and since the models were not significantly different in the lack-

Table 3-21 Optimum conditions for the preparation of the liquid-core hydrogel bead.

Parameter ¹		Dependent variables ²			Optimal conditions
		Y ₁	Y ₂	Y ₃	
Coded	X ₁	0.67	-0.70	0.27	-0.101
	X ₂	0.33	0.36	0.27	0.303
	X ₃	0.06	0.02	0.13	0.0202
	X ₄	1.00	0.45	-0.18	0.303
Uncoded	X ₁ (min)	31.70	18.00	27.70	23.99
	X ₂ (mole/L)	0.13	0.13	0.13	0.13
	X ₃ (min)	6.12	6.04	6.26	6.04
	X ₄ (mole/L)	0.075	0.061	0.046	0.058
Target		Maximum	Maximum	Minimum	
Predict value		27.99 N	87.37 %	21.25 %	
Predict value of optimization capability ³		26.08±0.59	86.17±0.83	26.71±0.72	
Experimental value of optimization capability ⁴		25.50±1.20	85.67±1.71	27.38±0.65	
Error (%) ⁵		2.21	0.57	-2.47	

¹X₁, primary gelation time; X₂, concentration of calcium lactate in primary gelation; X₃, secondary gelation time; X₄, concentration of calcium lactate in secondary gelation.

² Y₁, hardness (N); Y₂, encapsulation efficiency (%); Y₃, release profile of total phenolic compounds in simulated gastric digestion (%).

³The results of multiple response optimization were predicted by MINITAB statistical software with optimal conditions.

⁴The actual values of dependent variables of the liquid-core hydrogel bead which were prepared with optimal conditions.

⁵Error (%) = [(Predicted value – Experimental value) / Predicted value] × 100.

of-fit test, these dependent variables were used to search the optimal condition of preparing liquid-core hydrogel bead. Although the lack-of-fit test of the release profile of total phenolic compound in simulated gastric digestion (Y_4) was not significant either, the result of the RSREG procedure indicated that the eigenvalues of Y_4 were all positive. Positive eigenvalues show an upwards curvature, and if all eigenvalues are positive, the stationary point of the surface is the minimum point (Blows & Brooks, 2003). However, to ensure that the functional compounds could be absorbed efficiently, I expected the release profile of total phenolic compound in simulated gastric digestion should be high. In addition, the accuracy of optimal conditions was low when Y_4 was used as a dependent variable in multiple response optimization with Y_1 , Y_2 , and Y_3 in the pretest. From the reasons above, Y_4 was eliminated from the dependent variables of multiple response optimization.

In the first step of multiple response optimization, the conditions were optimized for each of the three dependent variables. As shown in Table 3-21, the optimized values of primary gelation time (X_1) ranged from 18.00 to 31.70 min, calcium lactate concentration in the primary gelation (X_2) was 0.13 mole/L, secondary gelation time (X_3) ranged from 6.04 to 6.26 min, and calcium lactate concentration in the secondary gelation (X_4) ranged from 0.046 to 0.075 mole/L. The overlay plot indicating the region of optimal process variable settings are shown in Figure 3-8. When X_1 , X_2 , X_3 , and X_4 were in the ranges of 13.58 to 31.81 min (coded variables -1.14 to 0.68), 0.08 to 0.18 mole/L (coded variables -0.91 to 1.49), 3.73 to 8.28 min (coded variables -1.14 to 1.14), and 0.033 to 0.084 mole/L (coded variables -0.67 to 1.35), respectively, the liquid-core hydrogel bead would show hardness over 20 N, encapsulation efficiency over 80 %, and release profile of total phenolic compounds in simulated gastric digestion less than 25 %.

In the second step, the target values of Y_1 =maximum, Y_2 =maximum, and Y_3 =minimum were set in multiple response optimization. The optimal conditions obtained were X_1 =23.99 min (about 23 min 59 sec), X_2 =0.13 mole/L, X_3 =6.04 min (about 6 min 2 sec), and X_4 =0.058 mole/L, and the liquid-core hydrogel bead demonstrated 25.50 N of hardness, 85.67 % of encapsulation

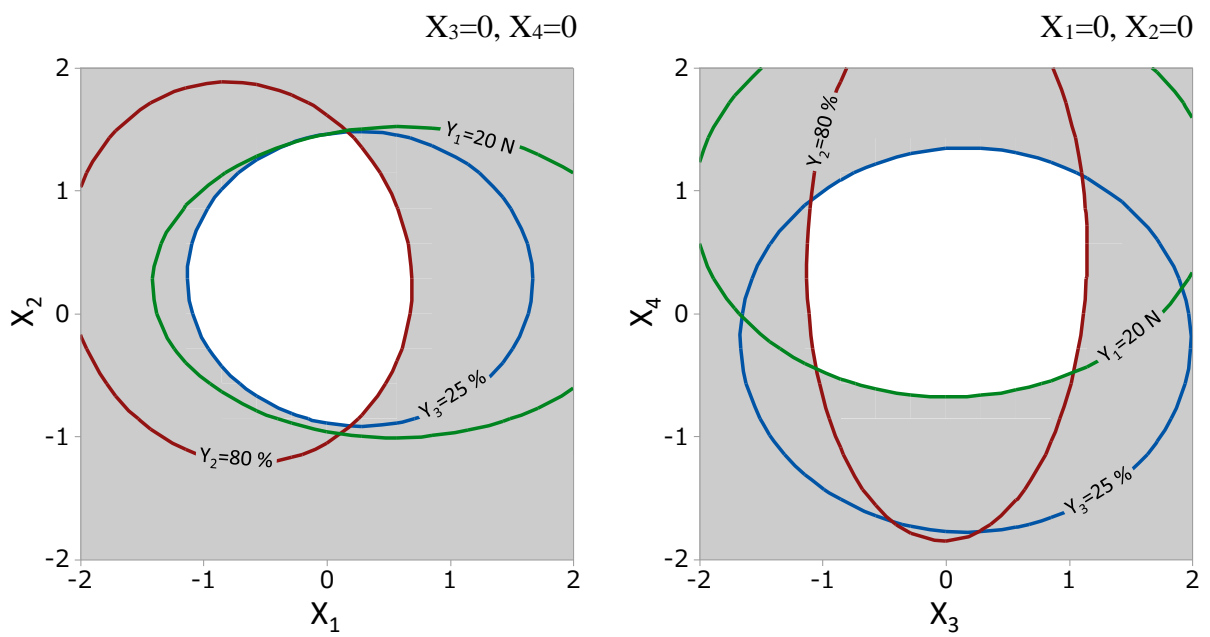


Figure 3-8 Overlay plot indicating the region of optimal process variable settings.

efficiency and release profile of total phenolic compounds in simulated gastric digestion of 27.38 % with small error-values (2.21, 0.57 and -2.47 %, respectively).

3.5. Conclusions

Our previous study (F. H. Tsai, Chiang, Kitamura, Kokawa, & Khalid, 2016) indicated that first and secondary gelation had different effects on physical properties of the liquid-core hydrogel bead; however, the importance of these preparation steps on each physical property were not studied. In this chapter, RSM was used for examining the effects and importance on different physical properties, and optimal conditions of the liquid-core hydrogel bead was investigated. Out of the seven dependent variables, average diameter, hardness (Y_1), encapsulation efficiency (Y_2), release profile of total phenolic compounds in simulated gastric (Y_3) and small intestinal (Y_4) digestion, swelling capacity (Y_5), and sphericity (Y_6), hardness, encapsulation efficiency, and release profile of total phenolic compounds in simulated gastric digestion were used for optimizing the conditions of the liquid-core hydrogel bead formulation because their lack-of-fit test showed no significant difference ($p > 0.05$). The optimized liquid-core hydrogel bead had a high hardness (25.50 N) and encapsulation efficiency (85.67 %), and low release profile of total phenolic compounds (27.38 %) in simulated gastric digestion with small error-values. The result demonstrated that the mathematical models obtained from the CCD were well fitted. Optimal conditions of the liquid-core hydrogel bead was primary gelation time of 23 min 59 sec, calcium lactate concentration of 0.13 mole/L in the primary gelation, secondary gelation time of 6 min 2 sec, and calcium lactate concentration of 0.058 mole/L in secondary gelation. Primary gelation time (X_1) had a relatively large effect on the encapsulation efficiency, sphericity, and average diameter; calcium lactate concentration in primary gelation (X_2) greatly affected total phenolic compounds release in simulated gastric digestion and simulated intestinal digestion; secondary gelation time (X_4) had a large influence on the hardness and the swelling capacity. The results indicated that the calcium lactate was a suitable calcium source

for preparing hydrogel particles and it could replace calcium chloride, which is more commonly used but has a bitter flavor. I expect that the liquid-core hydrogel bead prepared with reverse spherification could be used in commercial products.

4. Physical properties of liquid-core hydrogel beads with gum arabic and glycerol

I used reverse spherification, where radish by-product juice mixed with calcium ion are dropped into alginate/gum arabic and alginate/glycerol solution to produce liquid-core hydrogel beads, and evaluated the effect of different wall materials on the average diameter, sphericity, hardness, encapsulation efficiency, swelling capacity, and microstructure of alginate/gum arabic and alginate/glycerol bead. The different variations of liquid-core hydrogel bead were prepared by achieve alginate/gum arabic or alginate/ glycerol weight ratios of 0/1 (HB0), 0.25/0.75 (GA0.25 or GL0.25), 0.5/ 0.5 (GA0.5 or GL0. 5), and 0.75/0.25 (GA0.75 or GL0.75) in primary gelation. GA0.25 had the highest hardness and GA0.5 had the highest encapsulation efficiency (86.67 %). In the other hand, there are some cracks were observed on the surface of alginate/glycerol bead. The result demonstrated that gum arabic is a potential material for improving the physical properties of liquid-core hydrogel beads.

4.1. Introduction

Preparing the liquid-core hydrogel bead by reverse phase spherification has received increased attention in recent years. Materials which have high functionality and are suitable for reverse phase spherification processing have been searched for. Our studies demonstrated that liquid-core hydrogel bead, which produced with alginate, prevents the DPPH-scavenging ability of functional compounds from decreasing during storage (F. H. Tsai et al., 2016) and examined the release profiles of functional compounds during thermal and simulated gastrointestinal digestion (*in vitro*) (Fu Hsuan Tsai et al., 2017). These results indicated that alginate could be used as a potential delivery method.

However, properties such as encapsulation efficiency, hardness, and release characteristics in gastric digestion could be improved for more efficient delivery. Amine et al., (2014) indicated that ionotropically gelled alginate has a high permeability and entrapped compounds are released from alginate hydrogel beads rapidly due to their hydrophilic and porous structure.

Some studies have reported that improving physicochemical properties of alginate by adding other polymers as fillers, such as tapioca starch, chitosan and gum arabic (Chopra et al., 2015; Lozano-Vazquez et al., 2015; Mukhopadhyay, Chakraborty, Bhattacharya, Mishra, & Kundu, 2015). Furthermore, Ben Messaoud et al. (2016) indicated that mixing alginate with shellac polyesters could modify alginate shell properties of the liquid-core hydrogel bead.

Gum arabic, also known as gum acacia, is a highly branched natural polymer formulated from the tree sap of Acacia Senegal trees. The backbone of gum arabic consists of β -D-galactopyranosyl units and side chains are composed of L-arabinose, L-rhamnose, D-galactose, and D-glucuronic acid (Chopra et al., 2015; Nayak et al., 2012). It is an inexpensive biopolymer which is being extensively used as stabilizer, thickening agent, hydrocolloid emulsifier, and carrier in food, pharmaceutical, and cosmetic industries (Nami, Haghshenas, & Yari Khosroushahi, 2016).

Alginate and gum arabic are both biodegradable and biocompatible polymers as well as

generally regarded as safe (GRAS) by the United States Food and Drug Administration (USFDA). Fang et al. (2011) indicated that in the case of dry alginate beads, the addition of gum arabic reduced the side-by-side aggregation of the egg-box structure of the alginate. Side-by-side aggregation occurs when calcium alginate is dried. The egg-box junctions are drawn together due to the collapse of the alginate network, which results in further combining of the egg-box junctions by the presence of calcium ions. Side-by-side aggregation leads to a loss of the swelling capacity of calcium alginate. The combination of alginate and gum arabic has attracted attention for the protection of probiotic bacteria and drugs during drying, storage, and in the gastric tract (Chopra et al., 2015; Nami et al., 2016; Nayak et al., 2012).

The flexibility of polymers is improved by adding plasticisers. Some studies show that the addition of plasticizer could decrease the glass transition temperature and the melting temperature of polymer (Jost et al., 2014). Glycerol, one of plasticisers, is able to increase film flexibility, processability, and permeability to oxygen of edible film by reducing internal hydrogen bonding between polymer chains, increasing intermolecular spacing of polymer and attracting water. (Rojas-Graü, Tapia, Rodríguez, Carmona, & Martin-Belloso, 2007)

However, to our knowledge, little or no information is currently available on the liquid-core hydrogel bead prepared by alginate/gum arabic or alginate/ glycerol matrix.

4.2. Objectives

This part is the first study to prepare liquid-core hydrogel bead from alginate combined with gum arabic or glycerol by reverse spherification. The objectives of this work were to evaluate physical properties, average, sphericity, hardness, encapsulation efficiency, and swelling capacity, of the alginate/gum arabic bead and alginate/glycerol bead. Furthermore, the thermal prosperity and morphology of alginate/gum arabic and alginate/ glycerol outer layer was investigated.

4.3. Materials and methods

4.3.1. Materials

Radish leaves were obtained from a local farmer and prepared as described in the section 2.3.1. All chemicals in the investigation were commercially available and of analytical grade. The information of sodium alginate, chitosan 100, acetic acid, calcium lactate, sodium carbonate (Na_2CO_3), ethanol, and Folin-Ciocalteu reagent is described in the section 3.3.1. Gum arabic and glycerol were purchased from Wako Pure Chemical Industries, Ltd. (Japan). The viscosity of 1 % gum arabic was $3.1 \text{ mPa} \cdot \text{s}$ at 20°C .

4.3.2. Formulation of liquid-core hydrogel bead

Radish by-product juice was prepared as described in the section 3.3.2. Liquid-core hydrogel bead is a hydrogel particle that is composed of an alginate, alginate/gum Arabic, or alginate/glycerol outer layer and a core of liquid-core material (radish by-product juice, chitosan and acetic acid). The wall materials of liquid-core hydrogel bead were prepared from 100 mL of solutions containing 1 g of alginate and different amounts of gum arabic or glycerol (0.00, 0.33, 1.00, and 3.00 g), to achieve alginate/gum arabic or alginate/ glycerol weight ratios of 0/1, 0.25/0.75, 0.5/ 0.5, and 0.75/0.25, respectively. These different variations of liquid-core hydrogel bead were coded and shown in Table 4-1. Liquid-core material consists of 2 g chitosan, 1 mL acetic acid, and 3.70 g calcium lactate, and then adding radish by-product juice to achieve a final concentration of 0.12 mole/L of calcium lactate solution. Liquid hydrogel beads were prepared by following the method of the section 3.3.2. with dropping the liquid core material into the wall material through a 20G flat-tipped hypodermic needle with gentle stirring for 25 min. The beads were collected by filtration and rinsed sequentially with distilled water and 95% ethanol. Following secondary gelation, where liquid-core hydrogel beads were suspended for 6 min in 0.05 mole/L calcium lactate solution, liquid-core hydrogel beads were collected and rinsed sequentially with distilled water and 95% ethanol again.

4.3.3. Average diameter and sphericity

The average diameter and sphericity of each variation were measured by following the method of the section 3.3.3.

4.3.4. Hardness

The hardness of each variation was measured by following the method of the section 3.3.4.

Relative hardness was calculated with the following equation, using HB0 as a standard:

$$\text{Relative hardness (\%)} = \text{Hardness of each variation} / \text{Hardness of HB0} \times 100$$

4.3.5. Encapsulation efficiency

The encapsulation efficiency of each variation was measured by following the method of the section 3.3.5.

4.3.6. Swelling capacity

The swelling capacity of each variation was measured by following the method of the section 3.3.7.

4.3.7. Differential scanning calorimetry

According to the method of Lupo, Maestro, Gutiérrez, & González (2015) with some modifications. Alginate/gum arabic and alginate/ glycerol beads were dried by a freeze dryer (FD-1, Tokyo Rikakikai, Japan) for 12 h. Approximately 3 mg of dried alginate/gum arabic and alginate/glycerol outer layer was removed from each variation and sealed in an aluminum sample pan. The thermal property of outer layer was determined by a differential scanning calorimetry (DSC-60, Shimadzu Corporation, Japan). The sample was heated from 20 °C to 300 °C at a rate of 10 °C/ min with a flow rate of 30 mL/min of nitrogen and an empty aluminum

pan was used as a reference.

4.3.8. Morphology

Dry alginate/gum arabic and alginate/glycerol beads were prepared with a freeze dryer as described in the section 4.3.6. and then fixed on an stub with double-sided adhesive tape. The beads were coated with a platinum–palladium with a sputter coater (E-1045, Hitachi, Japan) under vacuum. The microstructure of the beads was observed by a scanning electron microscope (JSM-6330F, JEOL, Japan) with accelerating potential of 5kV.

4.3.9. Statistical analysis

All experiments were run at least in triplicate. The results were presented as the mean± standard deviation and analyzed using Statistical Analysis System software (Version 8.01, SAS Institute Inc., USA). One-way analysis of variance (ANOVA), followed by Duncan's multiple comparison test, was performed. Responses with p values <0.05 were considered significant.

4.4. Results and Discussion

4.4.1. Average diameter

The average diameter of different variation of alginate beads ranged from 4.58 to 5.66 mm (Table 4-2). HB0 showed a smallest diameter, and the average diameter increased with the increase of the amount of gum arabic and glycerol. There was no significant difference between HB0 and GA0.25 as well as between HB0 and GA0.5 ($p < 0.05$); however, GA0.75 showed a relatively larger diameter. The average diameter of GL 0.5 and GL 0.75 were also larger than HB0. Our former study (F. H. Tsai et al., 2016) demonstrated that semifinished beads tended to shrink during secondary gelation because alginate in the outer layer of alginate/gum arabic beads were pulled together by calcium ions. I inferred that GA0.75 showed a relatively higher diameter, which is similar to that of semifinished beads, because gum arabic was a barrier to

Table 4-1 Formulation of alginate/gum arabic and alginate/glycerol bead

Code		Ratio	Improver ¹ (g/100mL)	Alginate (g/100mL)
Alginate/ gum arabic beads	Alginate/ glycerol beads			
	HB0	0:1	0	1
GA0.25	GL0.25	0.25:0.75	0.33	1
GA0.5	GL0.5	0.5:0.5	1	1
GA0.75	GL0.75	0.75:0.25	3	1

¹ Improver means gum arabic or glycerol

Table 4-2 Average diameter of alginate/gum arabic and alginate/glycerol beads.

Ratio (GA ¹ or GL: alginate)	Average diameter (mm)	
	GA	GL
0:1	4.63±0.07 ^c	
0.25:0.75	4.58±0.02 ^c	4.78±0.30 ^{bc}
0.5:0.5	4.82±0.09 ^{bc}	5.03±0.14 ^b
0.75:0.25	5.66±0.16 ^a	5.00±0.28 ^b

¹ GA, gum arabic; GL, glycerol

Means of 3 replicates ± standard deviation.

^{a-c} Means each treatment with different superscript letters are significantly different at $p < 0.05$.

Table 4-3 Sphericity of alginate/gum arabic and alginate/glycerol beads.

Ratio (GA ¹ or GL: alginate)	Sphericity ($\times 10^{-2}$)	
	GA	GL
0:1	3.55±0.22 ^a	
0.25:0.75	1.36±0.01 ^b	3.27±0.99 ^a
0.5:0.5	1.76±0.29 ^b	2.43±0.89 ^{ab}
0.75:0.25	1.34±0.32 ^b	2.42±0.63 ^{ab}

¹ GA, gum arabic; GL, glycerol

Means of 3 replicates ± standard deviation.

^{a-b} Means each treatment with different superscript letters are significantly different at $p < 0.05$.

the combining of alginate.

4.4.2. Sphericity

Sphericity is an efficiency factor that evaluates the roundness of hydrogel beads. A higher value indicates a greater degree of deformation, and a value of zero indicates a perfect sphere. A hydrogel bead is considered a sphere if the sphericity is lower than 0.05 because the shape distortion cannot be obviously distinguished by human vision (Chan et al., 2009; Chew & Nyam, 2016). The result also showed that the addition of gum arabic decrease the sphericity and there is no significant difference with HBO and the beads which were modified with glycerol. During the primary gelation, which has been demonstrated to be the shape-determining step, the droplet of the liquid-core material is extruded from a syringe with a needle into the wall material solution. The liquid-core material is not a perfect sphere and is fragile to deformation as it passes through the surface of wall material solution, but returns to a spherical shape during in an appropriate primary gelation time. I inferred that the reason that HBO has a higher sphericity is because the conjugation of alginate without the interference, such as gum arabic, was so fast that the liquid-core material could not return to a perfect sphere before the shape was set. The glycerol had no significant interference during gelation because of the small molecule weight. However, the sphericity of all the variations were lower than 0.05, and they could thus, be considered as spheres.

4.4.3. Hardness

The results are shown in Table 4-4. A wide range of hardness could be observed by changing the ratios of alginate, gum arabic and glycerol in the formulation. The hardness of alginate/gum arabic bead and alginate/ glycerol bead ranged from 6.53 N to 26.68 N, and GA0.25 showed the highest hardness among all of the variation. Jost, Kobsik, Schmid, & Noller, (2014) indicated that even if alginate is good at holding water and controlling drug release, in addition

to being widely used as an air barrier, the brittleness of alginate film is one of the obstacles that needs to be overcome. The results demonstrate that gum arabic and glycerol have an ability to improve the hardness of alginate beads. However, an increase of gum arabic and glycerol break the balance of interactions between gum arabic/glycerol, alginate, and calcium, causing the hardness of alginate/gum arabic bead and alginate/glycerol bead to decrease (Chopra et al., 2015).

4.4.4. Encapsulation efficiency

Encapsulation efficiency was expressed as the ratio between the total phenolic compounds content in alginate/gum arabic beads and the total phenolic compounds content in the liquid-core material, the total amount used to prepare alginate/gum arabic beads. Low encapsulation efficiency could lead to a high cost of preparation and a less valuable product (Zucker et al., 2009). According to Table 4-5, GA0.5 showed the highest encapsulation efficiency (86.67 %), which was higher than that of HB0 (83.80 %). The result showed that the addition of the gum arabic could improve the encapsulation efficiency of alginate beads. The study of Chopra et al. (2015) also indicated that the encapsulation efficiency of alginate beads is increased by adding a proper concentration of gum arabic because of the interaction between alginate and gum arabic. Furthermore, the wall material of the alginate and gum arabic mixture has a higher viscosity, preventing the total phenolic compounds release during preparation (A. K. Nayak et al., 2012). However, increasing the gum arabic ratio greater than GA0.5 decreases the encapsulation efficiency. It was attributed to gum arabic is being unable to undergo a gelation by itself; therefore, total phenolic compounds leak out from alginate/gum arabic beads with that contain a high amount of gum arabic in the wall material (Fang et al., 2011). The encapsulation efficiency of alginate/glycerol beads ranged from 74.47 to 77.74 %. Glycerol is a high hydrophilic plasticizer, the drawback on leaching of ingredient during processing was reported by some study (Santana & Kieckbusch, 2013).

Table 4-4 Hardness of alginate/gum arabic and alginate/glycerol beads.

Ratio (GA ¹ or GL: alginate)	Hardness (N)	
	GA ¹	GL
0:1	21.46±1.27 ^c	
0.25:0.75	26.68±1.18 ^a	24.08±1.62 ^b
0.5:0.5	19.30±1.34 ^c	20.56±1.34 ^c
0.75:0.25	6.53±0.54 ^d	19.91±0.72 ^c

¹ GA, gum arabic; GL, glycerol

Means of 3 replicates ± standard deviation.

^{a-d} Means each treatment with different superscript letters are significantly different at $p < 0.05$.

Table 4-5 Encapsulation efficiency of alginate/gum arabic and alginate/glycerol beads.

Ratio (GA ¹ or GL: alginate)	Encapsulation efficiency (%)	
	GA ¹	GL
0:1	83.80±0.87 ^b	
0.25:0.75	85.65±0.52 ^{ab}	77.74±1.56 ^c
0.5:0.5	86.67±1.45 ^a	78.20±1.09 ^c
0.75:0.25	72.91±1.64 ^d	74.47±1.11 ^d

¹ GA, gum arabic; GL, glycerol

Means of 3 replicates ± standard deviation.

^{a-d} Means each treatment with different superscript letters are significantly different at $p < 0.05$.

Table 4-6 Swelling capacity of alginate/gum arabic and alginate/glycerol beads.

Ratio (GA ¹ or GL: alginate)	Swelling capacity (%)	
	GA ¹	GL
0:1	18.70±0.80 ^c	
0.25:0.75	16.89±0.81 ^d	25.20±1.14 ^a
0.5:0.5	14.26±0.98 ^e	21.23±0.68 ^b
0.75:0.25	7.10±0.50 ^g	11.83±0.39 ^f

¹ GA, gum arabic; GL, glycerol

Means of 3 replicates ± standard deviation.

^{a-g} Means each treatment with different superscript letters are significantly different at $p < 0.05$.

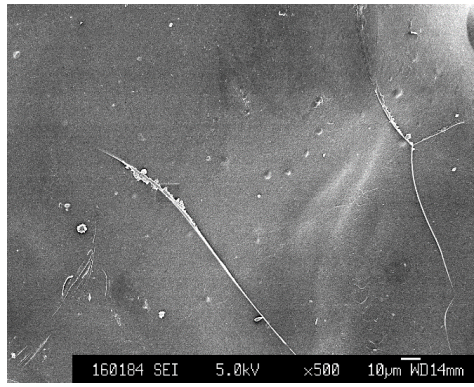
4.4.5. Swelling capacity

The swelling capacity of liquid-core hydrogel bead is considered to be related to the presence of osmotic pressure between liquid-core hydrogel bead and environment, and lower swelling capacity indicates higher stability. Some apertures may form because of alginate polymer bonding without combining with Ca^{2+} during gelation. When liquid-core hydrogel bead is suspended in a solution, water tends to fill these apertures, causing water absorption until the equilibrium state is reached (Pasparakis & Bouropoulos, 2006). The phenomenon causes the egg-box structure of alginate to become fragile, reduces the hardness of the liquid-core hydrogel bead and results in the release of compounds from the core. Table 4-6 shows that the swelling capacity of alginate/glycerol beads was higher than alginate/gum arabic bead. The study of Darmokoesoemo, Pudjiastuti, Rahmatullah, & Kusuma (2017) indicated that glycerol relaxes the intermolecular interaction of alginate, resulting in the stretching of polymer during dissolution process. On the other hand, the addition of gum arabic could reduce the swelling capacity of alginate beads. Gum arabic is an ampholytic polymer. This characteristic makes gum arabic attract alginate molecules, which are negatively charged, with electrostatic forces. Calcium ions do not only play a role as a crosslinker of alginate; they also react with the carboxylate groups of gum arabic (Fang et al., 2011; A. K. Nayak et al., 2012).

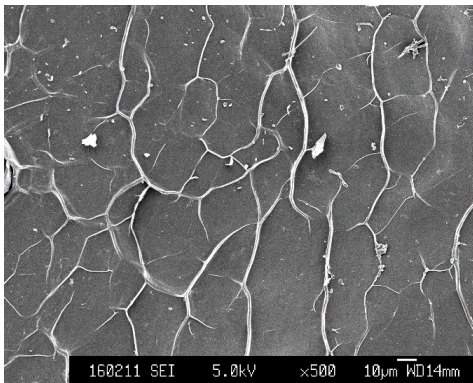
4.4.6. Microstructure

The microstructure of alginate/gum arabic bead and alginate/glycerol bead were visualized by SEM and is presented in Figure 4-1. These SEM photographs reveal some wrinkles on the surface of all variations of liquid-core hydrogel bead, which may be due to the partial collapse of the polymer during freeze drying (A. K. Nayak et al., 2016).

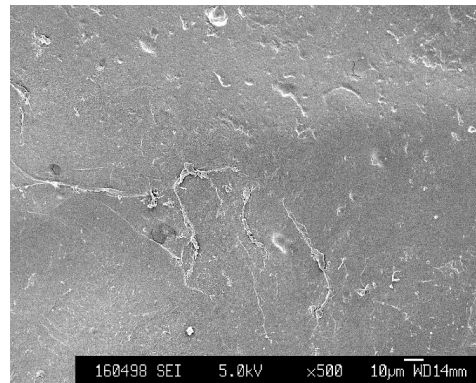
HB0 had a relatively smoother surface than other treatments (Figure 4-1a). With the increase of gum arabic ratio, the surface of alginate/gum arabic bead became rougher at first, and then became smooth again. The surface of GA0.25 was roughest, and a ridge structure was observed



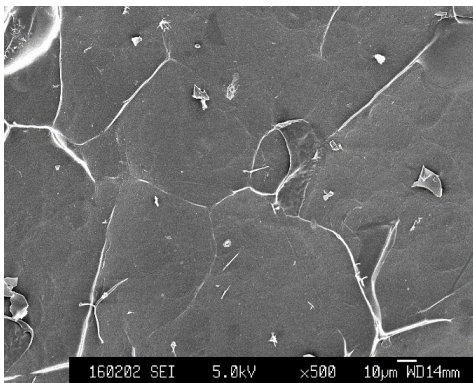
(a)



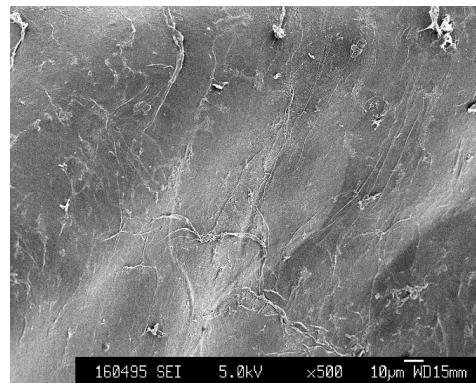
(b)



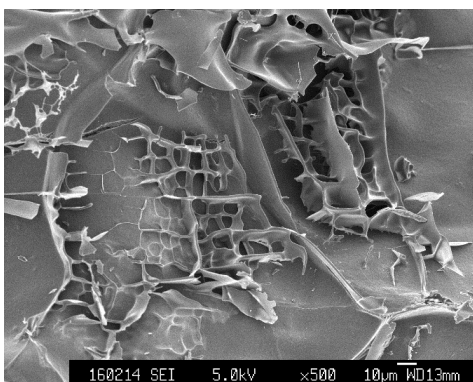
(c)



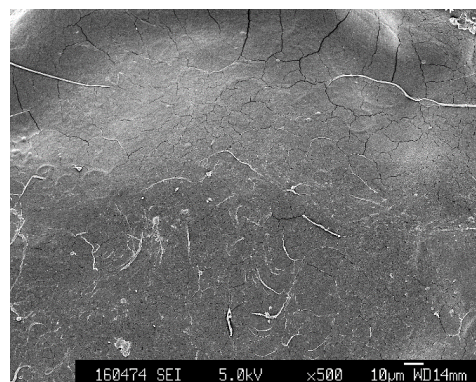
(d)



(e)



(f)



(g)

Figure 4-1 Microstructure of alginate/gum arabic and alginate/glycerol beads ($\times 500$).

(a) HB0; (b) GA0.25; (c) GL0.25; (d) GA0.5; (e) GL0.5; (f) GA0.75; (g) GL0.75.

(Figure 4-1b). The ridge structure was also observed on the liquid-core hydrogel bead which were prepared by reverse spherification with a high concentration of calcium chloride solution (Fu Hsuan Tsai et al., 2017). Interestingly, this study indicated that the liquid-core hydrogel bead in which the ridge structure was observed had a good controlled-release ability. This result is similar to that of this study: GA0.25, in which a clear ridge structure can be observed, also shows a slow total phenolic compounds release (Figure 5-6). Perhaps the ridge structure could be regarded as a feature of the liquid-core hydrogel bead indicating good controlled-release ability, although further studies are required for confirmation. GA0.75 exhibited a very porous surface with some tortuous flake structure (Figure 4-1d). The phenomenon resulted in the low encapsulation efficiency and hardness, and a poor ability for slowing down the release of total phenolic compounds of GA0.75. Some studies have indicated that alginate-based beads are characterized with a porous and collapsed structure (Belščak-Cvitanović et al., 2015). However, this phenomenon was not observed in the most of the alginate/gum arabic beads except GA0.75, which indicates that the influence of materials on the morphology of hydrogel beads depends on the preparation method used. Alginate/glycerol beads showed a smoother outer-layer than alginate/gum arabic beads. The film structures were observed on alginate/glycerol beads and these structures increased with the ratio of glycerol. The film structures could indicate the weak interaction between alginate. Moreover, GL0.75 showed some cracks on the surface. These phenomenon could explain the relatively lower hardness (Table 4-4) and encapsulation efficiency (Table 4-5) on GL0.75.

4.5. Conclusions

This study revealed the physicochemical properties of alginate/gum arabic and alginate/glycerol liquid-core hydrogel bead. According to this study, gum arabic is a good material to improve the physicochemical properties of alginate liquid-core hydrogel beads. The average diameter increased with the increase of the ratio of gum arabic or glycerol. All of the

variations showed a small sphericity (lower than 0.05) and demonstrated that the deformation of bead is not clearly visible by human eyes. The hardness of alginate/gum arabic bead (6.53 N to 26.68 N) changed significantly than the alginate/glycerol bead (19.91 N to 24.08 N). Alginate/ gum arabic bead showed the higher encapsulation efficiency and the lower swelling capacity than alginate/ glycerol bead. The SEM results showed that there are some cracks on the surface of alginate/ glycerol bead, resulting in the relatively lower hardness and encapsulation efficiency. In the future, this study may be useful for the quality improvement of delivery system.

5. Release behavior improvement of liquid-core hydrogel beads with gum arabic

Different weight ratios of alginate/gum arabic solutions were prepared to serve as the wall material of liquid-core hydrogel beads that were formulated to protect the total phenolic compounds of radish by-product juice from releasing during storage and in simulated gastrointestinal digestion. The liquid-core hydrogel bead formulated with 25 % gum arabic (GA0.25) was effective in preventing total phenolic compounds from losing during storage with a decay rate (k) of $6.10 \times 10^{-3} \text{ day}^{-1}$ and a half-life ($t_{1/2}$) of 113.63 days, it showed the slowest release of total phenolic compounds in simulated gastric digestion and the release mechanism followed Fickian diffusion. GA0.25 also showed the highest hardness among all of the variation. The results suggest that gum arabic is effective in improving the release properties of alginate.

5.1. Introduction

Reverse spherification, one of the encapsulation methods, is used for preparing liquid-core hydrogel beads. The method is performed by dripping droplets that contain ions and bioactive compounds, into an ionotropic polymer solution. The most common materials are Ca^{2+} and alginate. Alginate is a natural linear biopolymer consisting of 1,4-linked β -D-mannuronic (M residues) and α -L-guluronic acids (G residues) (Pawar & Edgar, 2012). Normally, it is extracted from brown algae. It is widely used to prepare hydrogel beads because it forms gels with multivalent cations (crosslink agents) such as calcium ions under gentle conditions. Gelation occurs while G residues coordinate with calcium ions, forming calcium alginate, a three-dimensional gel network known as an egg-box structure (George & Abraham, 2006; Paques, Van Der Linden, Van Rijn, & Sagis, 2014). Although, various ingredients have been encapsulated in gelled alginate beads, successfully. The leakage of these ingredients from the pores of gelled alginate during processing is a major limitation (Singh, Sharma, & Chauhan, 2010). A growing interest in the exploration of the natural, non-toxic, biocompatible, and biodegradable biopolymers as a modifier of alginate, currently (A. K. Nayak et al., 2012).

Gum arabic is a highly branched, slightly acidic natural polymer formulated from the tree sap of Acacia Senegal trees. It consisting a main chain of 1,3 linked β -D-galactopyranosyl units consisted of L-arabinose, L-rhamnose, D-galactose, and D-glucuronic acid with the side chain which formed of two to five linked β -D-galactopyranosyl units (Sarika, Cinthya, Jayakrishnan, Anilkumar, & James, 2014). It is widely used as stabilizer, thickening agent, hydrocolloid emulsifier, carrier, and release-controlled agent in food, pharmaceutical, and cosmetic industries (Nami, Haghshenas, & Yari Khosroushahi, 2016). Alginate and gum arabic are both regarded as safe (GRAS) by the United States Food and Drug Administration (USFDA).

Some reports have been provided that gum arabic beads have abilities on improving the encapsulation efficiency of alginate beads and alginate/ gum arabic beads provided a higher survival rates of probiotics at low pH and bile salt condition (Nami, Haghshenas, & Yari

Khosroushahi, 2016; A. K. Nayak et al., 2012). However, the study provided the first report on the *in vitro* release behavior and the storage stability of a liquid-core alginate/gum arabic bead which prepared by reverse spherification.

5.2. Objectives

Gum arabic was provided that it has a relatively better ability on improving the physical properties of liquid-core hydrogel beads than glycerol at chapter 4. The objectives of this part was to investigate a delivery of vegetable extract, which was composed with the alginate/gum arabic out-layer and a liquid vegetable extract core, in an attempt to protect its functional compounds from being destroyed in gastrointestinal tracts and during storage. The first change of hardness, swelling behavior, total phenolic compounds release behavior, and release kinetics in an *in vitro* digestion system were investigated. Finally, the stability of stored total phenolic compounds and their antioxidant ability were examined.

5.3. Materials and methods

5.3.1. Materials

Radish leaves were obtained from a local farmer and prepared as described in the section 2.3.1. All chemicals in the investigation were commercially available and of analytical grade and their information are described in the section 3.3.1. and 4.3.1. α, α -diphenyl- β -picrylhydrazyl (DPPH) was purchased from Sigma-Aldrich (USA).

5.3.2. Formulation of alginate/gum arabic bead and storage test

Radish by-product juice was prepared as described in the section 3.3.2. and the formation of an alginate bead (HB0) and alginate/gum arabic beads (GA0.25, GA0.5, and GA0.75) is showed in the section 4.3.2. (Table 4-1). The different variation of alginate/gum arabic bead were stored for 0 to 28 days at 4°C for evaluating the loss of total phenolic compounds and decrease in

antioxidant ability during storage. The results were compared with liquid-core material (LCM).

5.3.3. Total phenolic content

The amount of total phenolic compounds was determined with Folin-Ciocalteu method (section 3.3.5.). The amount of total phenolic compounds during storage was evaluated by a first-order kinetic model,

$$\ln M_t = \ln M_0 - kt$$

and the reduction rate (k) and half-life ($t_{1/2}$) were calculated using,

$$t_{1/2} = \ln 2/k$$

where M_t and M_0 are the amounts of total phenolic compounds at days t and 0 , respectively.

5.3.4. Antioxidant ability

The antioxidant activity of liquid-core hydrogel bead during storage was determined by DPPH assay. DPPH, a stable free radical, is widely used to evaluate the antioxidant abilities of phenols by capturing H atoms of phenols (Achat, Rakotomanomana, Madani, & Dangles, 2016). The DPPH-scavenging activity was determined by the method of Lai, Chou, & Chao (2001). The decrease of DPPH-scavenging activity during storage, reduction rate (k) and half-lives ($t_{1/2}$) were evaluated by formula in section 5.5.3. The alginate/gum arabic bead (0.5 g) or the liquid-core material (1 mL) was blended and centrifuged as described in the method of section 3.3.5. An aliquot of 1 mL of 0.2 mM DPPH in methanol was mixed with 1 mL of the supernatant. The mixture was mixed by vortexing and left at room temperature in the dark for 30 min. The absorbance of a sample (A_s), control (sample was replaced by distilled water, A_c), and blank (A_b) were measured at 517 nm by a spectrophotometer. DPPH-scavenging activity was calculated with the following equation:

$$\text{DPPH scavenging activity (\%)} = [1 - (A_s - A_b)/A_c] \times 100$$

5.3.5. *In vitro* release profile and release kinetic

The simulated gastric fluid and simulated intestinal fluid were prepared by following the method of the section 3.3.6. *In vitro* release experiments were performed by the method of Tsai, Chuang, Kitamura, Kokawa, & Islam (2017), using United States Pharmacopeia apparatus 2. The alginate/gum arabic bead (0.5 g) was left in 300 mL of simulated gastric fluid for 120 min and then transferred to simulated intestinal fluid for 240 min at 37 °C, with a paddle rotation speed of 50 rpm. Aliquots of 1 mL of the medium were withdrawn at specified times and replaced with fresh release medium. The amount of total phenolic compounds in the medium was measured by the method of section 3.3.5.

The release mechanisms of total phenolic compounds were evaluated with Korsmeyer-Peppas model: $M_t/M_\infty = Kt^n$

where M_t is the amount of total phenolic compounds at time t, M_∞ is the total amount of total phenolic compounds in the alginate/gum arabic bead, K is the release kinetic constants, and n is the release exponent, indicative of the drug release mechanism (Table 5-1).

5.3.6. Hardness

The hardness of each variation during *in vitro* release experiment were determined by following the method of the section 3.3.4.

5.3.7. Swelling capacity

The swelling capacity was determined by the method of Fu Hsuan Tsai, Chuang, et al. (2017). At regular time intervals during *in vitro* experiment, alginate/gum arabic beads were withdrawn from simulated gastric fluid, or simulated intestinal fluid, and excess water on the surfaces was gently removed with a paper towel. Swell capacity was calculated as follows:

$$\text{Swelling capacity (\%)} = [(W_2 - W_1)/W_1] \times 100$$

where W_t and W_0 are the weights of alginate/gum arabic bead at time t and 0.

Table 5-1 Release mechanism from polymeric delivery system

Release mechanism	Exponent (n) of Korsmeyer-Peppas model		
	Thin film	Cylinder	Sphere
Fickian diffusion	0.5	0.45	0.43
Anomalous transport	$0.5 < n < 1.0$	$0.45 < n < 0.89$	$0.43 < n < 0.85$
Case-II transport	1.0	0.89	0.85

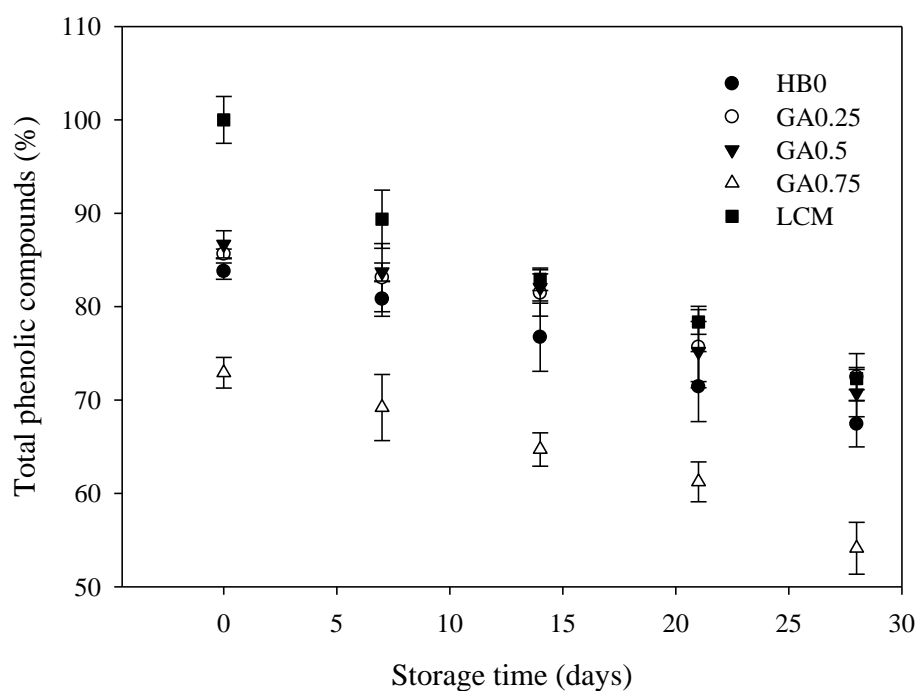


Figure 5-1 The amount of total phenolic compounds of alginate/gum arabic beads during storage.

5.4. Results and Discussion

5.4.1. Loss of total phenolic compounds

The amount of total phenolic compounds was expressed as the amount of total phenolic compounds found in alginate/gum arabic beads on a specific day of storage relative to the total amount of total phenolic compounds used to prepare the alginate/gum arabic beads. Figure 5-1 illustrates the decrease in total phenolic compounds during a storage test. The amount of total phenolic compounds in alginate/gum arabic beads was lower than that in liquid-core material due to total phenolic compounds loss during preparation. After 28 days of storage, there was no significant difference between the amount of total phenolic compounds of GA0.25 (72.46 %) and LCM (72.29 %).

The loss of total phenolic compounds was evaluated by the first-order kinetic model (Figure 5-1), and the kinetic parameters obtained are shown in Table 5-2. The results were well fit by the first-order kinetic model, indicated by the high (0.957 to 0.988) values of correlation (R^2). LCM had a high total phenolic compounds amount after 28 days of storage but the relatively higher k value ($1.11 \times 10^{-2} \text{ day}^{-1}$) showed that total phenolic compounds were easily destroyed when it was not protected by hydrogel beads. HB0 showed a lower k value than LCM. GA0.25 showed a low k value, but the k value increased from 6.10×10^{-3} to $1.03 \times 10^{-2} \text{ day}^{-1}$ with as the gum arabic ratio increased. The half-life ($t_{1/2}$) value indicates the days that were required for the amount of total phenolic compounds to be reduced by half. The half-life of total phenolic compounds in GA0.25 was more than 100 days but the half-life of total phenolic compounds without hydrogel protection (LCM) was only approximately 62 days. The result demonstrated that alginate/gum arabic beads were good at preventing total phenolic compounds from losing during storage.

5.4.2. Antioxidant activity

The antioxidant activity of alginate/gum arabic beads during storage was determined by DPPH

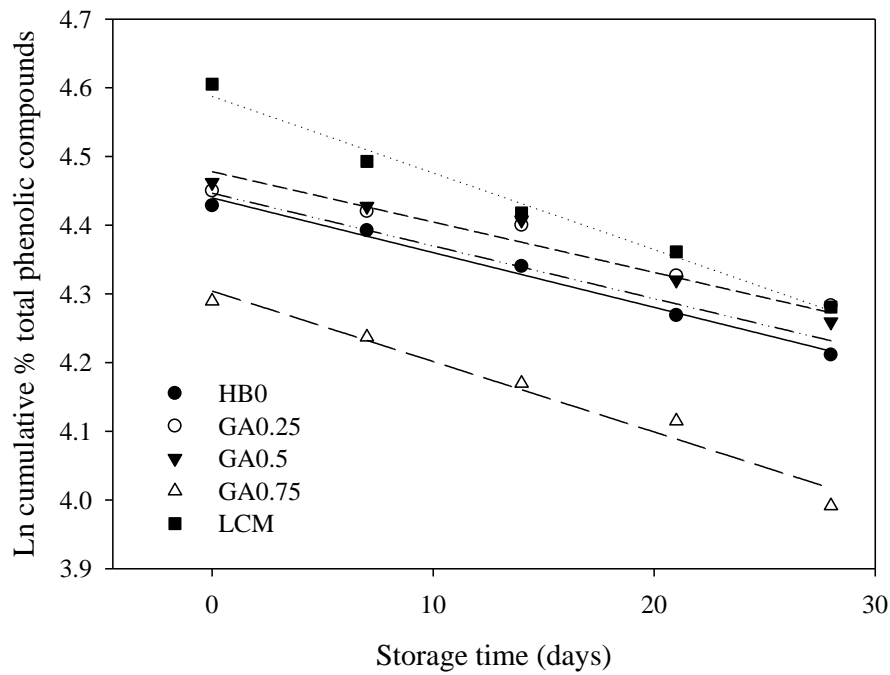


Figure 5-2 Total phenolic compounds loss kinetic during storage.

Table 5-2 Kinetic parameters for total phenolic compounds change during storage.

Code	Kinetic parameters		
	k^1 (day ⁻¹)	$t_{1/2}^2$ (day)	R ²
LCM ³	1.11×10^{-2}	62.45	0.988
HB0	8.00×10^{-3}	86.64	0.987
GA0.25	6.10×10^{-3}	113.63	0.957
GA0.5	7.30×10^{-3}	94.95	0.969
GA0.75	1.03×10^{-2}	67.30	0.986

¹ k represents the kinetic constant of first-order kinetic model.

² $t_{1/2}$ represents the half-lives of total phenolic compounds loss.

³ LCM, liquid core material; HB0, alginate beads; GA 0.25, GA 0.5, GA0.75, alginate/gum arabic bead which are coded according to Table 4-1

assay. DPPH, a stable free radical, is widely used to evaluate the antioxidant abilities of phenols by capturing H atoms of phenols (Achat et al., 2016). At the beginning of storage, the DPPH-scavenging ability of alginate/gum arabic beads varied between 75.37 % and 89.56 % and was lower than LCM (96.17 %) (Figure 5-3). After 28 days of storage, the DPPH-scavenging ability of GA0.25 and GA0.5 were higher than 70 %, on the other hand, GA0.75 showed the lowest DPPH-scavenging ability.

DPPH-scavenging ability reduction was found to be fit by first-order kinetics (Figure 5-4) with high correlation (R^2) (0.929 to 0.961) (Table 5-3). Hydrogel beads without gum arabic (HB0) showed that their DPPH-scavenging ability decay rate was $1.01 \times 10^{-1} \text{ day}^{-1}$ and their half-life was 68.63 days. GA0.25 resulted in a slower decay rate of DPPH-scavenging ability ($k = 8.00 \times 10^{-3} \text{ day}^{-1}$) and a longer shelf-life (half-life of 86.64 days); however, as the ratio of gum arabic increased, the decay rate of DPPH-scavenging ability increased and the half-life decreased. Tonon, Brabet, & Hubinger (2010) also indicated that anthocyanins in non-encapsulated black berry juice showed a higher degradation rate due to a greater contact with oxygen. Oxidation is one of the causes of total phenolic compounds degradation; however, alginate/gum arabic beads could eliminate the direct contact between core materials and environmental factors.

The trend of the DPPH-scavenging ability decrease was similar to the trend of the amount of total phenolic compounds (Figure 5-1). Phenolic compounds play an important role in antioxidant ability; therefore, more total phenolic compounds resulted in a higher DPPH-scavenging ability. I investigated the correlation between DPPH-scavenging activity and the amount of total phenolic compounds, and the result is shown in Figure 5-5. It was found that DPPH-scavenging activity positively correlated with the amount of total phenolic compounds ($R^2 = 0.92$).

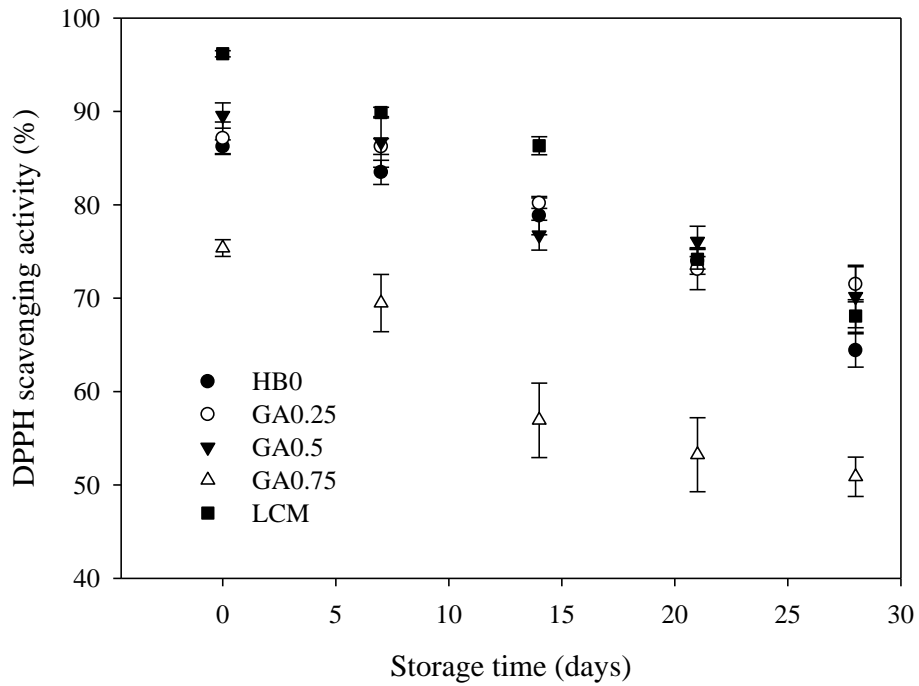


Figure 5-3 DPPH scavenging activity of alginate/gum arabic beads during storage.

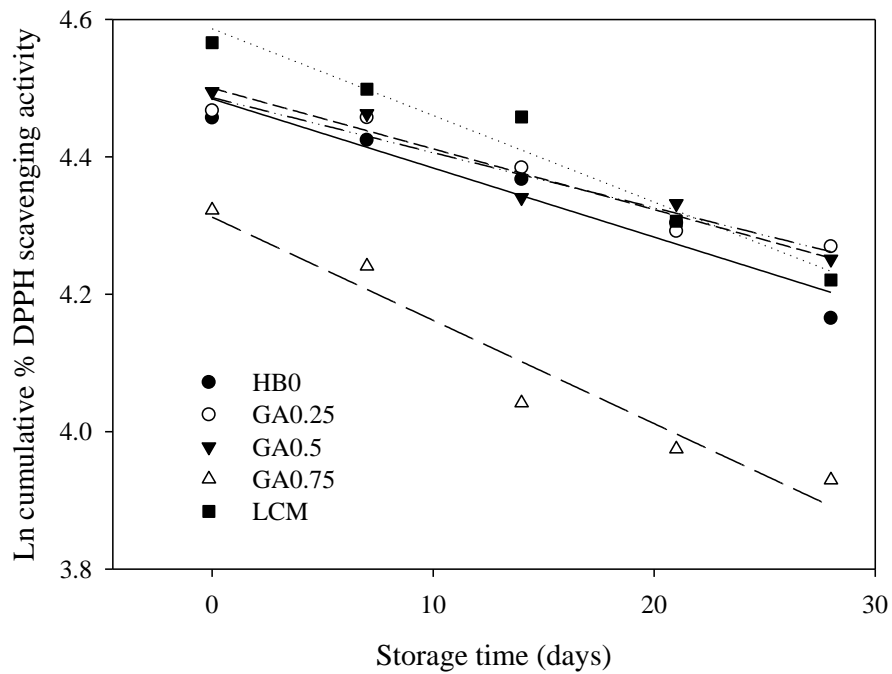


Figure 5-4 DPPH scavenging activity reducing kinetic during storage.

Table 5-3 Kinetic parameters for DPPH scavenging ability change during storage.

Code	DPPH scavenging activity		
	k^1 (day ⁻¹)	$t_{1/2}^2$ (day)	R ²
LCM ³	1.26×10^{-2}	55.01	0.961
HB0	1.01×10^{-2}	68.63	0.929
GA0.25	8.00×10^{-3}	86.64	0.942
GA0.5	8.80×10^{-3}	78.77	0.945
GA0.75	1.50×10^{-2}	46.20	0.942

¹ k represents the kinetic constant of first-order kinetic model.

² $t_{1/2}$ represents the half-lives of total phenolic compounds loss.

³ LCM, liquid core material; HB0, alginate beads; GA 0.25, GA 0.5, GA0.75, alginate/gum arabic bead which are coded according to Table 4-1

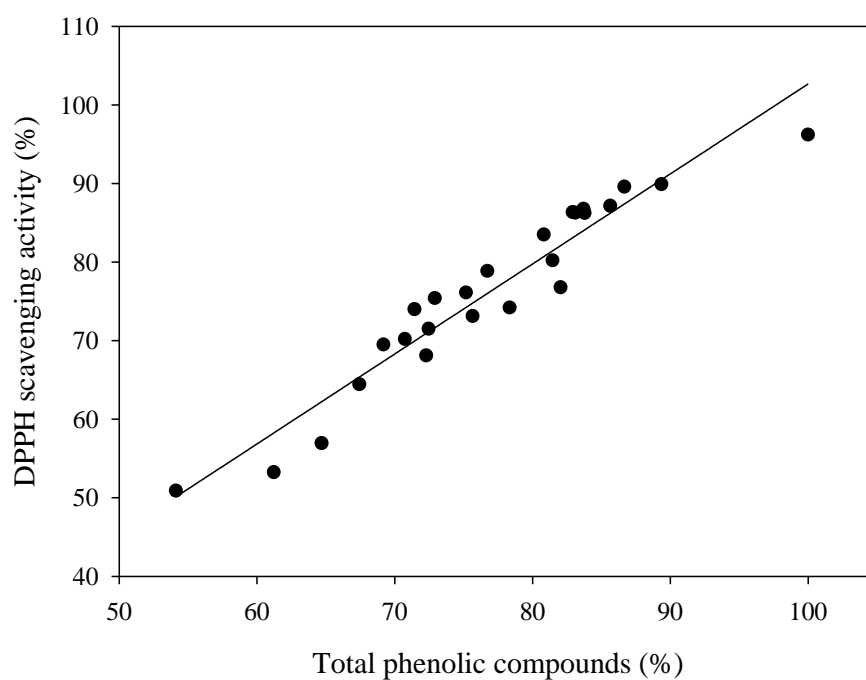


Figure 5-5 The correlation between DPPH scavenging activity and total phenolic compounds amount.

5.4.3. *In vitro* release profile and kinetics

The release behavior of alginate/gum arabic beads was investigated by an *in vitro* drug release experiment. Alginate/gum arabic beads were soaked in simulated gastric fluid (pH 1.2) for 2 h and then transferred to simulated intestinal fluid (pH 6.8) for 4 h. The appropriate technologies and materials of bead preparation should be chosen to effect ideal release behavior. Because of its pH-sensitivity, biocompatibility, and ease of manipulation, alginate has been widely used for carrying environmentally sensitive bioactives and oral delivery systems (Burey et al., 2008; Gong et al., 2011; Zeeb, Saberi, Weiss, & McClements, 2015). Some articles also report that the presence of pores in the alginate network is the major factor for release. The use of filler for delaying active compound release was deescribed (López Córdoba et al., 2013). To prevent core material from being destroying and releasing into stomach fluid, I tried to prepare a delivery system that can coat bioactives and protect them in simulated gastric digestion, for transport to the simulated intestinal digestion. Bioactives were expected to be released and absorbed in the intestinal tract. Thus, a low amount and slow release of total phenolic compounds in simulated gastric digestion was favored for this study. In constrast, a high amount and high-speed release of total phenolic compounds in simulated intestinal digestion was expected. Gum arabic was used as a filler in this work because of its ampholytic characteristics (Fang et al., 2011).

The effect of the alginate to gum arabic ratio on the total phenolic compounds release profile is shown in Figure 5-6. Alginate tends to shrink and has poor water solubility in acidic pH (Sinha et al., 2015), slowing the release of the compound from alginate/gum arabic beads. With the increase in gum arabic, the amount of total phenolic compounds released from alginate/gum arabic beads in simulated gastric digestion decreased for 2 h and then increased. GA0.75 showed the highest amount of total phenolic compounds release (53.15 %), which was about two times higher than that of GA0.25 (27.42 %) in the same time interval. The result indicates that a proper alginate to gum arabic ratio can prevent total phenolic compounds release because gum arabic play a role as a barrier in the pores in alginate (A. K. Nayak et al., 2012).

According to Figure 5-6, the amount of total phenolic compounds released by GA0.75 did not show any significant change after 180 min, HB0 and GA0.25 did not show any significant change after 300 min, and GA0.5 did not show any significant change after 210 min ($p < 0.05$). The result indicates that the amount of total phenolic compounds released for all variations reached their maxima in 6 h. HB0 released approximately 89 % of its total phenolic compounds in 6 h. On the other hand, the amount of total phenolic compounds released by all variations of alginate/gum arabic beads was higher than 90 %. If total phenolic compounds are not released from hydrogel beads within 6 h in an *in vitro* release system, they could form waste by exiting the body through the waste system. The results demonstrated that the addition of gum arabic could modify the release behavior of alginate.

The release profile was analyzed by fitting the results of the curve to the Korsmeyer-Peppas model, and the results were given in Table 5-4. Korsmeyer-Peppas is a simple but useful formulation to evaluate release mechanisms (Costa & Sousa Lobo, 2001). For a sphere, the release mechanism follows Fickian release when the release exponent (n) is approximately 0.43, when the n values are between 0.43 and 0.85, the release is defined as anomalous transport, and the release mechanism is defined as case-II transport when n is approximately 0.85. Fickian release indicates a diffusion-controlled release, in which compounds release from delivery by diffusion, anomalous transport represents a non-Fickian release, and case-II transport indicates a swelling-controlled release, in which water plays a role as a plasticizer (Siepmann & Peppas, 2001). The n values of all the samples ranged from 0.082 to 0.278, indicating that the release profile follows Fickian release. The release rate of total phenolic compounds in simulated gastric digestion showed an increase and then a decrease with an increasing amount of gum arabic, while GA0.25 showed the lowest release rate.

Gum arabic is an ampholytic polymer. This characteristic makes gum arabic attract alginate molecules, which are negatively charged, with electrostatic forces. Calcium ions do not only play a role as a crosslinker of alginate; they also react with the carboxylate groups of gum arabic

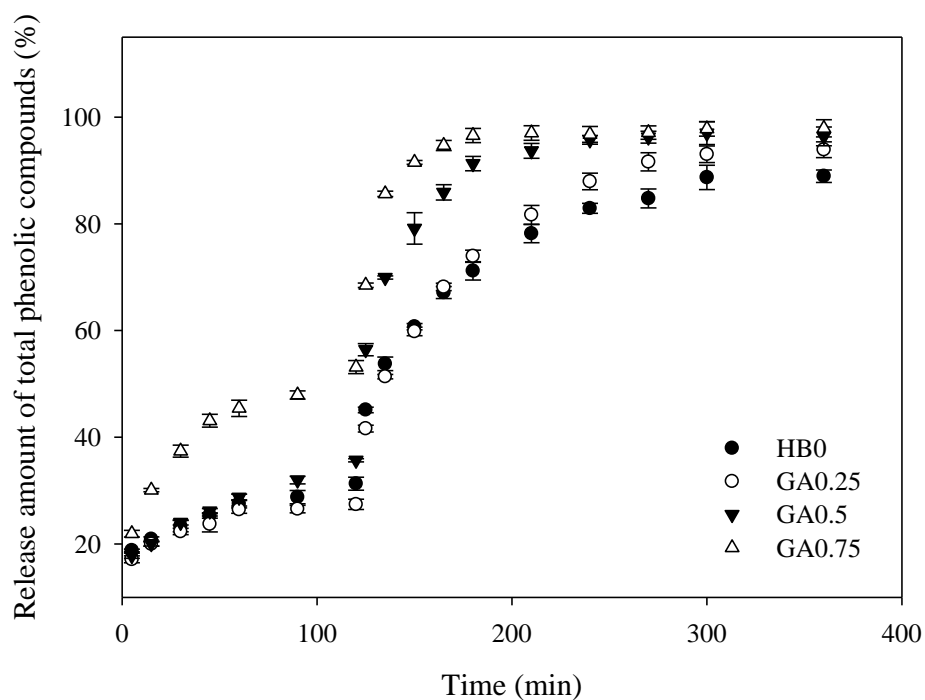


Figure 5-6 Total phenolic compounds release from alginate/gum arabic beads in an *in vitro* digestion system.

Table 5-4 Kinetic parameters for total phenolic compounds release from alginate/gum arabic beads in an *in vitro* digestion system.

Code	Simulated gastric digestion			Simulated intestinal digestion		
	k^1 (min ⁻ⁿ)	n^1	R ²	k (min ⁻ⁿ)	n	R ²
HB0	5.31×10^{-6}	0.162	0.972	2.71×10^{-3}	0.189	0.992
GA0.25	2.25×10^{-6}	0.155	0.981	4.09×10^{-3}	0.229	0.988
GA0.5	6.03×10^{-5}	0.221	0.964	5.61×10^{-3}	0.144	0.939
GA0.75	9.15×10^{-4}	0.278	0.991	6.09×10^{-3}	0.082	0.796

¹ k and n represents the kinetic constant and release exponent of Korsmeyer-Peppas release kinetics.

² HB0, alginate beads; GA 0.25, GA 0.5, GA0.75, alginate/gum arabic bead which are coded according to Table 4-1

(Fang et al., 2011; A. K. Nayak et al., 2012). Table 5-4 also shows that the relatively higher k values in simulated intestinal digestion were in the range from 2.71×10^{-3} to $6.09 \times 10^{-3} \text{ day}^{-1}$. The result demonstrates that total phenolic compounds were released from alginate/gum arabic beads were quicker in simulated intestinal digestion than in simulated gastric digestion. The faster release in simulated intestinal digestion might be due to the pK_a of carboxyl groups ($-\text{COOH}$), which is 4.75, being lower than the pH of simulated intestinal fluid (pH 6.8). Carboxyl groups deprotonate to carboxylate anions ($-\text{COO}^-$) and hydrogen ions (H^+). The electrostatic repulsive forces between carboxylate anions leads to alginate polymer swelling (Gong et al., 2011). GA0.75 in simulated intestinal digestion was fit worse by Korsmeyer-Peppas models and had the lowest R^2 (0.796) among all the variations. The release profile of total phenolic compounds released by GA0.75 was over 95 % at 180 min (Figure 5-6), and there were no significant difference between total phenolic compounds release profiles from 180 min to 300 min. I inferred that GA0.75 releases total phenolic compounds in simulated intestinal digestion quickly, resulting in a poorer fit to the Korsmeyer-Peppas model.

5.4.4. Hardness

Several mechanical properties can be evaluated by using a texture analyzer. The effect of the alginate/gum arabic ratio on hardness in an *in vitro* digestion system was evaluated by a compression model in this study. The results are shown in Figure 5-7. I used the sample of HB0 before soaking in an *in vitro* digestion system as a standard, and the relative hardness of alginate/gum arabic beads were calculated. The hardness of GA0.75 after 90 min was too low to be detected, and the hardness of other variations ranged from 8.37 to 15.87 % after 120 min. HB0 remained a relatively higher hardness after being suspended in simulated gastric fluid for 120 min. Furthermore, hardness of all of the variations was too low to be detected after 150 min. George & Abraham (2006) indicated that alginate is a pH-sensitive hydrogel. At a low pH environment, for example in simulated gastric fluid, alginate shrinks and converts into an

insoluble polymer, so-called alginic acid skin. Once transformed into a high pH environment, alginic skin is converted into a soluble polymer. The pK_a of carboxyl group (-COOH) is 4.75 which is lower than the pH of simulated intestinal fluid (6.8). Therefore, carboxyl groups release hydrogen ion, translating into the anionic form (-COO⁻), resulting in the hardness of alginate/ gum arabic beads decreasing (Gong et al., 2011).

5.4.5. Swelling capacity

Results of the swelling capacity are shown in Figure 5-8. Swelling capacity of all the samples was lower than 0 when suspended in the simulated gastric fluid (0-120 min) and decreased by time and then increased when suspended in simulated intestinal fluid. The results showed that alginate/ gum arabic bead shrunk at a low pH environment. GA0.75 changed in a relatively wider range than other treatments. Swelling capacity of HB0, GA0.25, GA0.5, and GA0.75 at 120 min were -18.28, -17.55, -21.12 and -42.74 %, respectively. On the other hand, swelling capacity of all variations increased when transferred into simulated intestinal fluid and then decreased by time. The swelling capacity of GA0.75 couldn't be detected after 125 min because the sample was too fragile.

Swelling capacity is affected by both osmotic pressure and pH, absorption and release of the bathing fluid occurred simultaneously in the dissolution system. Alginate/gum arabic beads tended to shrink when bathing fluid absorption was less than its release, and swell when bathing fluid absorption was greater than its release. In the simulated gastric digestion, low pH environment made the alginate layer of the alginate/gum arabic beads contract into an alginic acid skin, resulting in a greater bathing fluid release than absorption and a decrease in swelling capacity. In the first half of simulated intestinal fluid suspension (120-125 min), alginic acid skin swollen because the pH of simulated intestinal fluid (6.8) was higher than the pK_a of carboxyl group (-COOH) of alginate (4.75). Swelling capacity was calculated by the weight change between original beads and soaked beads. In the second half (after 125 min), the swollen

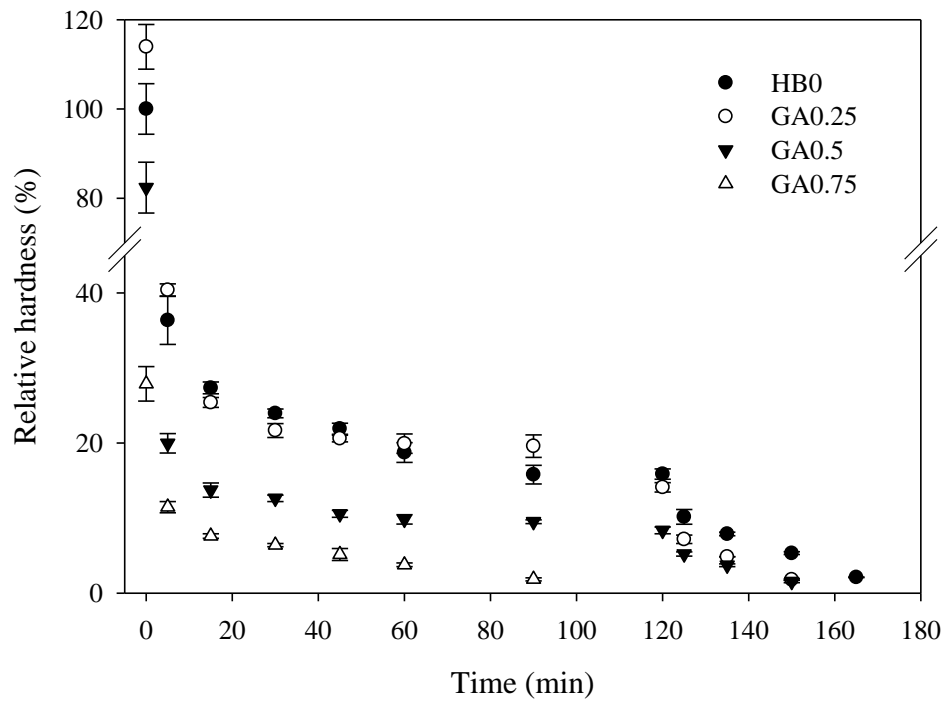


Figure 5-7 Hardness of alginate/gum arabic beads in an *in vitro* digestion system.

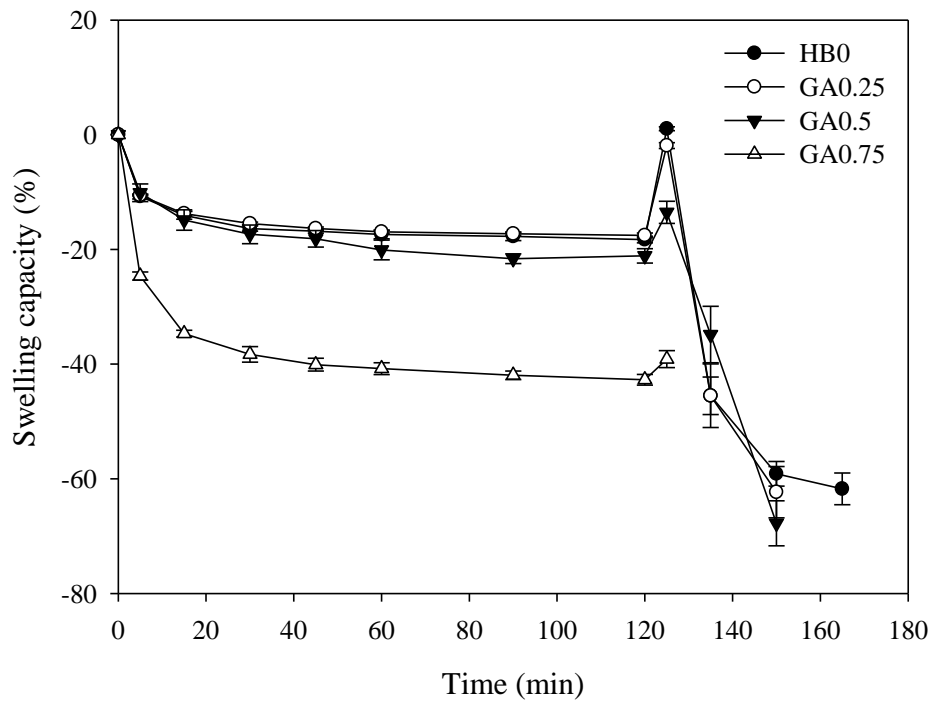


Figure 5-8 Swelling capacity of alginate/gum arabic beads in an *in vitro* digestion system.

alginic acid skin dissolved into the simulated intestinal fluid, resulting in the swelling capacity decreasing.

5.5. Conclusions

Storage tests of this study confirmed that the addition of gum arabic can prevent total phenolic compounds from losing, and the results were well fit by a first-order kinetic model, with R^2 ranging from 0.957 to 0.988. The half-life of total phenolic compounds decay in GA0.25 is over than 100 days. Gum arabic can also maintain antioxidant activity during storage. GA0.25 resulted in a slower decay rate of DPPH-scavenging ability ($k= 8.00 \times 10^{-3} \text{ day}^{-1}$) and a longer shelf- life (half- life of 86.64 days). *In vitro* release experiments indicated that the release profile of all the variation followed Fickian release. GA0.25 has a better performance in preventing the release of total phenolic compounds in simulated gastric digestion. GA0.75 showed the highest amount of the release of total phenolic compounds (53.15 %) in simulated gastric digestion, which was about two times higher than GA0.25 (27.42 %) in the same time interval. Thus, these results suggest that alginate/gum arabic bead can be used as potential carriers of radish by-product juice.

6. Conclusions and future prospective

Radish by-product liquid-core hydrogel was successfully prepared by reverse spherification. Firstly, the smallest particle size of radish by-product could be prepared with micro wet milling system at the rotation of 30 rpm. Some studies indicated that the functional compound could be released efficiently with the reduction of particle size of the fruit tissue and the orange juice, which was prepared micro wet milling system (Islam et al., 2017). The condition was used to prepare the radish by-product juice in the following chapter.

RSM was used for examining the effects and importance on different physical properties, and optimal conditions of the liquid-core hydrogel bead was investigated. Out of the seven dependent variables, average diameter, hardness (Y_1), encapsulation efficiency (Y_2), release profile of total phenolic compounds in simulated gastric (Y_3) and small intestinal (Y_4) digestion, swelling capacity (Y_5), and sphericity (Y_6), Y_1 , Y_2 , and Y_3 , were used for optimizing the conditions of the liquid-core hydrogel bead formulation because their lack-of-fit test showed no significant difference ($p > 0.05$). The optimized liquid-core hydrogel bead had a high hardness (25.50 N) and encapsulation efficiency (85.67 %), and low release profile of total phenolic compounds (27.38 %) in simulated gastric digestion with small error-values. The result demonstrated that the mathematical models obtained from the CCD were well fitted. Optimal conditions of the liquid-core hydrogel bead was primary gelation time of 23 min 59 sec, calcium lactate concentration of 0.13 M in the primary gelation, secondary gelation time of 6 min 2 sec, and calcium lactate concentration of 0.058 M in secondary gelation.

All of the variations showed a small sphericity (lower than 0.05) and demonstrated that the deformation of bead is not clearly visible by human eyes. and then the average diameter was approximately 4.58 mm to 5.66 mm. Gum arabic was provided that it is a good material to improve the physicochemical properties of alginate liquid-core hydrogel beads. The average diameter increased with the increase of the ratio of gum arabic or glycerol. The hardness of

alginate/gum arabic bead (6.53 N to 26.68 N) changed significantly than the alginate/glycerol bead (19.91 N to 24.08 N). Alginate/ gum arabic bead showed the higher encapsulation efficiency and the lower swelling capacity than alginate/ glycerol bead. Storage tests of this study confirmed that the addition of gum arabic can prevent total phenolic compounds from losing, and the results were well fit by a first-order kinetic model, with R^2 ranging from 0.957 to 0.988. The half-life of total phenolic compounds decay in GA0.25, which alginate/gum arabic or weight ratios of 0.25/0.75, is over than 100 days. Gum arabic can also maintain antioxidant activity during storage. GA0.25 resulted in a slower decay rate of DPPH-scavenging ability ($k= 8.00 \times 10^{-3} \text{ day}^{-1}$) and a longer shelf- life (half- life of 86.64 days). *In vitro* release experiments indicated that the release profile of all the variation followed Fickian release. GA0.25 has a better performance in preventing the release of total phenolic compounds in simulated gastric digestion. GA0.75 showed the highest amount of the release of total phenolic compounds (53.15 %) in simulated gastric digestion, which was about two times higher than GA0.25 (27.42 %) in the same time interval.

The study demonstrated that radish liquid-core hydrogel bead prevented total phenolic compounds from release in the simulated gastric digestion and loss during storage. In the future, I suggest that other biopolymer could be use as the wall material of liquid-core hydrogel bead, for example, chitosan and pectin, their release control ability have been proved (Jantrawut et al., 2013; Vandenberg, Drolet, Scott, & De la Noüe, 2001). The combination of biopolymer and the addition of modifier are also interesting topics. I believe that this study may be useful for the development and quality improvement of a delivery system and I expect that the liquid-core hydrogel bead prepared with reverse spherification could be used in commercial products

References

- Achat, S., Rakotomanomana, N., Madani, K., & Dangles, O. (2016). Antioxidant activity of olive phenols and other dietary phenols in model gastric conditions: Scavenging of the free radical DPPH and inhibition of the haem-induced peroxidation of linoleic acid. *Food Chemistry*, *213*, 135–142.
- Amine, K. M., Champagne, C. P., Salmieri, S., Britten, M., St-Gelais, D., Fustier, P., & Lacroix, M. (2014). Effect of palmitoylated alginate microencapsulation on viability of *Bifidobacterium longum* during freeze-drying. *LWT - Food Science and Technology*, *56*(1), 111–117.
- Anonymous. (2015). おいしいねっと. Retrieved December 16, 2017, from <http://o-e-c.net/syokuzai/daikon#syurui>
- Anonymous. (2017). 日本の起源. Retrieved December 16, 2017, from <http://www.m-gakusei.com/index.php?%E6%97%A5%E6%9C%AC%E3%81%AE%E8%B5%B7%E6%BA%90>
- Belščak-Cvitanović, A., Komes, D., Karlović, S., Djaković, S., Špoljarić, I., Mršić, G., & Ježek, D. (2015). Improving the controlled delivery formulations of caffeine in alginate hydrogel beads combined with pectin, carrageenan, chitosan and psyllium. *Food Chemistry*, *167*, 378–386.
- Ben Messaoud, G., Sánchez-González, L., Probst, L., Jeandel, C., Arab-Tehrany, E., & Desobry, S. (2016). Physico-chemical properties of alginate/shellac aqueous-core capsules: Influence of membrane architecture on riboflavin release. *Carbohydrate Polymers*, *144*, 428–437.
- Blows, M. W., & Brooks, R. (2003). Measuring Nonlinear Selection. *The American Naturalist*, *162*(6), 815–820.
- Burey, P., Bhandari, B. R., Howes, T., & Gidley, M. J. (2008). Hydrocolloid gel particles:

- formation, characterization, and application. *Critical Reviews in Food Science and Nutrition*, 48(789190280), 361–377.
- Cai, S., Zhao, M., Fang, Y., Nishinari, K., Phillips, G. O., & Jiang, F. (2014). Microencapsulation of *Lactobacillus acidophilus* CGMCC1.2686 via emulsification/internal gelation of alginate using Ca-EDTA and CaCO₃ as calcium sources. *Food Hydrocolloids*, 39, 295–300.
- Carley, K. M., Kamneva, N. Y., & Reminga, J. (2004). Response Surface Methodology. *Wiley Interdisciplinary Reviews: Computational Statistics*, 2(2).
- Chan, E. S., Lee, B. B., Ravindra, P., & Poncelet, D. (2009). Prediction models for shape and size of ca-alginate macrobeads produced through extrusion-dripping method. *Journal of Colloid and Interface Science*, 338(1), 63–72.
- Chew, S. C., & Nyam, K. L. (2016). Microencapsulation of kenaf seed oil by co-extrusion technology. *Journal of Food Engineering*, 175, 43–50.
- Chopra, M., Bernela, M., Kaur, P., Manuja, A., Kumar, B., & Thakur, R. (2015). Alginate/gum acacia bipolymeric nanohydrogels-Promising carrier for Zinc oxide nanoparticles. *International Journal of Biological Macromolecules*, 72, 827–833.
- Chung, D., Kim, S.-H., Myung, N., Cho, K. J., & Chang, M.-J. (2012). The antihypertensive effect of ethyl acetate extract of radish leaves in spontaneously hypertensive rats. *Nutrition Research and Practice*, 6(4), 308–14.
- CollinsDictionary.com. (2017). Retrieved December 18, 2017, from <https://www.collinsdictionary.com/dictionary/english/cost-in-use>
- Connell, J. J. (1975). The role of formaldehyde as a protein crosslinking agent acting during the frozen storage of cod. *Journal of the Science of Food and Agriculture*, 26(12), 1925–1929.
- Costa, P., & Sousa Lobo, J. M. (2001). Modeling and comparison of dissolution profiles. *European Journal of Pharmaceutical Sciences*, 13(2), 123–133.

- Darmokoesoemo, H., Pudjiastuti, P., Rahmatullah, B., & Kusuma, H. S. (2017). Novel drug delivery carrier from alginate-carrageenan and glycerol as plasticizer. *Results in Physics*, 7, 2979–2989.
- Fang, Y., Al-Assaf, S., Phillips, G. O., Nishinari, K., Funami, T., Williams, P. a., & Li, A. (2007). Multiple steps and critical behaviors of the binding of calcium to alginate. *Journal of Physical Chemistry B*, 111(10), 2456–2462.
- Fang, Y., Li, L., Vreeker, R., Yao, X., Wang, J., Ma, Q., Jiang, F., & Phillips, G. O. (2011). Rehydration of dried alginate gel beads: Effect of the presence of gelatin and gum arabic. *Carbohydrate Polymers*, 86(3), 1145–1150.
- Fu, H., Liu, Y., Adrià, F., Shao, X., Cai, W., & Chipot, C. (2014). From material science to avant-garde cuisine. the art of shaping liquids into spheres. *Journal of Physical Chemistry B*, 118(40), 11747–11756.
- George, M., & Abraham, T. E. (2006). Polyionic hydrocolloids for the intestinal delivery of protein drugs: Alginate and chitosan — a review. *Journal of Controlled Release*, 114(1), 1–14.
- Gong, R., Li, C., Zhu, S., Zhang, Y., Du, Y., & Jiang, J. (2011). A novel pH-sensitive hydrogel based on dual crosslinked alginate/N- α -glutaric acid chitosan for oral delivery of protein. *Carbohydrate Polymers*, 85(4), 869–874.
- Gouin, S. (2004). Microencapsulation: Industrial appraisal of existing technologies and trends. *Trends in Food Science and Technology*, 15(7-8), 330–347.
- Goyeneche, R., Roura, S., Ponce, A., Vega-Gálvez, A., Quispe-Fuentes, I., Uribe, E., & Di Scala, K. (2015). Chemical characterization and antioxidant capacity of red radish (*Raphanus sativus* L.) leaves and roots. *Journal of Functional Foods*, 16, 256–264.
- Hoffman, J. (2009). Q & A : Chemistry in the kitchen. *Nature*, 457(7227), 267.
- Islam, M. Z., Kitamura, Y., Kokawa, M., & Monalisa, K. (2017). Degradation Kinetics and Storage Stability of Vacuum Spray-Dried Micro Wet-Milled Orange Juice (Citrus

- unshiu) Powder. *Food and Bioprocess Technology*, 10(6), 1002–1014.
- Islam, M. Z., Kitamura, Y., Kokawa, M., Monalisa, K., Tsai, F. H., & Miyamura, S. (2017). Effects of micro wet milling and vacuum spray drying on the physicochemical and antioxidant properties of orange (*Citrus unshiu*) juice with pulp powder. *Food and Bioproducts Processing*, 101(2012), 132–144.
- Jantrawut, P., Assifaoui, A., & Chambin, O. (2013). Influence of low methoxyl pectin gel textures and in vitro release of rutin from calcium pectinate beads. *Carbohydrate Polymers*, 97(2), 335–342.
- Ji, C., Cho, S., Gu, Y., & Kim, S. (2007). The Processing Optimization of Caviar Analogs Encapsulated by Calcium-Alginate Gel Membranes. *Food Science and Biotechnology*, 16(4), 557–564.
- Jost, V., Kobsik, K., Schmid, M., & Noller, K. (2014). Influence of plasticiser on the barrier, mechanical and grease resistance properties of alginate cast films. *Carbohydrate Polymers*, 110, 309–19.
- Kim, B. R., Park, J. H., Kim, S.-H., Cho, K. J., & Chang, M.-J. (2010). Antihypertensive Properties of Dried Radish Leaves Powder in Spontaneously Hypertensive Rats. *The Korean Journal of Nutrition*, 43(6), 561.
- Koyama, K., & Seki, M. (2004). Cultivation of yeast and plant cells entrapped in the low-viscous liquid-core of an alginate membrane capsule prepared using polyethylene glycol. *Journal of Bioscience and Bioengineering*, 97(2), 111–118.
- Koyama, M., & Kitamura, Y. (2014). Development of a new rice beverage by improving the physical stability of rice slurry. *Journal of Food Engineering*, 131, 89–95.
- Lai, L. S., Chou, S. T., & Chao, W. W. (2001). Studies on the antioxidative activities of Hsian-tSao (*Mesona procumbens* Hemsl) leaf gum. *Journal of Agricultural and Food Chemistry*, 49(2), 963–968.
- Lee, P., & Rogers, M. A. (2012). Effect of calcium source and exposure-time on basic caviar

- spherification using sodium alginate. *International Journal of Gastronomy and Food Science*, 1(2), 96–100.
- Li, Y., Hu, M., Du, Y., Xiao, H., & McClements, D. J. (2011). Control of lipase digestibility of emulsified lipids by encapsulation within calcium alginate beads. *Food Hydrocolloids*, 25(1), 122–130.
- Liang, Y., Liu, W., Han, B., Yang, C., Ma, Q., Song, F., & Bi, Q. (2011). An in situ formed biodegradable hydrogel for reconstruction of the corneal endothelium. *Colloids Surf B Biointerfaces*, 82(1), 1–7.
- López Córdoba, A., Deladino, L., & Martino, M. (2013). Effect of starch filler on calcium-alginate hydrogels loaded with yerba mate antioxidants. *Carbohydrate Polymers*, 95(1), 315–323.
- Lozano-Vazquez, G., Lobato-Calleros, C., Escalona-Buendia, H., Chavez, G., Alvarez-Ramirez, J., & Vernon-Carter, E. J. (2015). Effect of the weight ratio of alginate-modified tapioca starch on the physicochemical properties and release kinetics of chlorogenic acid containing beads. *Food Hydrocolloids*, 48, 301–311.
- Luo, G. S., Chen, F., & Wang, Y. J. (2005). Mass transport and modeling of emulsion phase-inversion coating of hydrogel beads. *Chemical Engineering Science*, 60(7), 1995–2003.
- Lupo, B., Maestro, A., Gutiérrez, J. M., & González, C. (2015). Characterization of alginate beads with encapsulated cocoa extract to prepare functional food: Comparison of two gelation mechanisms. *Food Hydrocolloids*, 49, 25–34.
- MAFF. (2016). *Statistics of Agriculture, Forestry and Fisheries*.
- Maitra, J., & Shukla, V. K. (2014). Cross-linking in Hydrogels - A Review, 4(2), 25–31.
- Matalanis, A., Jones, O. G., & McClements, D. J. (2011). Structured biopolymer-based delivery systems for encapsulation, protection, and release of lipophilic compounds. *Food Hydrocolloids*, 25(8), 1865–1880.
- McKenna, B. A., Nicholson, T. M., Wehr, J. B., & Menzies, N. W. (2010). Effects of Ca, Cu,

- Al and La on pectin gel strength: implications for plant cell walls. *Carbohydrate Research*, 345(9), 1174–1179.
- Mohy Eldin, M. S., Kamoun, E. a., Sofan, M. a., & Elbayomi, S. M. (2014). l-Arginine grafted alginate hydrogel beads: A novel pH-sensitive system for specific protein delivery. *Arabian Journal of Chemistry*, 8(3), 355–365.
- Mowlick, S., Inoue, T., Takehara, T., Tonouchi, A., Kaku, N., Ueki, K., & Ueki, A. (2014). Usefulness of Japanese-radish residue in biological soil disinfestation to suppress spinach wilt disease accompanying with proliferation of soil bacteria in the Firmicutes. *Crop Protection*, 61, 64–73.
- Mukhopadhyay, P., Chakraborty, S., Bhattacharya, S., Mishra, R., & Kundu, P. P. (2015). pH-sensitive chitosan/alginate core-shell nanoparticles for efficient and safe oral insulin delivery. *International Journal of Biological Macromolecules*, 72, 640–648.
- Nami, Y., Haghshenas, B., & Yari Khosroushahi, A. (2016). Effect of psyllium and gum Arabic biopolymers on the survival rate and storage stability in yogurt of *Enterococcus durans* IW3 encapsulated in alginate. *Food Science & Nutrition*, (August), 1–10.
- Nayak, A. K., Das, B., & Maji, R. (2012). Calcium alginate/gum arabic beads containing glibenclamide: Development and in vitro characterization. *International Journal of Biological Macromolecules*, 51(5), 1070–1078.
- Nayak, A. K., Pal, D., & Santra, K. (2016). Swelling and drug release behavior of metformin HCl-loaded tamarind seed polysaccharide-alginate beads. *International Journal of Biological Macromolecules*, 82, 1023–1027.
- Nayak, A., Laha, B., & Sen, K. (2011). Development of hydroxyapatite-ciprofloxacin bone-implants using »Quality by design«. *Acta Pharmaceutica*, 61(1), 25–36.
- Neyraud, E., & Dransfield, E. (2004). Relating ionisation of calcium chloride in saliva to bitterness perception. *Physiology and Behavior*, 81(3), 505–510.

- Nguyen, K. T., & West, J. (2002). Photopolymerizable hydrogels for tissue engineering applications. *Biomaterials*, 23(22), 4307–4314.
- Ohi, M., & Isomura, Y. (2000). Phenotypic Variation and Relationship among Cultivars of *Raphanus sativus* L. Originated in Nagano Prefecture. *Journal of the Faculty of Agriculture Shinshu University*, 37(1), 49–55.
- Okine, A., Yimamu, A., Hanada, M., Izumita, M., Zunong, M., & Okamoto, M. (2007). Ensiling characteristics of daikon (*Raphanus sativus*) by-product and its potential as an animal feed resource. *Animal Feed Science and Technology*, 136(3-4), 248–264.
- Paques, J. P., Van Der Linden, E., Van Rijn, C. J. M., & Sagis, L. M. C. (2014). Preparation methods of alginate nanoparticles. *Advances in Colloid and Interface Science*, 209, 163–171.
- Pasparakis, G., & Bouropoulos, N. (2006). Swelling studies and in vitro release of verapamil from calcium alginate and calcium alginate–chitosan beads. *International Journal of Pharmaceutics*, 323(1-2), 34–42.
- Pawar, S. N., & Edgar, K. J. (2012). Alginate derivatization: A review of chemistry, properties and applications. *Biomaterials*, 33(11), 3279–3305.
- Robertson, V. K. (2013). *Applications of a Biorelevant In Vitro Dissolution Method Using USP Apparatus 4 in Early Phase Formulation Development*. University of Kansas.
- Rojas-Graü, M. A., Tapia, M. S., Rodríguez, F. J., Carmona, A. J., & Martin-Belloso, O. (2007). Alginate and gellan-based edible coatings as carriers of antibrowning agents applied on fresh-cut Fuji apples. *Food Hydrocolloids*, 21(1), 118–127.
- Santana, A. A., & Kieckbusch, T. G. (2013). Physical evaluation of biodegradable films of calcium alginate plasticized with polyols. *Brazilian Journal of Chemical Engineering*, 30(4), 835–845.
- Sarika, P. R., Cinthya, K., Jayakrishnan, A., Anilkumar, P. R., & James, N. R. (2014). Modified gum arabic cross-linked gelatin scaffold for biomedical applications. *Materials*

Science and Engineering C, 43, 272–279.

- Schmidt, S. J., Bohn, D. M., Rasmussen, A. J., & Sutherland, E. A. (2012). Using Food Science Demonstrations to Engage Students of All Ages in Science, Technology, Engineering, and Mathematics (STEM). *Journal of Food Science Education*, 11(2), 16–22.
- SELFNutritionData. (2014). Radishes, white icicle, raw. Retrieved December 17, 2017, from <http://nutritiondata.self.com/facts/vegetables-and-vegetable-products/2746/2>
- Shahidi, F., & Han, X. Q. (1993). Encapsulation of Food Ingredients. *Critical Reviews in Food Science and Nutrition*, 33(6), 501–547.
- Siepmann, J., & Peppas, N. a. (2001). Modeling of drug release from delivery systems based on hydroxypropyl methylcellulose (HPMC). *Advanced Drug Delivery Reviews*, 48(2-3), 139–157.
- Singh, B., Sharma, V., & Chauhan, D. (2010). Gastroretentive floating sterculia-alginate beads for use in antiulcer drug delivery. *Chemical Engineering Research and Design*, 88(8), 997–1012.
- Sinha, P., Ubaidulla, U., Hasnain, M. S., Nayak, A. K., & Rama, B. (2015). Alginate-okra gum blend beads of diclofenac sodium from aqueous template using ZnSO₄ as a cross-linker. *International Journal of Biological Macromolecules*, 79, 555–563.
- Stinco, C. M., Fernández-Vázquez, R., Escudero-gilete, M. L., Heredia, F. J., Meléndez-Martínez, A. J., & Vicario, I. M. (2012). Effect of Orange Juice's Processing on the Color, Particle Size, and Bioaccessibility of Carotenoids. *Jornal of Agricultural and Food Chemistry*, 60(6), 1447–1455.
- Šumić, Z., Vakula, A., Tepić, A., Čakarević, J., Vitas, J., & Pavlić, B. (2016). Modeling and optimization of red currants vacuum drying process by response surface methodology (RSM). *Food Chemistry*, 203, 465–475.
- Tonon, R. V., Brabet, C., & Hubinger, M. D. (2010). Anthocyanin stability and antioxidant

- activity of spray-dried açai (*Euterpe oleracea* Mart.) juice produced with different carrier agents. *Food Research International*, 43(3), 907–914.
- Trugo, L., & Finglas, P. M. (2003). Encyclopedia of Food Sciences and Nutrition, Second ed. In C. Thies (Ed.), *Microcapsule* (pp. 3892–3903). Atlanta: NewsRx.
- Tsai, F. H., Chiang, P. Y., Kitamura, Y., Kokawa, M., & Khalid, N. (2016). Preparation and physical property assessments of liquid-core hydrogel beads loaded with burdock leaf extracts. *RSC Advances*, 6, 91361–91369.
- Tsai, F. H., Chuang, P. Y., Kitamura, Y., Kokawa, M., & Islam, M. Z. (2017). Producing liquid-core hydrogel beads by reverse spherification: Effect of secondary gelation on physical properties and release characteristics. *Food Hydrocolloids*, 62, 140–148.
- Vandenberg, G. W., Drolet, C., Scott, S. L., & De la Noüe, J. (2001). Factors affecting protein release from alginate-chitosan coacervate microcapsules during production and gastric/intestinal simulation. *Journal of Controlled Release*, 77(3), 297–307.
- Wang, Q., Zhang, J., & Wang, A. (2009). Preparation and characterization of a novel pH-sensitive chitosan-g-poly (acrylic acid)/attapulgit/sodium alginate composite hydrogel bead for controlled release of diclofenac sodium. *Carbohydrate Polymers*, 78(4), 731–737.
- Zeeb, B., Saberi, A. H., Weiss, J., & McClements, D. J. (2015). Formation and characterization of filled hydrogel beads based on calcium alginate: Factors influencing nanoemulsion retention and release. *Food Hydrocolloids*, 50, 27–36.
- Zhao, Y., Hu, F., Evans, J. J., & Harris, M. T. (2011). Study of sol–gel transition in calcium alginate system by population balance model. *Chemical Engineering Science*, 66(5), 848–858.
- Zucker, D., Marcus, D., Barenholz, Y., & Goldblum, A. (2009). Liposome drugs' loading efficiency: A working model based on loading conditions and drug's physicochemical properties. *Journal of Controlled Release*, 139(1), 73–80.

中村美咲. (2016). 微細化処理が農産物中のホスファチジン酸生成に及ぼす影響の解明. 筑波大学.

Acknowledgement

I would like to express my gratitude to my supervisors Prof. Yutaka Kitamura and Mito Kokawa for their patience and support in overcoming numerous obstacles I have been facing through my research and helped me get results of better quality. I am also grateful to the committee of dissertation: Prof. Hitoshi Miyazaki, Prof. Shigeki Yoshida, and Marcos Neves for their insightful comments and suggestions.

I would like to thank the Japan-Taiwan Exchange Association for the financial support to conduct this Ph.D. study.

My sincere thanks also go to all the agriculture and food process laboratory members for their feedback, cooperation and of course friendship. It was great sharing laboratory with all of you during last three years. In addition I would like to express my gratitude to the staffs of the Appropriate Technology and Sciences for Sustainable Development and International Bioindustrial Sciences Course of the Graduate School of Life and Environmental Science.

I would like to thank my friends for accepting nothing less than excellence from me. Last but not the least, I would like to thank my family: my husband, parents and to my sister for supporting me spiritually throughout writing this thesis and my life in general.

Thanks for all your encouragement!